Temporal scale issues in flood simulation: estimation of instantaneous peak flow from maximum daily flow

VON DER FAKULTÄT FÜR BAUINGNIEURWESEN UND GEODÄSIE
DER GOTTFRIED WILHELM LEIBNIZ UNIVERSITÄT HANNOVER

Zur Erlangung des akademischen Grades

Doktor-Ingenieur

- Dr.-Ing. -

genehmigte Dissertation

Von

M.Sc. **Jie Ding**

geboren am 06.05.1986 in Changde, China

2015

Referent: Prof. Dr.-Ing. U. Haberlandt

Korreferent: Prof. Dr.-Ing. G. Meon

Tag der Promotion: 24. Juli 2015

Acknowledgement

The writing of this dissertation has been one of the most significant academic challenges I have ever faced. This study would hardly complete without the kind help and ever available support from my supervisor, my colleagues at the Institute of Water Resource Management, Hydrology and Agricultural Hydraulic Engineering, Leibniz Hannover University, my friends and my family. I own them my deepest gratitude:

In particular, I would like to express my utmost gratitude to Prof. Uwe Haberlandt for offering me the opportunity to conduct my research under his supervision and guidance. He has set a good example and showed me what a real scientist should be with his wisdom and the pursuit of high standards. Besides, he gives me a lot of useful and helpful advices to enrich my understanding of this research and it has always been enjoyable to discuss with him.

Dr. Makus Wallner and Hannes Müller are gratefully acknowledged. They offered excellent work in helping me to understand hydrological modeling and disaggregation rainfall model and for using the data they complied. The staff and technicians of the institute are thanked for their sincere cooperation and support to make a happy life here. Special thanks go to Christian Berndt, Ehsan Rabiei, Anne Fangmann, Sven van der Heijden and Ana Callau Poduje for their support and friendship.

I sincerely thank my committee Prof. Uwe Haberlandt, Prof. Günter Meon and Prof. Thomas Graf for their instructions and diligence in reviewing my thesis.

The financial support in the form a scholarship grant from the Chinese Scholarship Council is gratefully acknowledged.

I would like to thank my parents and my sister in Changde, half way across the globe, who have been supporting me unconditionally throughout my studies in Germany.

Finally, I wish to thank my friends in Hannover, for their encouragement and invaluable support to make my life easier here.

Declaration

I hereby explicitly declare that:

1. I know the Regulations for doctoral candidates at the Faculty of Civil Engineering and Geodetic Science and have met all the requirements.
2. I have completed the thesis independently and I have used no other sources excepts as noted by citations.
3. I did not pay any monetary benefits with regards to the content of my thesis.
4. The present dissertation has not been used as a M.Sc. or similar thesis before, or published before.
5. The same or substantially similar work has not been submitted at any other university or another academic institution.
6. I agree that my thesis can be evaluated regarding the compliance with scientific standards also using electronic data analysis.

All data, table, figures and text citations which have been reproduced from my own research papers, have been explicitly acknowledged as such:

In chapter 3, the content (text & figures) of sections 3.2, 3.3 and 3.4 are mostly from my first published paper (Hydrology Research, Ding, J., U. Haberlandt and J. Dietrich, Estimation of the instantaneous peak flow from maximum daily flow: a comparison of three methods. DOI: 10.2166/nh.2014.085). The permission to reproduce the above material has been granted from copyright holders, IWA publishing.

In chapter 4, the content of sections 4.2, 4.3 and 4.4 are mostly from my second submitted paper (Hydrological Processes, Ding, J., M. Wallner, H. Müller and U. Haberlandt, application of the HBV hydrological model in estimation of instantaneous peak flow from maximum mean daily flow)

Hannover, 8th June

Jie Ding

Kurzfassung

Daten der maximalen Scheitelabflüsse (Instantaneous peak flows IPF) sind die Grundlage für die Bemessung von Wasserbauwerken und für die Hochwasserstatistik. Die langen Abflussdatensätze, welche durch hydrologische Messanlagen aufgezeichnet werden, enthalten jedoch häufig nur mittlere tägliche Abflüsse, welche nur von beschränktem Wert für die Bemessung in kleinen Einzugsgebieten sind.
Prognosen und Vorhersagen von IPF können durchgeführt werden durch: (i) den Aufbau einer Beziehung zwischen Scheitelabflüssen und maximalen Tagesabflüssen, welche auf einer statistischen Analyse der verfügbaren, aufgezeichneten Tagesabflussdaten basiert oder (ii) die Verwendung eines Niederschlag-Abfluss-Modells mit hochauflösenden synthetischen Niederschlagsdaten. Da die konzeptionelle Struktur der hydrologischen Modelle eine Kalibrierung der Parameter benötigt, kann eine Regionalisierung von „IPF“ in unbeobachteten Gebieten durch (iii) eine vorgegebene Übertragungsfunktion zwischen den Modellparametern und den Eigenschaften des Einzugsgebiets erreicht werden. Die Arbeit ist nach den oben genannten Zielen wie folgt aufgebaut.

Im ersten Teil werden drei verschiedene Methoden verglichen, um Scheitelabflüsse (IPF) aus dem entsprechenden Tagesmaximum des Abflusses (MDF) zu schätzen. Im ersten Ansatz wird eine einfache lineare Regression angewendet um IPF aus MDF zu berechnen unter Verwendung wahrscheinlichkeitsgewichteter Momente (PWM) und Quantilwerten. Im zweiten Verfahren ermöglicht die Verwendung von schrittweiser multipler linearer Regressionsanalyse die wichtigsten Eigenschaften des Einzugsgebiets zu identifizieren. Die resultierende Gleichung kann angewendet werden, um MPF in IPF zu übertragen. Die dritte Methode untersucht die zeitlichen Skalierungseigenschaften der Zeitreihe des jährlichen maximalen Durchflusses auf Grundlage der Hypothese der stückweisen einfachen Skalierung kombiniert mit der generalisierten Extremwertverteilung (GEV). Die Ergebnisse aus diesem Teil zeigen: (1) die Skalierungsformeln, welche aus drei 15 Minuten Stationen entwickelt wurden, können auf alle Tagesstationen übertragen werden, um die IPF abzuschätzen, (2) das Verfahren der schrittweisen multiplen linearen Regression, liefert das beste Ergebnis im Vergleich zu den beiden anderen Verfahren , (3) die lineare Einfachregression ist bei

ausreichenden Daten am einfachsten anzuwenden, während die Skalierungsmethode die effizienteste Methode im Hinblick auf die Datennutzung ist.

Im zweiten Teil der Arbeit wird der Vergleich verschiedener Strategien um Häufigkeitsverteilungen der IPF abzuleiten mit einem hydrologischen Modell untersucht. Das hydrologische Modell wird mit täglichen und stündlichen Zeitschritten betrieben. Anschließend werden die GEV-Verteilungen auf die simulierten jährlichen Serien von täglichen und stündlichen extremen Abflüssen angepasst. Die resultierenden MDF Quantile der täglichen Simulationen werden unter Verwendung eines multiplen Regressionsmodells in IPF Quantile transferiert, sodass ein direkter Vergleich mit den stündlich simulierten Quantilen möglich ist. Solange keine Klimaaufzeichnungen mit hoher zeitlicher Auflösung zur Verfügung stehen, erfordern die stündlichen Simulationen eine Disaggregierung der Tagesniederschlagsmenge. Zusätzlich werden zwei Kalibrierungsstrategien angewandt: (a) Kalibrierung auf Abflussstatistiken; (b) Kalibrierung auf Ganglinien. Die Ergebnisse aus diesem Teil zeigen, dass: (1) das multiple Regressionsmodell in der Lage ist die IPFs mit den simulierten MDFs vorherzusagen; (2) sowohl die tägliche Simulation mit nachfolgender Korrektur der Abflüsse als auch die stündliche Simulation mit vorheriger Disaggregation des Niederschlags eine vernünftige Schätzung des IPFs ermöglichen, (3) die besten Ergebnisse mit Hilfe von disaggregierten Niederschlägen für die stündliche Modellierung mit einer Kalibrierung auf Abflussstatistiken erzielt werden kann, (4) wenn die IPF Beobachtungen nicht ausreichen um das hydrologische Modell anhand von Abflussstatistiken zu kalibrieren, die Korrektur von MDFs über die multiple Regression eine gute Alternative darstellt um die IPFs zu schätzen.

Im dritten Teil, wird die Abschätzung des Scheitelabflusses aus Tageshöchstwerten mit regionalisierten Parametern untersucht. Das hydrologische Modell wird anhand von täglichen Abflussstatistiken kalibriert und die Parameter werden unter Verwendung einer Übertragungsfunktion den Einzugsgebietseigenschaften zugeordnet. Es erfolgt eine simultane Modellkalibrierung für alle betrachteten Teileinzugsgebiete mit Hilfe der entsprechenden Gebietseigenschaften . Anschließend erfolgt eine Nachkorrektur der simulierten MDFs unter

Verwendung des multiplen Regressionsmodells . Die Ergebnisse dieses Teils zeigen: (1) die regionalisierten Parameter erhöhen den Schätzfehler der IPFs, während die multiple Regression in der Lage ist, diesen Fehler zu reduzieren. ; (2) zukünftige Untersuchungen zur Klassifizierung von Einzugsgebieten ist erforderlich um die Schätzfehler zu reduzieren.

Alle diese drei verschiedenen Untersuchungen wurden für das Aller-Leine Einzugsgebiet, Deutschland, durchgeführt. Der erste Teil der Forschung berücksichtigt 50 Pegel in diesem Bereich und die restlichen beiden Teile jeweils 18 Teileinzugsgebiete.

Schlagworte: der maximalen Scheitelabflüsse (IPF); Tagesmaximum des Abflusses (MDF); Aller-Leine Einzugsgebiet, Deutschland

Abstract

Instantaneous peak flow (IPF) data are the foundation of the design of hydraulic structures and flood frequency analysis. However, the long discharge records published by hydrological agencies contain usually only average daily flows which are of little value for design in small catchments. Prognoses and forecasts of IPFs can be carried out by: (i) building the relationship between instantaneous peak flow and maximum daily flow regarding the flood frequency analysis based on available flow data, (ii) operating the rainfall-runoff models using synthetic high resolution precipitation data, such as 1h as input. Since the conceptual structure of hydrological models needs a parameter calibration procedure, estimation of IPFs in ungauged areas can be derived by (iii) a predefined transfer functions between model parameters and catchment descriptors. According to the above three targets this thesis therefore is organized as follows.

In the first part, three different methods are compared to estimate the instantaneous peak flow (IPF) from the corresponding maximum daily flow (MDF). In the first approach, simple linear regression is applied to calculate IPF from MDF values using probability weighted moments (PWM) and quantile values. In the second method, the use of stepwise multiple linear regression analysis allows to identify the most important catchment descriptors of the study basin. The resulting equation can be applied to transfer MDF into IPF. With the third method, the temporal scaling properties of annual maximum flow series are investigated based on the hypothesis of piece wise simple scaling combined with the generalized extreme value (GEV) distribution. The results from this part show: (1) the scaling formulas developed from three 15_minute stations can be transferred to all daily stations to estimate the IPF, (2) the method based on stepwise multiple linear regression gives the best results compared with the other two methods, (3) the simple regression method is the easiest to apply given sufficient peak flow data, while the scaling method is the most efficient method with regard to data use.

In the second part, comparison of different strategies to derive frequency distributions of IPFs using the hydrologic model is investigated. The model is operated on a daily and an hourly time step. Subsequently, GEV distributions are fitted to the simulated annual series of daily

and hourly extreme flows. The resulting MDF quantils from daily simulations are transferred into IPF quantiles using a multiple regression model which enables a direct comparison with the simulated hourly quantiles. As long climate records with a high temporal resolution are not available, the hourly simulations require a disaggregation of the daily rainfall. Additionally, two calibrations strategies are applied: (a) calibration on flow statistics; (b) calibration on hydrographs. The results from this part show that: (1) the multiple regression model is capable to predict IPFs with the simulated MDFs; (2) both daily simulations with post-correction of flows and hourly simulations with pre-processing of precipitation enable a reasonable estimation of IPFs; (3) the best results are achieved using disaggregated rainfall for hourly modeling with calibration on flow statistics; (4) if the IPF observations are not sufficient for model calibration on flow statistics, the transfer of MDFs via multiple regressions is good alternative to estimate IPFs.

In the third part, estimation of the instantaneous peak flow from maximum daily flow using regionalized parameters is investigated. The model is calibrated on flow statistics on a daily time step and its parameter values are initially associated with the catchment descriptors using a transfer function. A simultaneous model calibration is performed for a number of sub catchments with these contrasting catchment characteristics. Post-correcting the simulated MDFs using multiple regression model is also involved. The results of this part show: (1) the regionalized parameters increase the estimation error of IPF while multiple regression is capable to deduce this error efficiently; (2) further work about classification may be needed to reduce the estimation error.

All these three different tests are carried out in Aller-Leine catchment, Germany. The first part of research takes into account 50 flow stations among this area and the rest two tests are investigated in 18 sub catchments of this area.

Keywords: instantaneous peak flow (IPF); maximum daily flow (MDF); Aller-Leine catchment, Germany

Table of Contents

Lists of Figures

Lists of tables

Symbols and abbreviations

symbol	Definition	Dimention
GEV	Generalized extreme value distribution	
PWM	Probability weighted moments	
LM	Linear moments	
HBV	Hydrologiska Byråns Vattenbalansavdelning	
DEM	Digital Elevation Model	
IPF	Instantaneous peak flow	$[m^3/s]$
MDF	Maximum daily flow	$[m^3/s]$
P	precipitation	[mm]
ET	Evapotranspiration	[mm]
Q	Runoff	$[m^3/s]$
HQ	Quantiles of runoff	$[m^3/s]$
SD	Snow depth storage	[mm]
SM	Soil moisture	[mm]
UZ	Upper zone	[mm]
wsmf	Wet snow melt factor	$[mm^{-1}]$
LZ	Lower zone	[mm]
dd	Degree day factor	$[mm°C^{-1}d^{-1}]$
tt	Threshold temperature	[°C]
fc	Field capacity	[mm]
Kc	Crop coefficient	[-]
lp	Limit potential evaporation	[-]
β	Exponent parameter	[-]
hl	A threshold parameter in upper zone	[mm]
Q_0	Surface runoff	$[m^3/s]$
Q_1	Interflow	$[m^3/s]$
Q_{perc}	Percolation to the lower zone	$[m^3/s]$

Q_2	Base flow	$[m^3/s]$
K_0	Recession coefficient of surface flow	[d]
K_1	Recession coefficient of interflow	[d]
K_{perc}	Recession coefficient of percolation	[d]
K_2	Recession coefficient of base flow	[d]
ms	Triangular unit hydrogaph	$[\Delta t^{-1}]$
mk	Muskingum storage coefficient	[h]
mx	Muskingum weighting coefficient	[-]

Chapter 1

1 Introduction

1.1 Flood risk and flood consequences

Floods are one of the most damaging natural hazards in the world while the evolution of human society always depended on the dynamics of water. The catastrophic floods occurred during the last decades caused several problems to our societies including the loss of human lives, damage on the goods as well as all kinds of environmental issues. The knowledge of flood risk and its consequences is essential for the development of flood management, flood control, improvement of resilience and risk reduction. Better understanding on this extreme phenomenon is also essential for flood forecasting which is carried out to reduce the damage and help to prepare the adequate alternatives.

Flood risk is considered as the combination of a vulnerable system susceptible to suffer loss, the hazardous phenomenon of flooding and probability. Basic knowledge for apprehending the flood risk therefore concerns the frequency and intensity of floods, human sensitivity to floods and their susceptibility to suffer damage, the exposition of humans and assets to flooding. Since it brings variable aspects together, such as economic, human, natural and environmental, the consequences of floods can be distinguished as negative and positive types. The floods that have adverse impacts on the natural system, social system or the building environment are referred as damaging floods, i.e. the catastrophes occurred in the Yellow River floodplain in China and the Europe (Merz et al. 2010); In August 2002, scenes of devastated villages, cities and landscapes were flashed around the world, with tragic loss of life and massive economic damage estimated in billions of Euros (see Table 1.1). On the other hand, the floods are potential to generate benefits since the effects of flooding on the environment can differ between the assessment of the impacts of flooding and ecological communities, e.g. the cases of Mississippi delta, improving the agricultural lands and keeping the elevation above sea level, and the flood in “1’ Aude” in France 1999 improving solidarity between towns (D4E 2007; Montz and Tobin 1997).

It is highly probable that the mixture of climate change and human interference is responsible for human suffering and the losses across the world. Responding to the people’s demand and the enormous damage, different actions and management are conducted for managing the risks of floods. Examples are the Act on Flood Protection, the recently published directive of the European Commission on the sustainable flood protection and the 5-point program of the

German Government (Damm 2010). Technical protection measures (dams, diversion canals, river and coastal defences) are taking place as well. To understand further about flood risk, the following subsections are presented to bring some essential concepts about floods.

Table 1.1 Economic damage of the most severe flood events in Germany since 1990

Rank	Month/Year	Rivers	Damage [m.€]	Insured damage [m.€]
1	08/2002	Elbe, Danube	11600	1800
2	12/1993	Rhine	530	160
3	05/1999	Danube, Rhine	430	75
4	07/1997	Oder	330	32
5	01/1995	Rhine	235	95

Source: (Damm 2010)

What is a flood?

A flood is characterized as an overflow of water that submerges land which is usually dry. The European Union Floods Directive defines a flood as a covering by water of land not normally covered by water. Several factors, such as extreme climate conditions, concentration of water in riverbeds can promote a flood event. Some floods develop quite fast just a few minutes and may without visible signs of rain while others can develop slowly. Additionally, floods can be very large which affects the whole river basins. They can also be local, only impacting a community or neighborhood. A flood situation can be described according to its causes (overbank flooding, engineering issues), geography (ice jam flooding) or speed (flash floods).

Flood effects and flood forecasting

Floods generate several effects in a direct or indirect way and they can be defined as all objective changes on human, economical systems and natural. Nowadays, flooding has been considered as the first unfavorable natural hazard in the world since their benefits almost certainly outweigh their negative aspects. The primary effects of flooding include loss of life, damage to social system and built environment. Flood waters typically inundate farm land, cities, making the transport unworkable and preventing crops from being planted or harvested. Meanwhile, there are some psychological damages to people who suffered the loss of property and serious injuries especially. However, for some smaller floods or in particular more frequent ones can also bring many benefits, such as increasing nutrients in soils, recharging ground water, providing water in arid and semi-arid regions. Therefore, the

flooding phenomenon is a natural process which is considered as a risk if the society is potentially affected by the floods. The effects of floods are defined as all objective changes generate by floods on human, natural and economical systems. The following scheme (Figure 1.1) represents these concepts.

Flood forecasting is a complex process of estimating flow rates and water levels for periods ranging from a few hours to days ahead, especially the peak flow rate, by using the real-time precipitation and stream flow observations and rainfall-runoff models to forecast the possible flood events across the target watershed.(Messner et al. 2007). The main goal of flood forecasting is to anticipate floods before occurring which allows for people to be warned and precautions to be taken. For example, emergency services can make provisions to prepare enough resources available in advance to respond to emergencies as they occur, farmers can also remove animals from the dangerous flood areas if needed. To make accurate flood forecast, it is best to have long time series of historical flow data. In addition, the real time knowledge about volumetric capacity in target basin, such as ground water levels, degree of saturation and spare capacity in reservoirs are also useful in order to make more accurate flood forecasts. For more details, refer to (Saddagh and Abedini 2012; Wu et al. 2013; Yu and Tseng 1996)

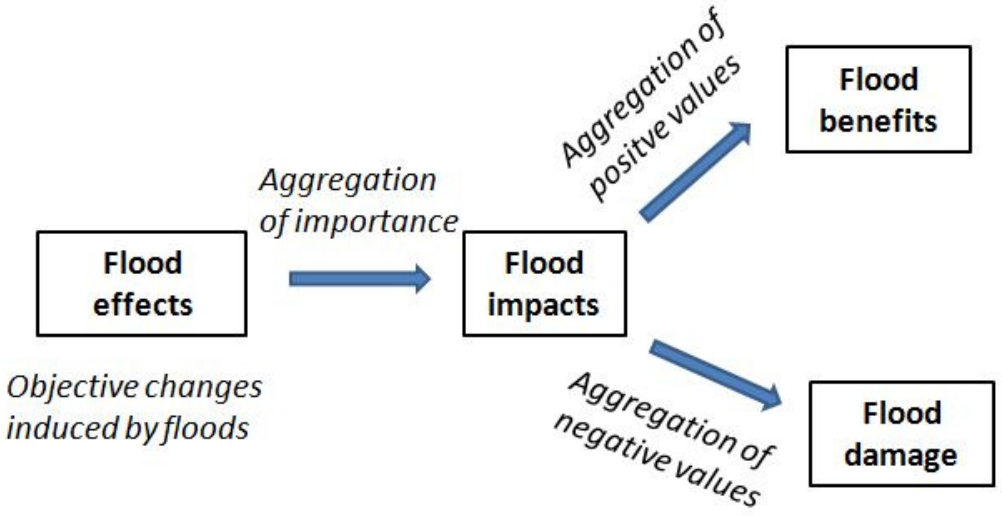

Figure 1.1: Effects, impacts and damage linked to floods (edited after Eleutério 2012)

Flood control

Flood control refers to all techniques or practices used to reduce or prevent the detrimental effects of flood waters with dams, artificial channels, etc. e.g. The largest and most elaborate flood defenses are found in the Netherlands, where they are called 'Delta Works' with the Oosterschelde dam as its crowning achievement. In China, some rural areas are used as flood diversion areas to be deliberately flooded in emergencies in order to protect cities. Basically, two alternatives are employed to reduce damage induced by floods: (1) to reduce the potential damage by the construction of infrastructure, e.g. dams, retention basins, rectification and deviation of waters. These measures imply interventions on the physical world, (2) to reduce the vulnerability of assets exposed hazards by focusing on the behavior of individuals, in this context, the non-structural measures, such as evacuation plans, education and rescue organization, are used to modify the behavior of the individuals to become able to reduce their own vulnerability. The structural measures on the infrastructures and buildings can be adopted to reduce their susceptibility to suffer damage. The control of urbanization is one of important strategies for flood control in a long term perspective. (Bouwer et al. 2011; Colin et al. 2011)

Due to global climate change, meteorological and hydrological variables and patterns have been changing. Several regional models have concluded that there are dramatic impacts of the rising temperature on rainfall and runoff generation process. It is necessary therefore to take some measures and actions to deduce the flood risks, although with some unavoidable uncertainties from these regional models.

1.2 Estimation of design flood peak

Estimation of design flood peak provides an effective way of design of hydraulic structures, water resources planning and flood risk management although reliable estimation of flood frequency in terms of peak flows is still a challenge in hydrology (Cameron et al. 1999). Flood frequency estimation is concerned with quantification of rarity. The main objective of it is to estimate how large a flood will be for a particular probability of exceedance, or how often a specific flood event will occur. For the preservation of human life and property, it is quite necessary in the design, planning and operation of hydraulic structures, such as dam spillways, bridges and culverts (Pegram and Parak 2004; Reis Jr and Stedinger 2005).

Most of the reported design methods are based on frequency analysis assuming stationary conditions in a certain time window representing current and future hydrological conditions. The peak flows are then treated to be random and independent variables. However, in reality

there are nonstationarities in probability distribution of peak flows because of land use changes, climate changes and human disturbance on flow regimes by damming and other hydraulic constructions (Bradley and Potter 1992; Gebregiorgis and Hossain 2012; Sivapalan and Samuel 2009; Villarini et al. 2009a; Villarini et al. 2009b). Despite the controversial issue of stationarity of annual peak flow series, statistical flood frequency analysis is still commonly applied for the design of hydraulic structures and flood management given reasonable assumption of stationarity (Gebregiorgis and Hossain 2012; Villarini et al. 2009a; Xiong and Guo 2004).

Several techniques for design flood peak estimation have been developed in many regions. A direct estimate of the flood peak for a given exceedance probability can be obtained by frequency analysis of observed flood peaks. Since rainfall records are generally longer and less variable over time than the flow records, rainfall runoff modeling based techniques are often used for the determination of the design flood peak. If the observed flow data are not available at the site of interest, the event based methods or some alternate regionalization approaches have to be used. USACE (1994) summarizes the use of statistical estimation of design flood based on the observations, regionalization approaches for ungauged areas and rainfall-runoff modeling based methods. The decision tree for the selection of design flood peak estimation method is presented in Figure 1.2.

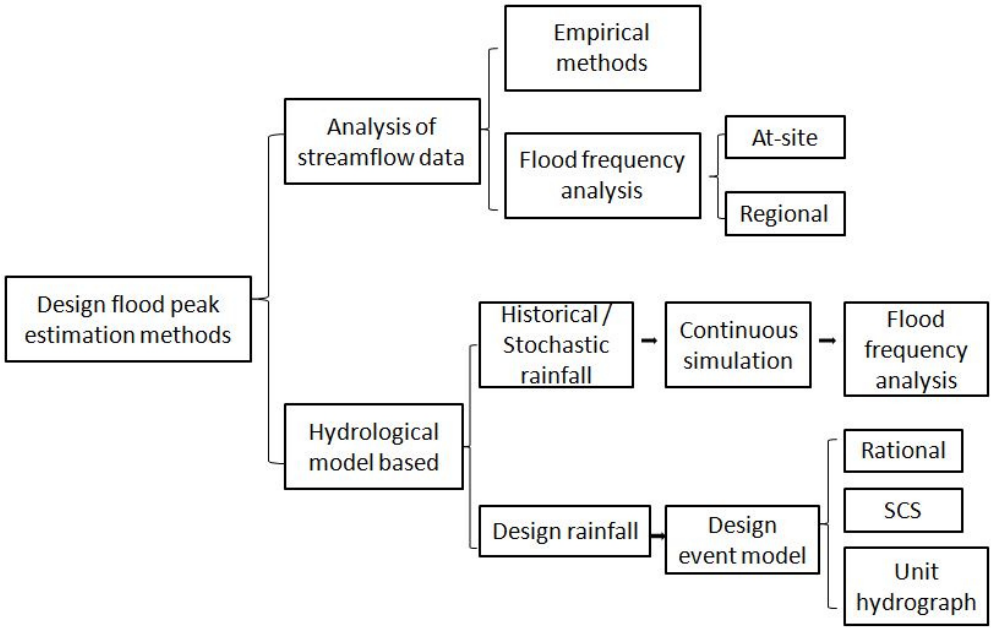

Figure 1.2: Approaches to design flood peak estimation

1.2.1 Statistical approaches

The methods based on the analysis of observed flood samples which are probabilistic by nature are hence suitable for estimating design flood peaks. They can be summarized as flood frequency analysis method at sites and regional flood frequency analysis for catchment with no data.

Flood frequency analysis (FFA) at a gauging site

Design flood peak estimation using FFA at sites method requires the frequency analysis of observed instantaneous peak flow data, from a flow gauge, that are adequate in both quality and length. A direct estimation of the design flood peak for a given exceedance can then be obtained via frequency analysis. The following assumptions are generally made for the peak flow series data:

- The collected peak flow data are supposed to be independent from each other. Thus, in a random process, the value of the variant does not depend on previous or next values.

- It is assumed that the sample is representative of the population and the selected annual peak flows conform to a stationary and identically distributed random process.

There are two procedures included for the probabilistic analysis (Alexander 2001):

1. summarise the observed flood peak data.
2. select the appropriate probability distribution while estimating the parameters

The summarization of the observed flood peak data includes ranking either the annual maximum series (AMS) or partial duration series (PDS) in a descending order of magnitude and assigning an exceedance probability to the plotted values subsequently. The AMS are defined as the highest instantaneous peak flow value in each hydrological year for the whole record period (Chadwick et al. 2004; Schulze 1995). The PDS which has been denoted to be advantageous for the flood statistics to represent more than one peak flow per year, is also referred to as an peak over threshold (POT) series. In the selection procedure of PDS, it includes all events above some arbitrary threshold values and entails that some of the annual maximum peaks may be exclude in the series using this threshold exceedance value (Kite 1988). Several hydrologists have discussed previously the use of the AMS and PDS in their studies. According to Madsen et al. (1997), PDS is more suitable for analyzing flood frequency when secondary flood peak values are important and also for short data records. Additionally, the PDS design estimates can be more accurate than the AMS by including the extreme cases which may be exclude in the AMS for not be the largest event in a specific year (Stedinger et al. 1993b). On the other hand, Adamson (1981) pointed out that, the AMS according to its easy usage instead of theoretical efficiency in characterizing the flood peak series are more favorable than the PDS. Therefore, the AMS seems to be much more applied in hydrologic studies than PDS, since the extraction of peaks to include in the AMS is a straightforward task (Madsen et al. 1997).

Numerous plotting position formulas have been suggested to assign an exceedance probability to flood peaks. Most have the general formula:

$$P = \frac{i - a}{n + 1 - 2a} \tag{1.1}$$

where P is exceedance probability; i is the ranked number of peak flows in descending order, varies from a to 0.5 and n is the total number of observations.

Five of the most commonly-used formulas are shown in Table 1.3:

Table 1.2 Plotting position formulas included in the theoretical probability distributions

Reference	a	Formula
Weibull(1939)	0	i/(n+1)
Blom(1958)	0.375	(i-0.375)/(n+0.25)
Cunnance(1978)	0.4	(i-0.4)/(n+0.2)
Gringorten(1963)	0.44	(i-0.44)/(n+0.12)
Hazen (1914)	0.5	(i-0.5)/n

The Weibull formula has long been used as the standard reference for determining flood frequencies and for plotting flow duration and flood frequency curves in the United States (Langbein 1960). The Blom formula is preferred in probability plots for comparing data quantiles to those of anormal distribution. The advantages of Cunance formula are: firstly, it is acceptable for normal probability plots, which is very close to Blom; secondly, this formula has been proved by Cunnane that it outperforms Weibull when calculating exceedance probabilities. Chambers et al. (1983) have applied the Hazen formula for comparing two or more data sets using Quantile-Quantile plots.

Parameters estimation methods available for fitting theoretical probability distribution to observed flood peaks include: Maximum likelihood (ML), Method of Least-Squares (MLS), Method of Moments (MM), Probability Weighted Moments (PWM) and Linear Moments (LM) (Chow et al. 1988; Kite 1988; Stedinger et al. 1993b; Yevjevich 1982). Estimation the parameters of a theoretical probability distribution based on a specific sample is always within limits when using all these methods (Kite 1988). LM estimators are used commonly and widely as a standard procedure by hydrologists for the purpose of screening discordant data, testing clusters for homogeneity and flood frequency analysis. They have been proved better than ML estimators in terms of variance for sample sizes and bias (Hosking 1985) and well defined for most of the different distribution functions. Besides, they are more robust against outliers than standard MM estimators. Compared with the equivalent PWMs (Hosking 1994), LM estimators are more convenient because they are more easily interpretable as measures of distributional shape (Stedinger et al. 1993a). However, Alexander (2001) criticizes LM are too robust against outliers since both low and high outliers are significant characteristics of flood peak maxima. The suppression of the effect of outliers cold result in unrealistic estimates of longer return periods values. Thus, further investigation is needed when adopt these methods.

Based on the limited available information, an appropriate theoretical probability distribution fitted to the observations allows fitting to a frequency with some systematic extrapolation procedures and also provides a smoothed and compact way to present the frequency distribution of the population (Smithers and Schulze 2000a). Many statistical distributions therefore have been investigated in hydrology for different countries. Annual flood peak series are found to be often skewed, which leads to the development of many skewed distributions, such as Generalized Extreme Value (GEV) distribution, Gumbel (EV1), the Log Pearson Type III (LP3) and 3-parameter Lognormal (LN3) (Pilon and Harvey 1994). In 1984, A worldwide survey involving 55 agencies from 28 countries reveals that, in spite of recent popularity of GEV distribution in flood frequency analysis, there is only one country employing it in comparison with the other most common distributions (such as: EV1, two parameter lognormal (LN2), P3 and LP3). (Cunnane 1988).

Regional flood frequency analysis (RFFA)

Given the facts that frequently no or inadequate observed flood peak data at flow-gauging sites are available and the sampling errors are correspondingly large, the use of regional flood frequency analysis becomes necessary. The index flood method is one of the first approaches to regional flood estimation (see Dalrymple (1960)). It consists of two major parts. The first is to identify the homogeneous regions which can provide a basis for information transfer to the target region. Different classification techniques and similarity measures are utilized in practice. The second part is to perform the regional estimation methods estimating the flood frequency at the target region based on data from the regions identified in the first part of analysis. Thus, an appropriate frequency distribution for the selected regions has to be included here. In essence, the assumption in regional flood frequency analysis is that in a homogeneous region, the probabilistic behaviors of extreme flows are similar for all different sites, therefore, the flow data from various single stations can be combined to produce a single regional flood frequency curve after justifiable scaling techniques. This determined regional frequency curve is intended to be the result for any site (Smithers and Schulze 2003). More details about it can be found in (Cunnane 1988; Dawdy et al. 2012; GREHYS 1996).

The advantages of RFFA for design flood peak estimation are evident from the literature. For example, Potter (1987) expressed a regional method will be more efficient than the application of an at-site analysis in nearly all practical situations. Cordery and Pilgrim (2000) concluded that a well conducted regional frequency analysis will yield quantile estimates accurate enough to be useful in improving flood prediction and many practical applications. This leads to the adoption of a RFFA approach as the recommended approach for design flood peak estimation by some countries, such as UK and Australia. However, one should be

careful to ensure that such an approach is not applied outside of the range of observations used to develop the method or outside of the region where the method was derived.

1.2.2 Derived flood frequency analysis (DFFA) approach

Rainfall-runoff models are used for design flood peak estimation to simulate flood events or continuous time series of runoff for which the quantiles of a given recurrence can be determined. These methods that seek to integrate rainfall-runoff modeling and statistical frequency analysis are referred to as derived flood frequency analysis (DFFA) approaches (Eagleson 1972). The advantages of using rainfall-runoff models for design flood peak estimation can be summarized as follows (Lamb 2006):

1. Compared with the available flow data, the rainfall records at most of the sites are generally longer and with better quality for analysis and the hydrological models can be driven by also long synthetic rainfall data.
2. The changing catchment conditions, measurement errors or inconsistencies in the data can render non-stationary flow records which are not suitable for direct frequency analysis.
3. Physical characteristics of a catchment can be incorporated into a rainfall-runoff model. In addition, it can also model the different land use and climate situations in historical, current or future conditions within a catchment.

Design event models

An established complement to statistical flood frequency analysis is simulating flows for discrete design storms with event based procedures. The widespread use of design event models, such as Unit Hydrograph, Rational and Soil Conservation Services (SCS), is due to their ability to estimate the individual design flood peaks in a robust and simple manner. They lump the complicated, heterogeneous catchment processes into a single process prior to the occurrence of a flood event. Similar to any conceptual rainfall-runoff model, the structures of design event models also combine loss and attenuation modules.

This event based methods can make good use of the available rainfall data, which itself brings potential advantages in catchments where longer rainfall records exist or where rain gauge network in more extensive than the flow gauge network. One of the limitations of design event based models in the assumption that, the frequency of input rainfall and the estimated runoff is equal, while being influenced by model parameters and catchment representative inputs (Viglione et al. 2009). Namely, if the catchment is at an ‘average’ condition, the T-year recurrence interval rainfall will generate the T-year flood peak. This assumption takes into account the probabilistic natural of rainfall but ignores the probabilistic behavior of other

inputs (e.g. antecedent soil moisture condition) and parameters. Thus, it is likely to introduce significant bias in the estimation of design flood peak and the validity of this assumption is crucial to the accuracy of this approach.

Continuous simulation methods

In order to overcome the limitations associated with event based design models, continuous simulation is proposed to generate extended time series of flow data, from which it is easy to extract different features of interest, such as peak flows, measure of flow duration and volumes above a threshold. There are three elements included in the continuous simulation methods:

- A series of climate data, derived from observations or a stochastic model as input
- Simulation the catchment processes with a model
- The extraction of important flood features from the simulated flow time series data.

In contrast to the event based design models, these continuous simulations have the advantage that no assumptions on the return period of the design rainfall, its intensity and duration and the antecedent soil moisture have to be made (Boughton and Droop 2003; Cameron et al. 1999). Any rainfall-runoff models could be used, ranging from a black box transfer function approach to a distributed, detailed physically based model. It can provide a complete hydrograph and continuous simulation of antecedent moisture conditions.

Rainfall inputs are clearly of paramount importance for model simulation. One of the motivations for continuous simulation is that rainfall data can often give more information than flow data since the rain gauge networks are denser, longer and more extensive established. In some cases, there may be an interest in simulating flows directly from the observed rainfall when the flow records are not good enough to undertake the frequency analysis. In addition, if the rainfall records are too short to drive the length of simulation needed for sampling floods, the continuous simulation could still provide a way of estimation the design flood peak due to the currently increasing computational power coupling with long stochastically generated rainfall series. A long series of artificial discharge data can be used for flood frequency estimation subsequently (Blazkova and Beven 2002; Faulkner and Wass 2005; Sivapalan et al. 2005).

1.3 Motivation, objectives and outlines of the thesis

Motivation

Over the last few decades, enormous importance and attention have been given on flood management and hydraulic engineering projects. In Hannover, Germany, Aller-Leine river is an important source of irrigation, but the increasing flooding along Aller led to heavy losses for agriculture in this region.

The severity of floods is often poorly captured using conventional daily flow gauge networks which are not sufficient to fully describe the temporal characteristics of flood events and may increase the risk of failure due to an underestimation of design floods (Pilon 2004). In fact, the bad understanding of this phenomenon is due to peak discharges are unknown in the catchments of concern, or the length of the records is too short for a flood frequency analysis. However, the design of hydraulic structures often depends on the instantaneous peak flows as the maximum daily values are always smaller than the corresponding instantaneous peak flows, using the daily data to estimate the design flood flow may cause a significant under estimation. in particular, there can be some serious stream flow fluctuations within hours or even minutes in some small basins (Fill and Steiner 2003).

Figure 1.3 shows the difference of quantile value (T=100 years) of IPF and MDF for 56 flow gauges in Aller-Leine catchment, where the relative error is defined as:

$$\mathrm{Re}\,lative\ error = \frac{HQ_{IPF} - HQ_{MDF}}{HQ_{IPF}} \cdot 100\% \tag{1.2}$$

where the HQ_{IPF} and HQ_{MDF} are the 100- year quantile values for peak and daily series respectively.

It can be seen that the difference between the IPF and MDF is decreasing with the basin area while for the some small regions (Area<500km^2) the relative error can reach over 50%. Besides, most of the regions of interest are not large enough (Area<1000km^2) to ignore the estimation differences from MDF. Thus, investigations into the link between the IPF and MDF are needed to derive the IPF from the available MDF which can further extend our knowledge for flood risk management.

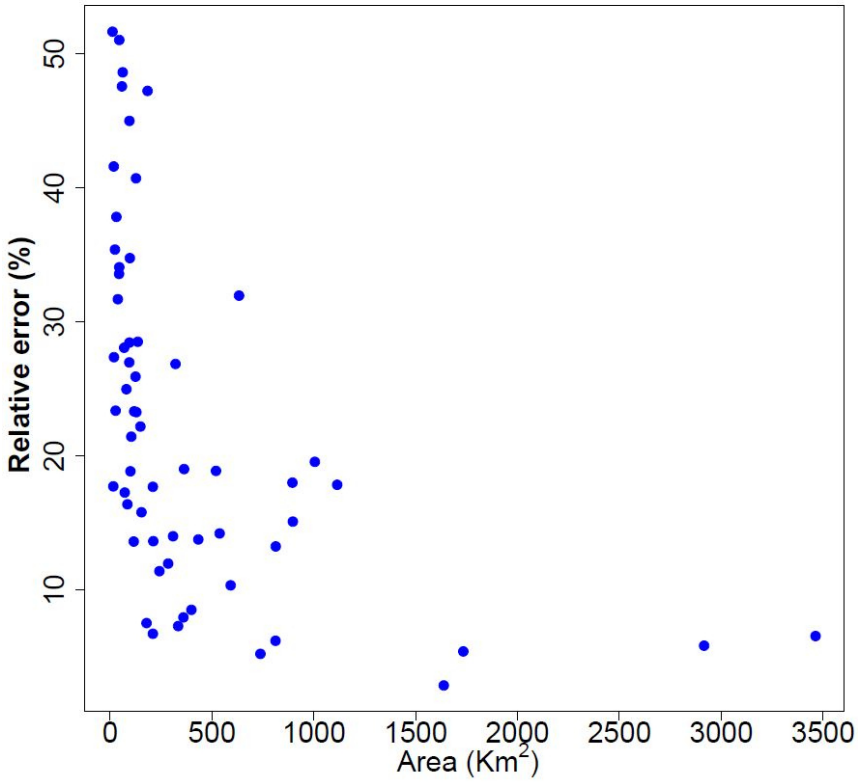

Figure 1.3: The difference of IPF and MDF in Aller-Leine catchment

Concerning the impact of change in land use, climate and management on extreme runoffs, the available MDF data may not be trusted while the assessment of the safety of existing infrastructures is needed. As a result, estimation of the design flood peak requires more robust and reliable approaches. With the help of hydrological models, stochastic rainfall models and flood frequency analysis techniques, there are probabilities that the design flood peak could be estimated by taking into account the dynamic changes in the catchments.

Conceptual models which provide a simplified representation of key hydrological processes using a perceived system, on the other hand, are well-known for their moderate data requirement. This deficiency cause problems when dealing with ungauged basins since the model parameters have to be obtained through calibration. Due to the fact that the hydrological models only perform well with calibration based on the historical hydrological data, the conceptual basis of these models will reduce their ability to deal with climate/land use changes taking place in most regions. In a broad and practical sense, estimation of design flood peak based on the simulated extremes requires regionalization methods which relate easily measured watershed characteristics to hydrological model parameters. This may enable not only the predictions of ugagued sites but also the sites within the emerging context of climate change.

Objectives and procedures

The main objectives of this frequency analysis study are:

- To determine suitable methods of finding the instantaneous peak flow and maximum daily flow relationship, also called IPF-MDF relationship for Aller-Leine catchment, Germany;

- To compare two different strategies to derive frequency distribution of IPFs with a hydrologic model, namely, calibration of the model on daily step with post correction of simulated MDFs (post-correction) and calibration of the model on hourly step with disaggregated daily rainfall as input (pre-procession);

- To present the application of parameter regionalization in estimation of IPFs from simulated MDFs in ungauged catchments.

A preliminary step in building the IPF-MDF relationship is based on the annual maximum statistical models. This requires knowledge of the flood peak characteristics of a specific region including examination of probability plots, descriptive statistics, examination of suitability of candidate distribution and seasonal analysis. The obtained information can further lead to the identification of appropriate probability distribution for describing the flood situation in the target region. The goodness of fit tests such as Chi-square ($\chi 2$), Kolmogorov-Smirnov test and $n\omega 2$ test, are often used to examine the suitability of candidate distributions. In this procedure, the assumed parent distribution will be tested to check if it is capable to produce random variables with the same statistical characteristics as the observed sample series. The annual peak and daily extremes are assumed to have an unique probability distribution throughout the whole Aller-Leine catchment.

The simple regression method provides an easy and simple way to relate the IPFs with MDFs:

$$HQ_{IPF} = a \cdot HQ_{MDF} \tag{1.3}$$

$$PWM_{IPF} = b \cdot PWM_{MDF} \tag{1.4}$$

where HQ is the quantiles of IPF and MDF data series; PWM_{IPF} and PWM_{MDF} are the probability weighted moments calibrated from IPF and MDF data series respectively. a, b are the regression coefficients that can be derived by the leave one out cross validation method. In the coefficients determination process, one station will be selected randomly while the HQ_{IPF}

and $HQ_{MDF,}$ or PWM_{IPF} and PWM_{MDF} values from the remaining flow stations are regressed linearly.

Based on the previous studies, multiple linear regression analysis is employed to describe the IPF as a function of MDF and catchment properties. It is important therefore to know which properties should be selected as the explanatory variables for the final regression function. The effective identification of the explanatory variables is governed by two selection analysis. A descriptive statistical analysis is used to give a perspective about the relationship between the flow and the candidate catchment properties. A stepwise regression analysis is then to eliminate the redundant selected variables from last step and determine the final ones.

It has been observed that the scaling properties of extreme runoff series of different time scales exist. The piecewise scaling method is proposed to explore the scaling theory in runoff based on the assumption that equality holds in the probability distribution of the observed runoff rate at two different time scales. The relationship regarding the moments of IPFs and MDFs can be described as:

$$M_{IPF} = \lambda \cdot M_{MDF} \tag{1.5}$$

where λ is the scaling factor and M is the moments of any order. Hence the quantiles of IPF can be estimated by the scaled moments from observed MDF data series. A detailed validation of the scaling hypothesis is required in this context.

Given the obtained relationship between IPF and MDF from the above analysis, the objective of hydrological modeling is to contribute to the understanding of how the two different strategies used to derive IPFs quantiles and also help the decision makers to clarify ideas about choosing the proper estimation strategy conditioned on available data.
A conceptual rainfall-runoff model, HBV model has been chosen to simulate the IPFs and MDFs on both hourly and daily time steps for 18 catchments in Aller-Leine area, Germany. Two calibration schemes are performed, which are based on flow statistics and traditional hydrographs respectively. Four different aspects of the runoff statistics are included: the winter (November-April) extremes distribution, summer (May-October) extremes distribution, flow duration curve and annual extreme series. An automatic optimization procedure based on dynamically dimensioned search algorithm (DDS) algorithm is used for solving a single overall objective calibration problem. The frequency analysis of the extreme values is based on the generalized extreme value distribution (GEV) with L moments (see Hosking and Wallis (1997)). Figure 1.4 gives an overview of the workflow used in this investigation. Since there is no time step associated with the instantaneous peak flows (IPFs), the hourly peaks are assumed to be the IPFs here.

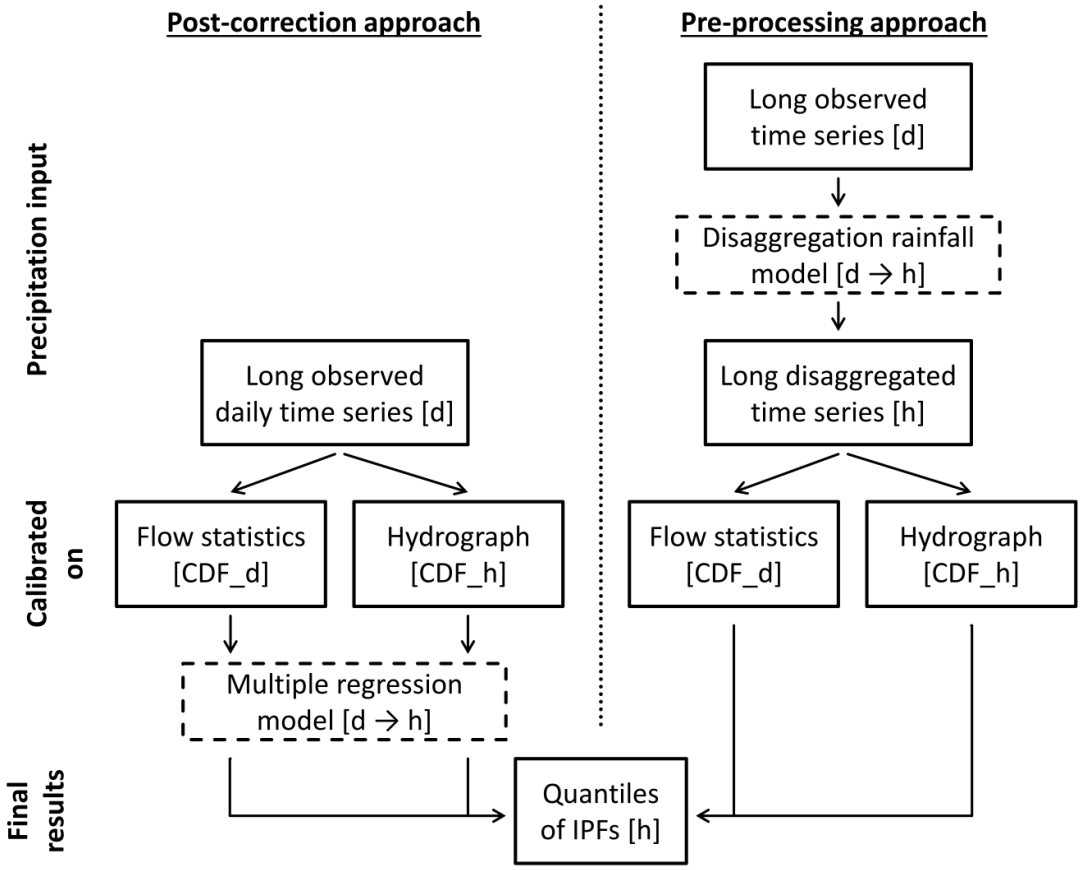

Figure 1.4: Scheme of the two approaches; the temporal resolution of the data is given in brackets.

For the post-correction approach the hydrologic model is operated at a daily time step using the two calibration strategies respectively. The quantiles from the simulated MDFs data series will then be post-corrected into IPFs by the above derived multiple regression equation. An advantage of this method is making good use of the available daily flow and climate data since they often have the longer, more extensive and better observations than the corresponding hourly ones. The pre-processing approach provides a basis for the direct simulation of IPFs using the synthetic hourly rainfall with high temporal and sufficient spatial resolution which can be generated from the long-term recorded daily rainfall by a disaggregation rainfall model.

Quantification of the IPF in ungauged areas has been an interesting topic for several hydrologists in many countries. However, there has been limited knowledge to guarantee a quantitative relationship between the simulated MDFs using regionalized parameters and the observed IPFs. In addition, the faith one can put on hydrological models in predicting the IPFs depends on the uncertainty associated with model parameters. In this part of work, the HBV model is used and calibrated to selected gauged sub catchments with contrasting

catchment characteristics from different parts of the Aller-Leine basin. The calibration is carried out to estimate the regional values of the model parameters as functions of the catchment descriptors. The obtained MDFs are then corrected into IPFs by the above mentioned multiple regression.

Outline of the thesis

Besides the current chapter, the remaining part of the thesis is structured as follows:

Chapter 2 describes the state of the art of this research which is concentrated on investigating the ideas and methods of estimating the instantaneous peak flow based on maximum daily flow. It covers some historical reviews on examination of IPF-MDF, flood frequency modeling and calibration techniques.

Chapter 3 presents three statistic approaches to estimate the IPF from the corresponding MDF based on the observed records. The comparison results of the advantages and disadvantages of these three methods can give an insight into how to choose the proper method due to the specific catchment condition.

Chapter 4 reports about the estimation of IPF from MDF using hydrologic models. This chapter gives a detailed account of two estimation strategies: post-correction and pre-processing approach. The necessary comparisons are also made between them to provide the guidelines for engineering practice in flood peak estimation.

Chapter 5 gives estimation of IPF from MDF using hydrologic models with regionalized parameters. A simultaneous model calibration is carried out for all the studied sub catchments with a predefined function between the model parameters and catchment descriptors. The simulated MDFs are then post-corrected into IPFs by the multiple regression derived in Chapter 3. It gives a new insight of estimating IPFs in catchments without flow data.

Chapter 6 provides a summary, the conclusions and the outlook of the study.

Chapter 2

2 State of the art in this research

Whoever wants to reach a distant goal take many small steps. – Helmut, Schmidt

2.1 Estimation of IPF from MDF using statistical methods

The first known study about estimating the relationship between annual instantaneous peak flow (IPF) and its corresponding maximum daily flow (MDF) is Fuller's study (Fuller 1914). He analyzed flow data from 24 river basins with drainage areas varying from 3.06 to 151,592 km^2 in the Eastern United States and developed an equation to calculate IPF from MDF as a function of the basin area. Following Fuller's method, there have been several studies investigating the relationship between the ratio of IDF and MDF and basin area. For instance, Langbein (1944) illustrated that the ratio of IPF to MDF is a function of the ratio of the daily discharge of the preceding day to the discharge of the maximum day and the ratio of the daily discharge of the succeeding day to that of the maximum day. Since this method does not permit generalized conclusions, it was further improved by Sangal (1983) and Fill and Steiner (2003). Additionally, Canuti and Moisello (1982) studied a group of basins in Tuscany to determine the probability distribution of the IDF on the basis of the MDF using the ratio of IDF and MDF as a function of its geomorphic catchment characteristics, such as mean altitude, basin magnitude, basin relief and channel slope, where the basin area does not seem to be the most important predictor.

Tanguas et al. (2008) developed a three-step procedure to find possible linear relationships of IPF—MDF in semi-arid areas of Spain. The first step is a preliminary analysis and involves categorizing basins into different groups according to the coefficient of determination (R^2) of the regressions between IPF and MDF. The second step is the identification of the most important hydrological and topographic characteristics of the watersheds that will be included in IPF-MDF regional equations by using Principal Components Analysis (PCA). The third step is the development of regional equations to calculate the peak flow based on the influence of different attributes of the studied areas. The results showed a significant improvement in comparison to the traditional method of Fuller. The influence of the catchment properties on the hydrological response is an accepted concept in hydrology, upon which many models are built (Beven et al. 1988). Muñoz (2012) developed a reliable peak flow estimation method for the design of hydraulic structures in Chile to relate instantaneous peak flow with rainfall and several other geomorphological descriptors.

As such, in this study, to effectively use the available flow data in IPF—MDF studies, there is a need to develop other potential techniques to relate instantaneous peak flow and maximum daily flow. One approach to tackle this problem is by using simple regression between observed peak and daily data regarding their PWM and quantile values. This method focuses on the average correlation performance between the IPF and MDF rather than on the empirical function within a region. As one of the key driver, an visual impression of the differences in IPF and MDF can be obtained from this direct comparison of their PWM and quantile values. Given the data series of all stations being available, the simple regression method can be easily operated.

On the other hand, the link between annual instantaneous peak flow and maximum daily flow in this study is further investigated in a more comprehensive and easier manner, compared with the former researches. It is assumed assumed that the peak discharge response of a catchment is dependent on the regional runoff mechanism and climate and is also a reflection of different watershed characteristics, such as river slope, land use, land cover and rainfall intensity. A multiple linear regression analysis is therefore performed. The selection of the most important catchment descriptors has extended the work of further constructing a functional linear relationship between IPF and MDF.

During the last decades, self computing approaches have evolved with several applications in hydrology. Dastorani et al. (2013) employed artificial neural networks (ANN) and adaptive neuro-fuzzy inference systems (ANFIS) to derive IPF from MDF. The authors compared their results with the methods of Fuller (1914), Sangal (1983) and Fill and Steiner (2003). ANFIS showed the highest accuracy of all methods. A general limitation of machine-based learning techniques is the need for training data. Thus, they need at least a short time series of IPF. In addtion, several disaggregation methods have been developed and performed in different areas to construct streamflow series at a finer temporal scale (Stedinger and Vogel 1984; Tarboton et al. 1998; Kumar et al. 2000; Xu et al. 2003; Acharya and Ryu 2014). It is suggested that many of these disaggregation algorithms are capable to produce streamflow realizations. However, the uncertainty existed in estimating parameters, high dimensionality of the disaggregation problem and the intensive computational resources mightily limit the application of disaggregation methods.

Another potential approach is based on the concept of scaling which has gained increasing awareness recently in the field of geophysics and hydrology. Gupta & Waymire (1990) introduced the “multiplicative cascade” modeling framework for studying spatial variability of probabilistic structures of the rainfall process by introducing the concepts of simple and multiple scaling. Smith (1992) developed a lognormal cascade model to represent the basin scale in flood peak distributions and used a lognormal multi-scaling model to fit observed flood series in the Appalachian region of the United States. Gupta et al. (1994) applied a

multi-scaling theory at the regional scale to study the invariance of the probability distributions of peak flows on a basis of log-levy stable distributions. De Michele and Rosso (1995) proposed an assessment of regionalization procedures to show that the spatial variablility of flood probabilities of a small basin in Italy can be well presented by simple scaling. Yu et al. (2004) investigated the regional Intensity-Duration-Frequency formulas based on the scaling theory. It involves the hypothesis of piecewise simple scaling combined with the Gumbel distribution and the analysis of the temporal scaling properties of annual maximum precipitation series for various durations and return periods in northern Taiwan. These studies reveal that scaling theory is capable of finding a synthesis of the regularities in different temporal scales to characterize extreme storm probabilities.

Thus, the scaling theory is adopted in this study to investigate the scaling properties of extreme flow for different time scales and to estimate IPF from MDF data. It proposes to build the scaling equations in three 15min flow stations while no such work has been done in the literature on relating the IPF with MDF. This scale-invariant model, scales flow data from one temporal resolution to another which give us a new insight into overcoming the lack of the instantaneous peak flow data and regionalization.

Generally, all these methods are based on the purpose of estimation of IPF from MDF in a simple and reasonable manner. The state of art of this part of study can be summarized as:

1. The transfer function of IPF-MDF is further improved by correlating their PWM and quantile values and new catchment descriptors have been found to establish a new multiple regression analysis in Aller-Leine basin, Germany.

2. Although the scaling theory is quite popular and developed in the rainfall studies, it is not fully explored in the application of runoff, especially in the field of building the relationship between IPF and MDF. Here, the piecewise simple scaling combined with the GEV distribution is applied to estimate the moments of IPF form the observed MDF data series and subsequent quantile values of IPF.

2.2 Estimation of IPF from MDF using hydrological modeling

Various statistical methods can be found to estimate design peak flow in case there are long enough recorded stream flow data available. However, in many circumstances, the measured stream flow data are often too short to perform robust statistical inference at the site of interest. Under such conditions, Rainfall-runoff modeling is one of the most important and efficient method for the solution of extreme flows estimation problems, as well as for analysis of catchment and climate change or for theoretical investigation of controls on the flood

frequency curve (Cameron et al. 1999; Haberlandt and Radtke 2014). Additionally it can be quite useful to estimate IPFs for ungauged sites, where no measurements are available. In this case, regionalization of hydrological model parameters is commonly used to transfer information from gauged or partially gauged sites to the target site (Hundecha and Bárdossy 2004; Merz and Blöschl 2004; Oudin et al. 2010; Seibert 1999; Sivapalan 2003; Wallner et al. 2013). Consequently, the IPFs magnitudes and return periods can be estimated by the frequency analysis of flow data generated by a hydrological model with the transferred parameters.

One main problem in hydrological modeling has been the lack of high resolution climate data. One possible solution would be to run the hydrological model with stochastically generated high resolution rainfall data (Blazkova and Beven 2004; Cameron et al. 1999; Haberlandt et al. 2008; Haberlandt and Radtke 2014; Viglione et al. 2012). Another alternative would be to use a daily time step in hydrological modeling with the longer available daily climate forcing data. Then scale the simulated flows or derived extreme values afterwards. Unfortunately, it is not known which of the two options, namely, calibrating the daily model with subsequent correction of simulated MDFs and calibrating the hourly model with the disaggregated daily rainfall as input, provides better results.

A state-of-art assessment regarding the performances of these two methods is proposed in this study. To make an appropriate choice for a specific design problem, the estimates of IPFs from daily simulations with post-correction of flows and hourly simulations with pre-processing of precipitation are compared. The simulated annual maximum daily and hourly extremes are subsequently analyzed for different return periods. Since the results from hourly simulation lead to estimations of IPFs with the desired recurrence interval, it is referred as pre-processing approach. On the other hand, the obtained maximum daily flow (MDF) quantiles are subsequently transformed into IPFs with a multiple regression model. This is called post-correction approach.

Hydrological models are selected and applied as a basis for decision making about water resources management. The degree of belief people have in model predictions is often dependent on how well the model is able to reproduce observations, especially, to simulate the extremes. In this study, two calibrations strategies for the hydrological model using the hydrograph and using flow statistics, respectively, are compared through application for both post-correction and pre-procession approaches. The use of additional information during parameter estimation in the form of flow statistics, such as cumulative distribution function and flow duration curves, may help reduce uncertainties in simulating extremes (Cameron et al. 1999; Haberlandt and Radtke 2014; Westerberg et al. 2011; Yu and Yang 2000).

2.3 Estimation of IPF from MDF in ungauged catchments

The estimation of design floods in ungauged catchments is a common problem in hydrology since there are numerous ungauged basins in the world. The most commonly adopted methods for this task include Index Flood (Method Hosking and Wallis 1993), the Quantile Regression Technique (Haddad and Rahman 2012; Tasker and Stedinger 1989) and Probabilistic Rational Method (Rahman et al. 2011; Young et al. 2009). These methods are limited to peak flows and hence are not particularly useful when the estimation of complete streamflow hydrograph is needed. The rainfall-based Design Event Approach has been recommended by a lot of countries, e.g. Australia and England. In this approach, the probabilistic nature of rainfall depth is considered in the rainfall-runoff modeling, but it ignores the probabilistic behavior of rainfall temporal patterns and runoff (Hill and Mein 1996).

With the development of computational power, rainfall-runoff models have been commonly used to estimate the design flood peak in ungauged catchments since modeling has been proven to be an efficient and useful tool for estimating the elements of the water cycle in a lot of different catchments. The model parameters for these areas can be estimated using regional information. One can assume that catchments with similar characteristics have a similar hydrological behavior and thus can be operated using similar model parameters. It is therefore plausible for regionalization of model parameters on the basis of catchment characteristics.

Regionalization techniques including the parameter regression approach (Fernandez et al. 2000; Merz and Blöschl 2004; Seibert 1999; Servat and Dezetter 1993), nearest neighbor approach (Bárdossy and He 2006; Chiew and Siriwardena 2005; Merz and Blöschl 2004) and parameter regionalization (Kapangaziwiri and Hughes 2008) are implemented to transfer model parameters from one catchment to another catchment defined with similar climatic and hydrological characteristics. Parajka et al. (2005) compared a range of different regionalization methods using both snow cover data runoff data to estimate the model parameters**.**

Although the regression-based approach was strongly doubted by McIntyre et al. (2005) who suggest to investigate the relationship between model parameter and the catchment descriptor to produce a joint distribution function of the model parameters which however requires a large number of observed catchments, it is still the main-stream regional calibration approaches. Earlier on, there are two steps involved in the regression-based regional approaches: (1) estimation of watershed model parameters at each individual catchment independently, followed by (2) attempts to relate the model parameters to catchment characteristics. Examples of this method can be found in Abdulla and Lettenmaier (1997) and Sefton and Howarth (1998). However, the transfer of parameters is difficult due to the non-uniqueness of the model parameters. In principle, it is not easy to estimate the flow elements

in ungauged areas by calibrating the transfer function between model parameters with the characteristics of the catchment. To improve this weakness, a one step approach is proposed by Hundecha and Bárdossy (2004) where the calibration is carried out with the reference to the coefficients of the predefined regression function instead of the model parameters. In this approach, Model parameters are regionalized through simultaneous calibration of the same hydrological model on different catchments.

Here, one step regression-based regionalization approach is used for the purpose of estimating the IPFs from simulated MDF in ungauged areas. A predefined function between model parameters and catchment descriptors is proposed. All the sub basins in in Aller-Leine catchment, Germany are calibrated simultaneously with the dual objective of reproducing the flow statistics of observed daily streamflows and additionally to obtain four quantile values of IPF. The HBV model is operated only on a daily time step. The simulated annual maximum daily extremes are subsequently analyzed for four return periods (T=10, 20, 50, 100yr). The obtained maximum daily flow (MDF) quantiles are subsequently transformed into IPFs with a multiple regression model. In addition, the calibrations strategy for the hydrological model is using flow statistics.

Chapter 3

3 Estimation of IPF from MDF using statistical methods

Given the available observed flow data, these three statistical methods developed in this chapter are performed to seek a relationship between the instantaneous peak flow (IPF) and mean daily flow (MDF). Such a regression function should prove to be attractive and useful to the people who want to determine peak flows based on the available often longer recorded daily flows. They are applied to a series of flow stations in Germany and compared to the traditional method available in the literature. The idea of the fist approach is to apply a simple regression between observed IPF and MDF data regarding their probability weighted moments (PWM) and quantile values. It can directly give us an impression of the differences and significance of correlation between IPF and MDF. The second method including a multiple linear regression analysis constructs a functional linear relationship between IPF and MDF with the selected catchment descriptors. The last scaling method proposes to extend the former research and build a scale-invariant model scaling the flow data from one temporal resolution to another. It gives us a new insight into overcoming the lack of the instantaneous peak flow data and regionalization.

3.1 Methods

3.1.1 Simple regression using quantiles and probability weighted moments (PWMs)

L-moments are linear functions of Probability weighted moments (PWMs), introduced by Greenwood et al. (1979). PWMs can be written as:

$$\beta_i = \int_0^1 x\left(F'\right)F'dF \tag{3.1}$$

where i=0, 1, 2…is positive integer. When i =0, β_0 is equal to the mean of the distribution; F is cumulative distribution function (CDF) for x and $x\left(F'\right)$ is inverse CDF of x evaluated at the probability F.

The ith L-moments γ_i are related to the ith PWM through

$$\gamma_{i+1} = \sum_{j=0}^{i} \beta_k (-1)^{i-j} \binom{i}{j} \binom{i+j}{j} \tag{3.2}$$

For instance, the first three L-moments are related to PWMs using

$$\begin{aligned} \gamma_1 &= \beta_0 \\ \gamma_2 &= 2\beta_1 - \beta_0 \\ \gamma_3 &= 6\beta_2 - 6\beta_1 + \beta_0 \end{aligned} \tag{3.3}$$

L-moments ratios are defined by Hosking 1990 as follows:

$$\begin{aligned} L-CV &= \gamma_2 / \gamma_1 \\ L-skew &= \gamma_3 / \gamma_2 \\ L-kurt &= \gamma_4 / \gamma_2 \end{aligned} \tag{3.4}$$

where L-CV is a termed the L-coefficient of variation, L-skew is referred to as L-skewness while L-kurt is referred to as L-kurtosis.

Extreme value distributions are the statistic models to measure events which occur with very small probability and they are quite useful in flood risk modeling as risky events per definition happen with low probability. The class of Extreme value distributions essentially involves three types of extreme value distributions, namely, type I, II and III.

The Gumbel distribution (type I) is named after the German mathematician Emil Gumbel, one of the pioneer scientists in practical applications. It has been extensively used in various fields including hydrology for modeling extreme events (Benito et al. 2006; Fortin et al. 1997; Guo and Cunnane 1991; Martins and Stedinger 2001; Veijalainen et al. 2010). The type II distribution is named after a French mathematician Maurice Fréchet who developed a possible limiting distribution for a sequence of maxima with convenient scale normalization. This has been applied often in modeling of market-returns in France which are often heavy tailed. The Weibull distribution is named after a Swedish engineer and scientist Waloddi Weibull who is famous for his work on fatigue analysis and strength of materials. Due to its flexibility Weibull distribution is widely used in various areas although it was originally devised to address the problems in material sciences for minima arising.

The Generalized Extreme Value (GEV) distribution arises from the extreme value theorem as the only possible limit distribution of properly normalized maxima of a sequence of independent and identically distributed random variables (Fisher and Tippett 1928). It is a family of continuous probability distributions combining the Gumbel, Fréchet and Weibull families and has been fairly applied to model the maxima of long sequences of random

variables. GEV distribution has been recommended for use in flood frequency analysis by many hydrologists (Ahilan et al. 2012; Bobee 1999; Wallis et al. 2007). The cumulative distribution function of GEV has the following form (Jenkinson 1955):

$$F(x)=\begin{cases}\exp\left\{-\left[1+k\left(x-u\right)/a\right]^{-1/k}\right\} & k\neq 0\\ \exp\left\{-\exp\left[-\left(x-u\right)/a\right]\right\} & k=0\end{cases} \tag{3.5}$$

where k=0, k>0, and k<0 correspond respectively to the Gumbel, Fréchet and Weibull distribution; $u\in\mathbb{R}$ is the location parameter, a >0 is the scale parameter and $k\in\mathbb{R}$ is the shape parameter. Hosking et al. (1985) showed that probability weighted moments (PWM) provide more efficient and less biased parameters than using the maximum likelihood method for the short sample sizes encountered in flood frequency analysis.

The simple regression analysis consists of three steps:

Step 1: select the proper frequency distribution function for fitting of annual extreme flow series by the Chi-square test;

The first step of the method will decide the possible probability distribution for peak and daily extreme values. Eight commonly employed probability distributions for extreme values are considered as the candidate distribution. These are: two-parameter Weibull (Wei), gamma distribution (Gam), three-parameter generalized extreme value (GEV), Pearson type III, generalized pareto distribution, kappa distribution, five-parameter wakeby and generalized logistic distribution (GlO). For the Chi-square goodness of fit procedure, the acceptability of the distribution functions are selected on the basis of a p-value with a confidence level of 95% (α=0.05). The null hypothesis will therefore be rejected if the p-value is smaller than the 5% significance level. Following Hosking & Wallis (1997), L-moments are utilized for the parameter estimation in the second step.

Step 2: estimate the flood quantiles (T=10, 20, 50, 100 years) for annual maximum daily and annual peak flow series respectively;

Step 3: apply linear regression without intercept to obtain a regional regression model based on the quantile and PWM values derived from step 2.

In the third step, the linear regression with no intercept is carried out using the quantiles for the return periods of T= 10, 20, 50, 100 years and alternatively the first four PWMs for each flow station within our study area. The details of the final regression equations are presented

as follows. Eq. (3.6) describes the quantile regression for a single return period, where for testing c_q is determined by the leave one out cross validation method. In this procedure, one station is selected randomly while the peak and daily flow quantiles based on the observed IPF and MDF data series from the remaining flow stations are regressed linearly. The slope of the regression line is the parameter c_q for the station left out. Eq. (3.7) is used for the PWM regression and for testing the parameter c_m is estimated using the same procedure.

$$HQ_{peak}^{est} = c_q \cdot HQ_{day}^{obs} \tag{3.6}$$

$$PWM_{peak}^{est} = c_m \cdot PWM_{day}^{obs} \tag{3.7}$$

where c_q and $c_m$are the quantile regression coefficient and the PWM regression coefficient respectively; HQ_{day}^{obs} and PWM_{day}^{obs} are the derived daily quantile flows and probability weighted moments from observed MDF data series; HQ_{peak}^{est} and PWM_{peak}^{est} are the corresponding estimated instantaneous peak flow values and moments.

3.1.2 Multiple linear regression method

Multiple regression analysis is often applied to test the influence of independent variables (predictors) on a single dependent variable (criterion). Given a data set of n statistical units, the model can be described as (Draper and Smith 1998):

$$\begin{bmatrix} Y_1 \\ Y_2 \\ Y_3 \\ \vdots \\ Y_{n-1} \\ Y_n \end{bmatrix} = \begin{bmatrix} X_{a1} & X_{b1} & X_{c1} \\ X_{a2} & X_{b2} & X_{c2} \\ X_{a3} & X_{b3} & X_{c3} \\ \vdots & \vdots & \vdots \\ X_{a(n-1)} & X_{b(n-1)} & X_{c(n-1)} \\ X_{an} & X_{bn} & X_{cn} \end{bmatrix} \begin{bmatrix} B_1 \\ B_2 \\ B_3 \\ \vdots \\ B_{n-1} \\ B_n \end{bmatrix} \tag{3.8}$$

where Y is a column vector containing a series of the criterion variables; X is a matrix containing list of all the independent variables that are related with Y; B is also a column vector containing the regression coefficients.

Here, this idea is further employed to the following objectives:

- To study the geomorphologic and hydrological factors that can restrict the basin responses;
- To explore the possible relationships of between annual instantaneous peak flow (IPF) and the corresponding daily flow (MDF);

- To develop the final regional equations based on the selected catchment characteristics to calculate the IPF.

This method consists of the following three steps:

As the first step of the method, in order to obtain a perspective about the relationship between extreme flow rate and the selected explanatory variables as well as the interrelation among the latter by a descriptive statistical analysis is carried out. In addition, Pearson's correlation coefficient r with p value is calculated to measure the strength of linear association between two variables.

$$r = \frac{\sum_{i=1}^{n}\left(x_i - \bar{x}\right)\left(y_i - \bar{y}\right)}{\sqrt{\sum_{i=1}^{n}\left(x_i - \bar{x}\right)^2}\sqrt{\sum_{i=1}^{n}\left(y_i - \bar{y}\right)^2}} \tag{3.9}$$

where x and y are variables; n is the sample size.

The correlation coefficient r is a number between -1 and 1. There are 3 types of correlation by describing the relationship between a pair of variables that is as one variable increases what happens to the other variable:

1. Negative correlation: the other variable is predicted to decrease, with the value of -1 for a perfect negative correlation;
2. Positive correlation: the other variable is predicted to increase, with the value of 1 for a perfect positive correlation;
3. No correlation: the other variable does not show any increase or decrease tendency.

On the other hand, the p value shows the statistical significance of the predictors related with IPF since the correlation does not imply an underlying causal relationship between them. Given that the p value is less than the significance level (traditionally α=0.05), there is a significant linear correlation between the selected variable with IPF can then be concluded. Consequently, this descriptive statistical analysis can give one a sense of the data to select the proper catchment descriptors into the next step.

Secondly, a stepwise regression analysis based on the selected catchment characteristics derived in the first step is performed.

The stepwise regression procedure used here is a combination of forward and backward selection techniques. It therefore involves removing or adding variables to the regression

equation step by step and eliminating the variable which contributes least to the prediction of a group membership (see Figure 3.1).

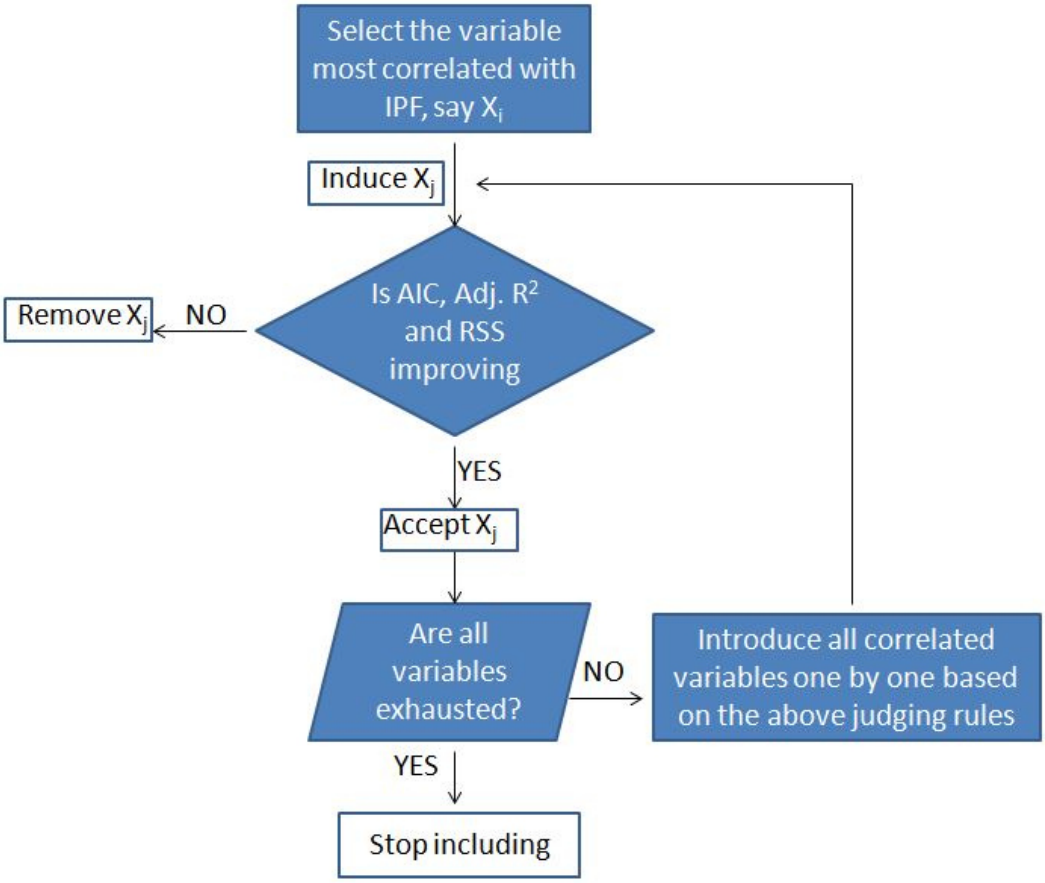

Figure 3.1: The scheme of stepwise multiple regression

To begin with, the variable which has the highest correlation with IPF is the first to be added in the regression equation. The second variable to be added is the one that explains the largest remaining candidate variation in the IPF. At this stage the first variable is tested for significance and retained or discarded depending on the results of this test. It is guided by the AIC (Akaike information criterion) score which allows for an immediate ranking of the candidate models. The model with the minimum AIC score has the smallest divergence (see Bozdogan 1987). Furthermore, the adjusted coefficient of determination (Adj. R^2) and Residual Sum of Squares (RSS) are also considered. RSS is the sum of the squared differences between the actual and estimated IPF. This procedure is repeated till a situation is reached when all the factors not included in the equation are insignificant, and all the factors included in the equation are significant. This is a very good approach to use but care must be exercised to ensure that the resulting equation is rational.

The final step is to eliminate redundant explanatory variables within the selected regression models through a partial correlation analysis and compare the final multiple regression model with the traditional Fuller equation. The aim of the last step is to evaluate the performance of the final multiple regression model in comparison to Fuller's equation (see Eq. (3)). Fuller's equation is one of the most commonly used methods describing the relationships between IPF and its corresponding MDF, where the drainage area is the only physical descriptor. Further details about Eq. (3) are referred in Fuller (1914).

$$Q_{peak} = Q_{day} \cdot \left(\beta_0 + \beta_2 \cdot A^{\beta_1}\right) \tag{3.10}$$

where β_0 ... β_2 are regression coefficients; A= drainage area (km^2); Q_{day} is the maximum mean daily flow (m^3/s) and Q_{peak} is predicted peak flow (m^3/s).

3.1.3 Simple scaling theory

The importance and recognition of scale issues in hydrology has grown enormously within the last few decades. In particular, people want to know what attributes become different and what attributes keep invariant under scale change. Proper notions of scale invariance and scale transformation are therefore proposed and tested in science and engineering. Ideas of statistical simple scaling and multi-scaling generate a natural framework to understand the hydrological processes within a region and physical structure of floods (Gupta et al. 1994; Gupta and Waymire 1990; Smith 1992). One of the most important issues recently is the recognitions of runoff organization at different temporal scales. The scaling properties including scaling exponents by using the observed annual maximum runoff data at recording station are investigated for various durations and return periods. Since scaling theory has been investigated far less in runoff study in comparison with extreme rainfall, The theory with the basic equations applied in rainfall studies are introduced first.

The scaling hypothesis is that equality holds in the probability distribution of the observed runoff depth at two different time scales (see Koutsoyiannis et al. 1998; Yu et al. 2004), as described by Eq. (3.11).

$$Q_{\lambda h} \overset{d}{=} \lambda^{\alpha} Q_h \tag{3.11}$$

where $\overset{d}{=}$ is understood in the sense of equality of the probability distributions of $Q_{\lambda h}$ and Q_h; Q_h is the 15_minute flow series; α is the scaling exponent and λ denotes a scale factor. It suggests that $Q_{\lambda h}$ and $\lambda^{\alpha} Q_h$ have the same probability distribution.This property is referred to

as ‘simple scaling in the strict sense’ by Gupta and Waymire (1990). If both variables have finite moments of an order k, their relationship regarding moments can be then described as Eq. (3.12) which implies that the raw moments $M^{k}_{\lambda h}$ of any order are scale invariant.

$$M^{k}_{\lambda h} \overset{d}{=} \lambda^{\alpha^{k}} M^{k}_{h} \tag{3.12}$$

In order to acquire the scaling exponent α, Eq. (3.12) can be log-transformed into Eq. (3.13):

$$\log M^{k}\left(Q_{\lambda h}\right) = \log M^{k}\left(Q_{h}\right) + \alpha^{k} \log \lambda \tag{3.13}$$

where α^{k} is the scaling exponent. The scaling exponent can be estimated from the linear regression slope between the ratio $\left(\log M^{k}\left(Q_{\lambda h}\right) / \log M^{k}\left(Q_{h}\right)\right)$ and scale parameter $\left(\log \lambda\right)$ for various orders of moments (k).

When the scaling exponents and their corresponding order of moment have a linear relationship with the scaling exponent of order 1, namely, $\alpha^{k} = k\alpha^{1}$, it is usually referred to simply as ‘wide sense simple scaling’. If the this linear relationship cannot be found in the target variable, the other approach namely, multi-scaling can be considered (see Gupta & Waymire 1990).

For the analysis in this method, piecewise scaling approach is used to deal with the multi-scaling problem and five steps are carried out as follows:

1. Select the peak flow series using the peak over threshold (POT) method (see Katz et al. 2002);

2. Assess the scaling properties in the maximum flows of various durations by scaling analysis of probability weight moments (PWM);

3. Validate the scaling hypothesis in runoff;

4. Determine the scaling formulas based on the scaling property of fractal;

5. Estimate the quantile values of instantaneous peak flows from daily flows with downscaling of the PWMs using Eq. (3.12) computed in the above step and the GEV distribution. The application of this step for unobserved gauges without IPF data involves the assumption of spatial consistence of the relationship within the transfer region.

3.1.4 Evaluation criteria

Leave-one-out cross validation (LOOCV) illustrated in Figure 3.2 is the degenerate case of k-fold cross validation. In LOOCV, the original sample is randomly partitioned into N equal size subsamples and N is the total number of observation in the original sample. It incorporates using one subsample as the validation set and the remaining (N-1) subsamples as the training set. This procedure is repeated N times on all ways to cut the original sample on a validation set of one observation and a training set. This has the benefit that each observation in the sample will be utilized once as validation data and avoids splitting the sample with their limited size into independent calibration and validation datasets. LOOCV has also been proven to be an almost unbiased estimator of prediction risk by Cawley and Talbot (2003). Here, it is used to assess the performances of all three models.

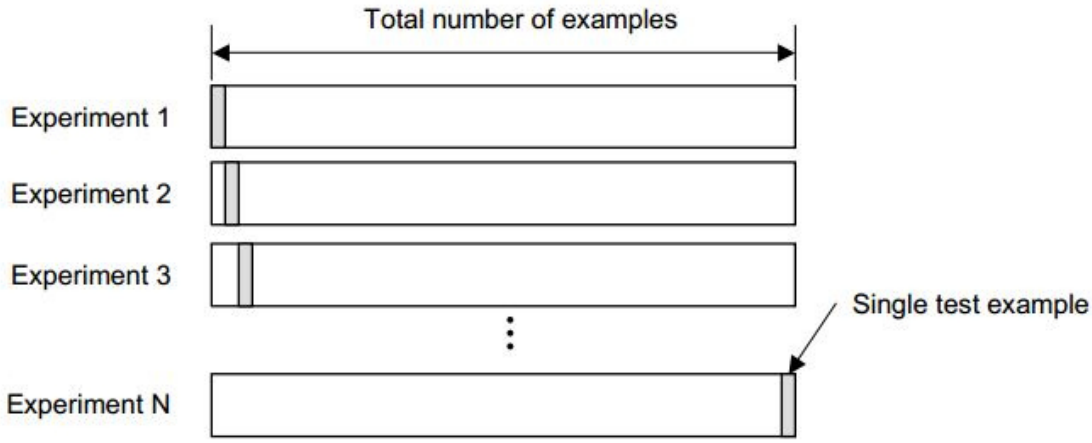

Figure 3.2: The scheme of leave one out cross validation (LOOCV)

Root mean square error (RMSE) and bias are the criteria applied for the evaluation of model performance. The root mean square error normalized with the average observed flow is given by:

$$RMSE = \sqrt{\frac{1}{N}\sum_{i=1}^{N}\left(\frac{HQ_i^* - HQ_i}{HQ_i}\right)^2} \tag{3.14}$$

and the normalized bias criterion is given by:

$$Bias = \frac{1}{N} \cdot \sum_{i=1}^{N} \left(\frac{HQ_i^* - HQ_i}{HQ_i} \right) \tag{3.15}$$

where N is the number of stream flow stations; HQ_i^* and HQ_i denote the quantile values based on estimated and observed peak flow values respectively.

3.2 Study area and data

The Aller-Leine river basin is located in the federal state of Lower Saxony in northern Germany. The total basin area is 15,803 km^2 and the basin is physiographically diverse. Mean elevations in this catchment range from 5m.a.s.l (meters above sea level) to 1140m.a.s.l (see Figure 3.3). In the northern part of the basin, the highest elevation is 169m.a.s.l, compared to southern the Harz middle mountains where elevations reach up to 1140m.a.s.l. In the Harz mountains most aquifers are fractured with some areas of karst. The flatland of the Lüneburger Heide is characterized by sandy soils, porous quaternary aquifers and heath and moor vegetation. 58.2% of the total area is agriculture and 32.5% forest. The climate is characterized by high annual precipitation with mean annual precipitation ranging from 500mm to approximately 1600 mm. Frost is present in the winter season.

According to the locations of discharge gauges, there are 45 delineated sub-basins. For each basin, 16 catchment descriptors are derived (see Table 3.1). Their geomorphologic characteristics, such as drainage area, minimum and maximum elevation, longest flow path, river slope and basin slope, are obtained from a Digital Elevation Model (DEM) with a resolution of 10 meters. The shape length is taken as the perimeter of each catchment, and the derivation of time of concentration (Tc) is based on Kirpich's formula. The soil properties of effective field capacity (Fc) and saturated hydraulic conductivity (K_f) are estimated from the German digital soil data base BÜK1000 (see Hartwich et al. 1995). The portion of different land use types is derived from the land cover map CORINE2000 (see EUR 1994). Mean annual areal precipitation is computed using point observations from 244 daily precipitation stations, which are interpolated on a 1×1 km raster through Ordinary Kriging (OK) and aggregated over space. Finally, mean daily temperature is interpolated for all available climate stations by External Drift Kringing (EDK) with elevation as additional information (see Haberlandt et al. 2015).

Table 3.1 Physical and hydrologic catchment descriptors for the 45 sub-basins

Variable description	Symbol	Units
100-year of peak flow	HQ1	m^3/s
100-year of daily flow	HQ2	m^3/s
Shape length of subbasins	shape_len	m
Subbasin area	Area	Km^2
Basin slope	basin_sl	‰
Mean concentration time	Tc	h
Longest flow path	lst_fp	m
River slope	river_sl	-
Max elevation	Elv_up	m
Min elveation	Elv_ds	m
Mean elevation	mean_Elv	m
Mean conductivity	Kf	mm/h
Mean field capacity	FC	Vol-%
Ratio of city	City	%
Ratio of agriculture	agriculture	%
Ratio of forest	Forest	%
Annual precipitation	PCP	mm/year
Mean daily temperature	Tem	°C

Figure 3.4 displays box plots of the hydrological attributes for all 45 sub-basins. It shows that minimum elevations vary between 33 m and 580 m, the size of the catchments from 40 km^2 to 1000 km^2, and the longest flow path from 10 km to 70 km. The sampling of annual flood flow series is done in a way that instantaneous peak flow (IPF) and maximum daily flow (MDF) always belong to the same event. The primary daily and peak discharge data for analysis herein are employed from a total number of 45 flow stations which are illustrated in Figure 3.3. However, only three 15 min continuous flow stations can be used for the scaling analysis, since the record length of all other stations is inadequate. The record lengths of the three 15_minute flow stations used are from 2000 to 2008, from2002 to 2008 and from 2003 to 2008 respectively. It can be seen from Figure 3.3 that all the three selected 15 min continuous flow stations are located within the higher elevated area of the catchment.

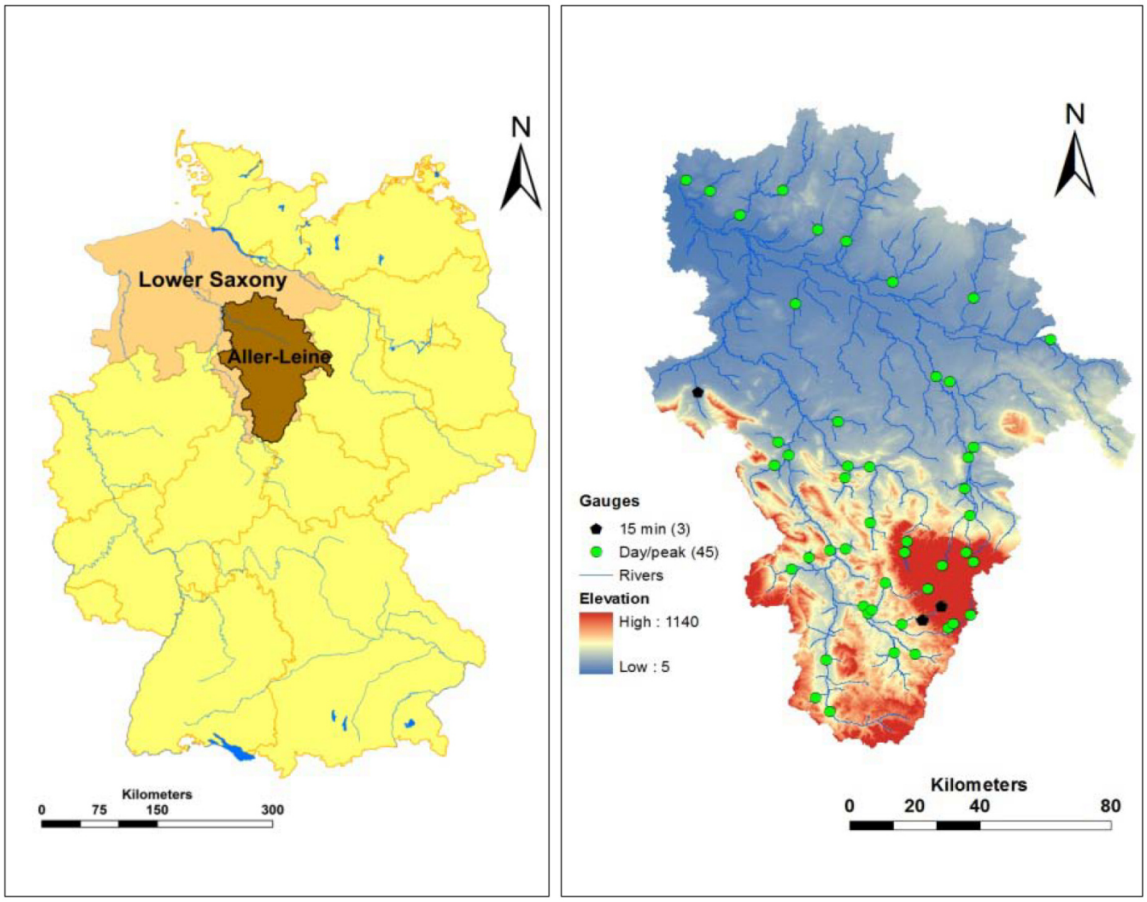

Figure 3.3: Study region showing the Aller-Leine catchment within Germany and the federal state of Lower Saxony; the right figure displays the topographic structure of the catchment, the location of 45 daily flow stations including 3 stations with 15_minute continuous flow record.

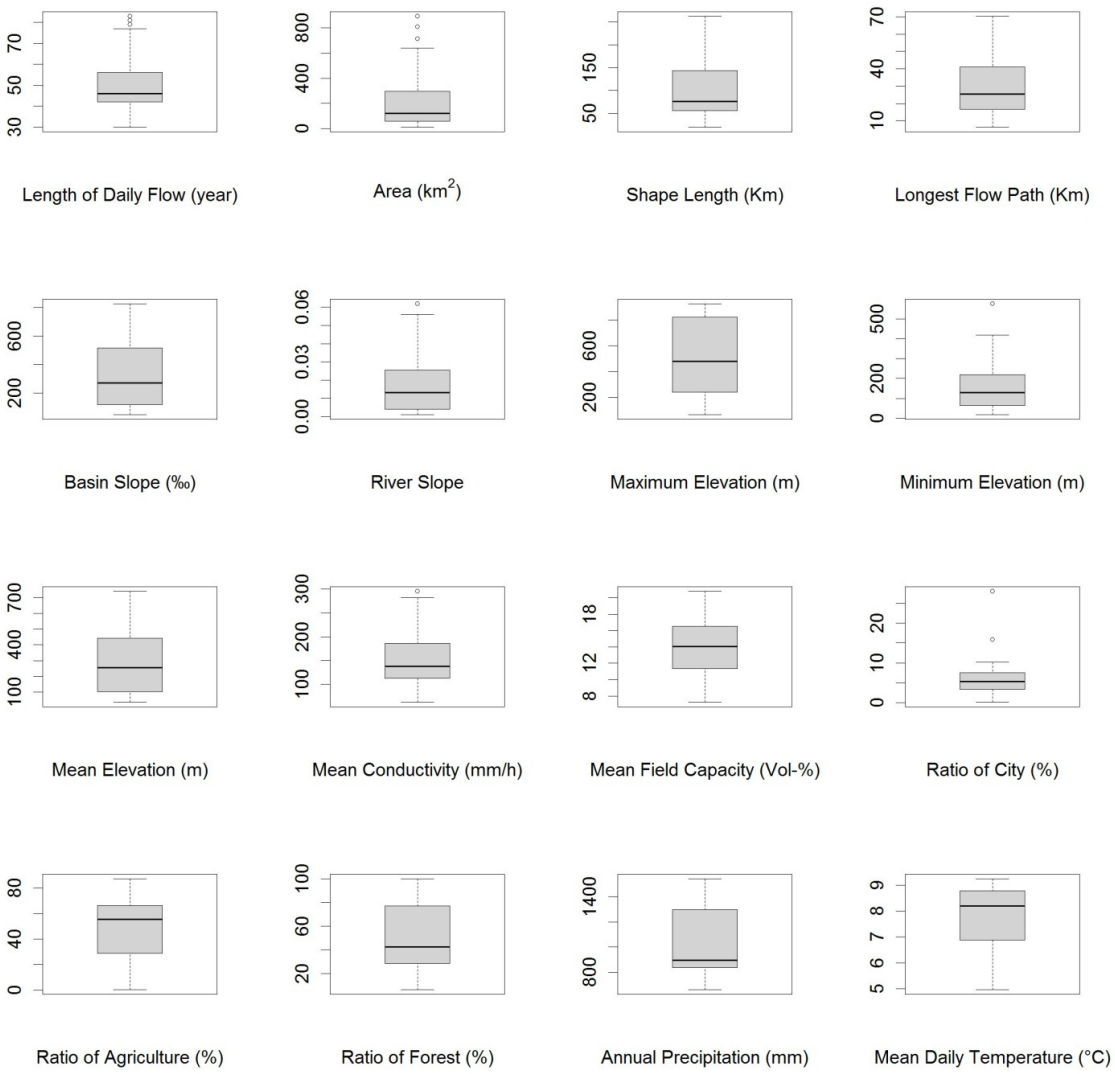

Figure 3.4: Box-plots of stream flow gauges and hydrological attributes of the 45 sub-basins

3.3 Results

In this section, three different models presented in chapter 3 are used to explore the relationship between instantaneous peak flow and maximum daily flow regarding their frequency analysis. The performance of these models is measured by leave one out cross validation based on RMSE and bias criteria for a total number of 45 flow stations in northern Germany. It is important to note that for the first two models long-term observed annual IPF and MDF data series are used, whereas for the third model the observed MDF and the short-term 15_minute continuous flow data for three flow stations are used.

3.3.1 Simple regression approach

In the first method, a simple regression model is obtained by direct comparison between the observed annual instantaneous peak flow (IPF) and maximum daily flow (MDF) series regarding their quantile and probability weighted moments (PWM) values. Here only the best fitting four probability distributions, according to Chi-square test performed on each of the 45 discharge gauges, are shown here (see Figure 3.5). The red solid line in the figure indicates a 5% significance level. As can be seen, the best fitted probability model is the generalized extreme value distribution (GEV) with hardly any rejection of the null hypothesis for all flow gauges that the GEV fits the flow data (p-value > 0.05) for both MDF and IPF data series.

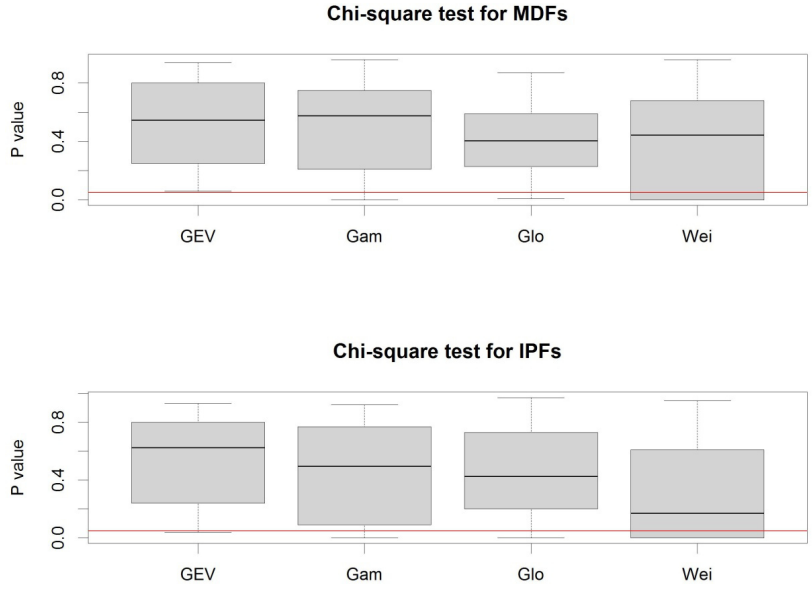

Figure 3.5: P-value results obtained from chi-square test for maximum daily flow (MDF) and instantaneous peak flow (IPF) data series

(a)

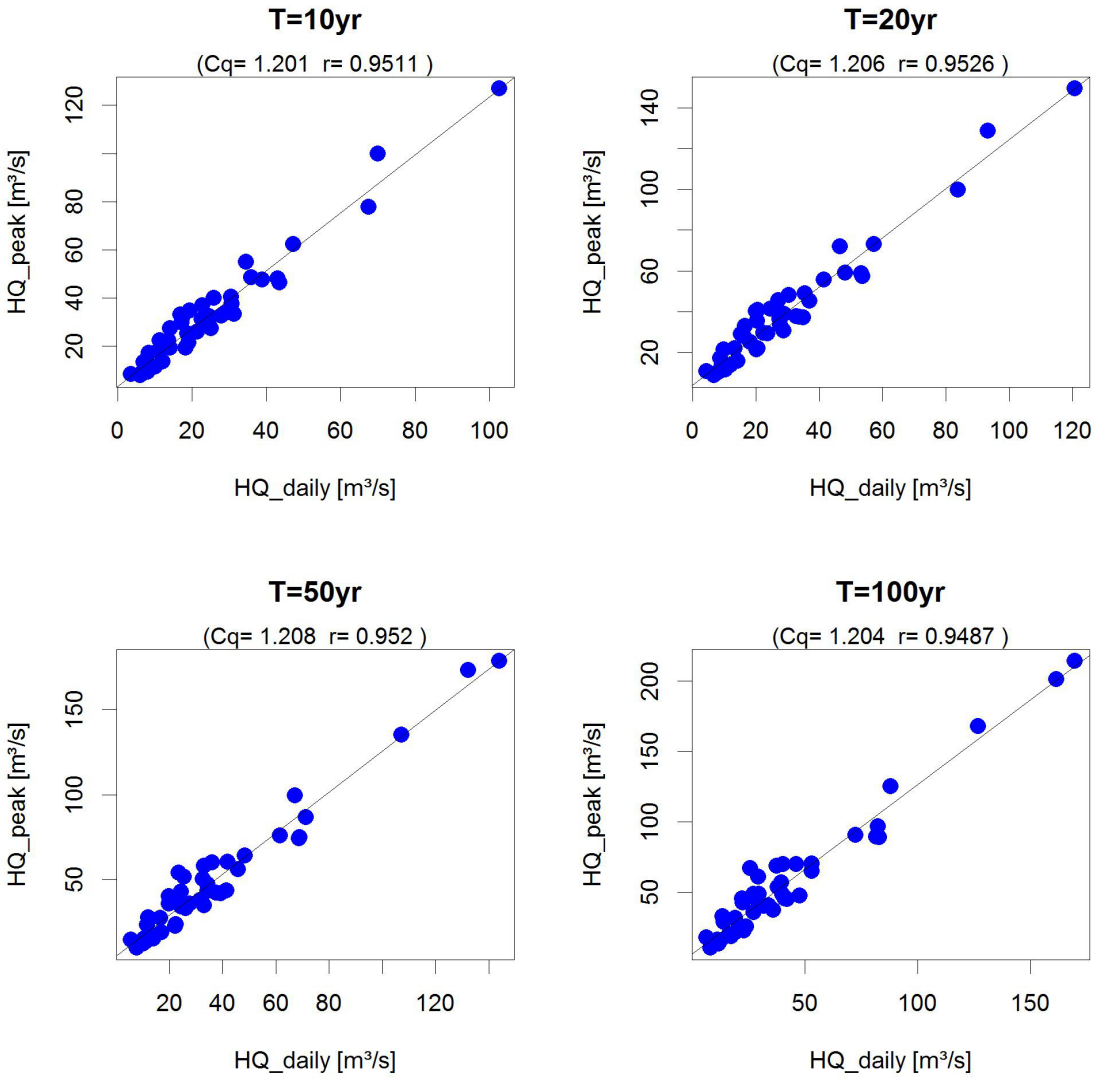
T=10yr
(Cq= 1.201 r= 0.9511)
HQ_peak [m³/s]
HQ_daily [m³/s]
T=20yr
(Cq= 1.206 r= 0.9526)
HQ_peak [m³/s]
HQ_daily [m³/s]
T=50yr
(Cq= 1.208 r= 0.952)
HQ_peak [m³/s]
HQ_daily [m³/s]
T=100yr
(Cq= 1.204 r= 0.9487)
HQ_peak [m³/s]
HQ_daily [m³/s]

(b)

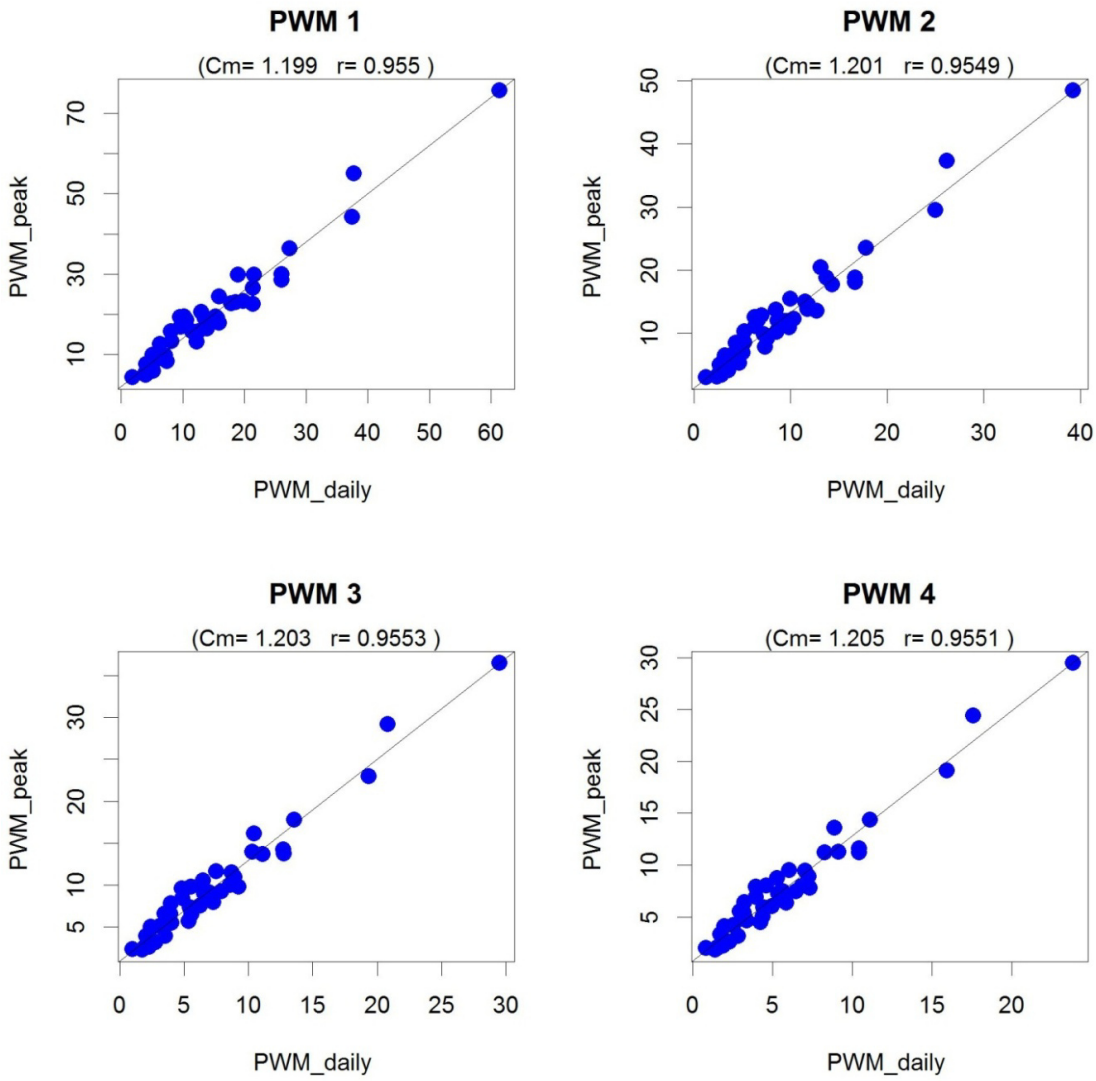

Figure 3.6: (a) shows the relationship between the annual peak flow and maximum daily flow series regarding regarding their quantile values, whereas c_q is the regression coefficient and r is the correlation coefficient; (b) shows the relationship between the annual peak flow and maximum daily flow series regarding probability weighted moments (PWM); c_m is the regression coefficient and r is the correlation coefficient.

It can be seen that peak and maximum daily flow are highly correlated with each other in the sense of their quantiles and PWMs, with correlation coefficients larger than 0.95 for the four return periods and the first four orders of PWMs. Hence, it is reasonable to estimate the

design IPF though correcting the underestimation of its corresponding MDF. In addition, the strength of PWMs and the quantile values regression are very similar. As such, the performance of the simple regression models regarding the PWM and quantiles are expected to be similar, as shown in Figure 3.7.

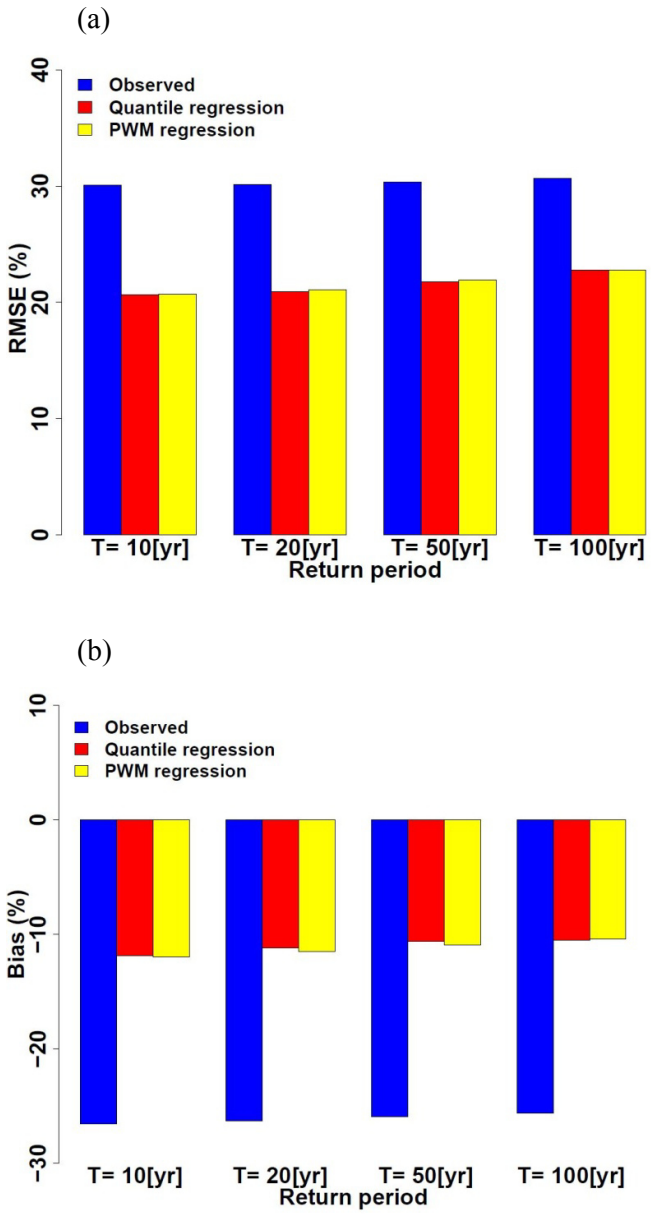

Figure 3.7: The RMSE (a) and Bias (b) of the simple regression model regarding probability weighted moments (PWM) and quantiles averaged for all 45 flow gauges

Figure 3.7 (a)-(b) display the root mean square errors (RMSE) and bias from the simple regression model using cross validation. The IPFs based on the observed annual peak flow series are considered to be the reference for assessment of the performance of the following three models. The first blue column is the observed error representing the difference between the peak flows and maximum daily flows from observed IPF and MDF series; while the red and yellow columns denote the estimation error from the simulated peak flows using the observed annual MDF series. On average, the RMSE is approximately 20% for the simple regression model for these four different recurrence intervals in comparison with an observed error of over 30%. The results in Figure 3.9 (b) show the biases from the simple regression model are approximately -11% and the observed errors around -26%. This means that the simple regression model reduces considerably the error in estimating the design peak flow compared to using the observed MDF data, although still with some negative bias.

3.3.2 Multiple regression analysis

Figure 3.8 shows a scatter plot matrix with a combined correlation for HQ1 and all explanatory variables. The symbols of all explanatory variables are indicated in the diagonal of the matrix and their definitions can be referred to in table 1. In the cells of the upper part of the matix (above the diagonal), the correlation coefficients and P values are presented. For the remainder of the matrix, scatter plots are shown between variables pairs. The scales of each variable are indicated on the margins of the matrix.

As an arbitrary decision rule to determine the significance of the predictors related with HQ1, the p value limit of 0.05 is considered to be important, although the absolute values of the simple correlation coefficients for some variables may be less than 0.5. For instance, the Elv_up is selected as one of the importand predictors even though the simple correlation coefficient between Elv_up and HQ1 is 0.36 while the p value is less than 0.05. It can be seen from the top two rows, that Area has the strongest positive correlation with HQ1 and HQ2, followed by lst_fp and shape_len. In addition to these three aforementioned variables, Elv_ds is also selected for the next step, as it has the strongest negative correlation with HQ2 (P value=0.057, r=-0.29). Below the second row, it is shown that many of the explanatory variables are highly interrelated with one another (e.g. Area~lst_fp, Area~shape_len). This fact must be taken into account for further analysis and possible exclusion of variables from the final model.

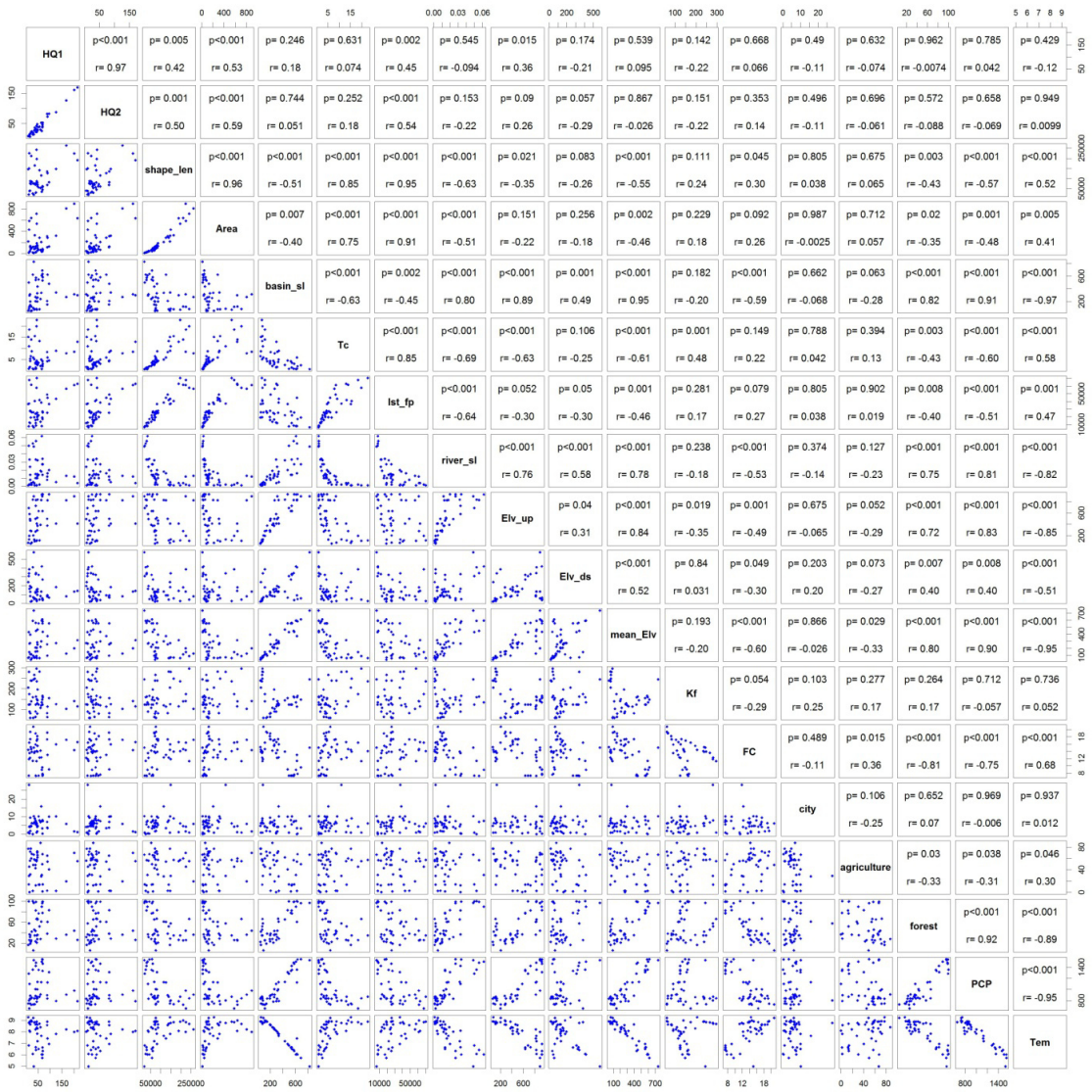

Figure 3.8: Scatter plot and correlation matrix for the basin properties and the instantaneous peak flow

A stepwise multiple regression analysis is carried out in the next step. According to the number of predictors, six regression models are selected from their specific combination groups (see Table 3.2). The adjusted coefficients of determination of the last five models are almost equal while the first model with HQ2 as the only predictor, possesses the least correlation with the target variable (Adj.R^2=0.94). For the Residual Sum of Squares RSS, the first two models produce almost twice as large errors as the other models. Given the simplicity and overall performance of the regression model, the fourth model with shape_len, lst_fp, Elv_ds as predictors, seems to be the most suitable model with the least AIC value (189.47) while the third model is the next most suitable.

Table 3.2 Stepwise regression results for peak flow

Number	Variables	Adj.R^2 (-)	RSS $(m^3/s)^2$	AIC (-)
1	HQ2	0.9423	4607	208.65
2	HQ2,Elv_ds	0.9553	4575	191.21
3	HQ2,lst_fp,Elv_ds	0.9602	2650	190
4	HQ2,shape_len,lst_fp,Elv_ds	0.9630	2600	189.47
5	HQ2, shape_len,lst_fp,Elv_ds,Area	0.9636	2551	190.64
6	HQ2, shape_len,lst_fp,Elv_ds,Area,ELV_up	0.9648	2539	192.44

As shown in Table 3.3, there is a significant correlation between the longest flow path (lst_fp) and shape length (shape_len), with a partial correlation coefficient of 0.921. This can lead to multi-collinearity and thus can have negative impacts on the stability and quality of the regression model. Therefore, the third model in Table 3.2 is determined to be the final multiple regression model. It further proves that peak flow can be determined with an appreciable degree of accuracy using just three predictors, namely, the maximum daily flow, longest flow path and minimum elevation (see Eq. (3.16)).

$$HQ_{peak}^{est} = \alpha_1 \cdot HQ_{day}^{obs} + \alpha_2 \cdot lst\_fp + \alpha_3 \cdot Elv\_ds \tag{3.16}$$

where $\alpha_0 \ldots \alpha_3$ are regression coefficients; HQ_{day}^{obs} denotes the derived daily flow quantiles obtained from observed MDF data series and HQ_{peak}^{est} denotes the estimated instantaneous peak flow quantiles.

Table 3.3 Partial correlation matrix of basin descriptors and hydrologic response

Variables	Maximum daily flow (HQ2)	Shape length (shape_len)	Longest flow path (lst_fp)	Minimum elevation (Elv_ds)
HQ2	1	-0.045	0.005	0.012
shape_len		1	0.921	-0.188
lst_fp			1	-0.044
Elv_ds				1

A comparison of the performance between the Fuller equation and the developed multiple regression model, through the RMSE and bias, is presented in Figure 3.9.

It can be seen that both methods are able to reduce the error compared to using the observed annual MDF data series. However the multiple regression model outperforms the traditional Fuller equation. For the Fuller equation, the RMSE values increase with increasing return period, ranging from 18.12% RMSE for the 10 year recurrence interval to around 23% RMSE for the 100 year recurrence interval. Additionally, the bias also rises from -10% to -17%, which implies that for a higher return period the underestimation is larger. In contrast, for the multiple regression model proposed here, the errors are independent of the recurrence instead. Some physical explanations for the selected regression are:

(1) The differences between peak flow and daily flow are due to the catchment retention. Therefore, basins with longer flow paths have greater potential to show differences between MDF and IPF.
(2) The significance of other commonly used predictors will become weaker for larger basins. The differences between their mean climate, soil or basin slope characteristics is not obvious, whereas the distinctive minimum elevation in each basin can be more representative.
(3) According to the initial investigation in our study area, the available maximum daily flow data are the most important resource to relate the instantaneous peak flows.

(a)

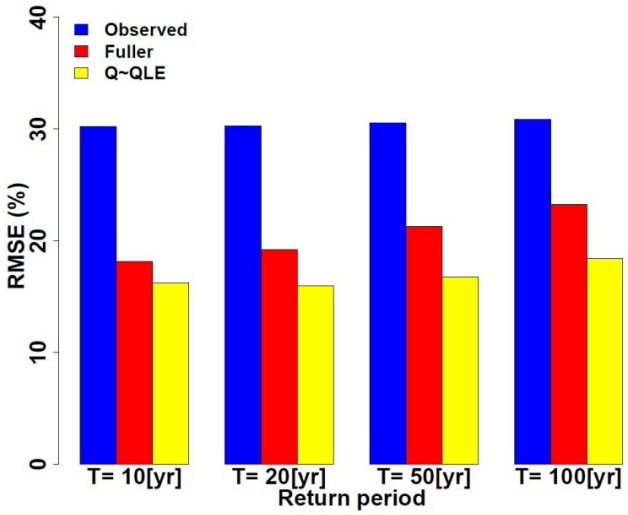

(b)

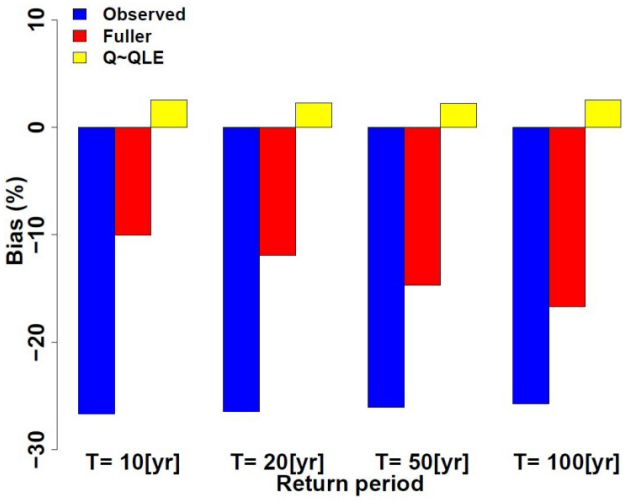

Figure 3.9: The RMSE (a) and bias (b) of stepwise multiple regression model averaged for all 45 flow gauges

3.3.3 Scaling analysis

In the first step of the scaling analysis the annual peak flow series are extracted from three short term 15_minute flow stations. The observed 15_minute flow data for each gauge are aggregated into 27 different time scales (see Table 3.4). For each time scale, the peak over threshold (POT) is adopted to extract approximately 30 extreme values. Briefly, the peaks will be extracted at an average rate of four events each year from those aggregated flow time series data sets. According to the characteristics of the flood events in our study basin, a minimum separation period of 45 days is imposed to ensure independence of selected peaks within the one year. The PWMs of the runoff extremes including all 27 time scales are consequently derived.

Table 3.4 The definition of 27 scales

Time scales	1	2	3	4	5	6	7	8	9	10	11	12	13	14	15	16	17	18	19	20	21	22	23	24	25	26	27
Flow duration (h)	0.25	0.5	0.75	1	1.25	1.5	1.75	2	2.5	3	3.5	4	4.5	5	5.5	6	7	8	9	10	12	14	16	18	20	22	24

Next, the property of simple scaling of runoff of various durations in the three selected sample stations is demonstrated according to Eq. (3.13). Here, the parameter h is defined as the runoff duration of 0.25h; the scale parameter λ is a multiplier to convert runoff duration h to λh and $Q_{\lambda h}$ denotes the runoff intensity of λh hours. Figure 3.10 gives the regression results after a logarithmic transformation between PWM and durations of the flow data for all 5 moment orders and three 15_minute flow stations. As can be seen, the whole period (15 minute— 24h)

can be visually divided into 3 pieces (15 minute—2h, 2h—10h, and 10h—24h) where the slope of the linear regression line for each piece gives the values of the scaling exponent α^k for various orders of moments k. For each piece the linear regression lines are almost parallel to one another. This characteristic implies that the scaling exponents (the slopes of linear regression lines) of each piece will be very similar for various orders of PWM, which is demonstrated in Figure 3.11.

(a) Station1

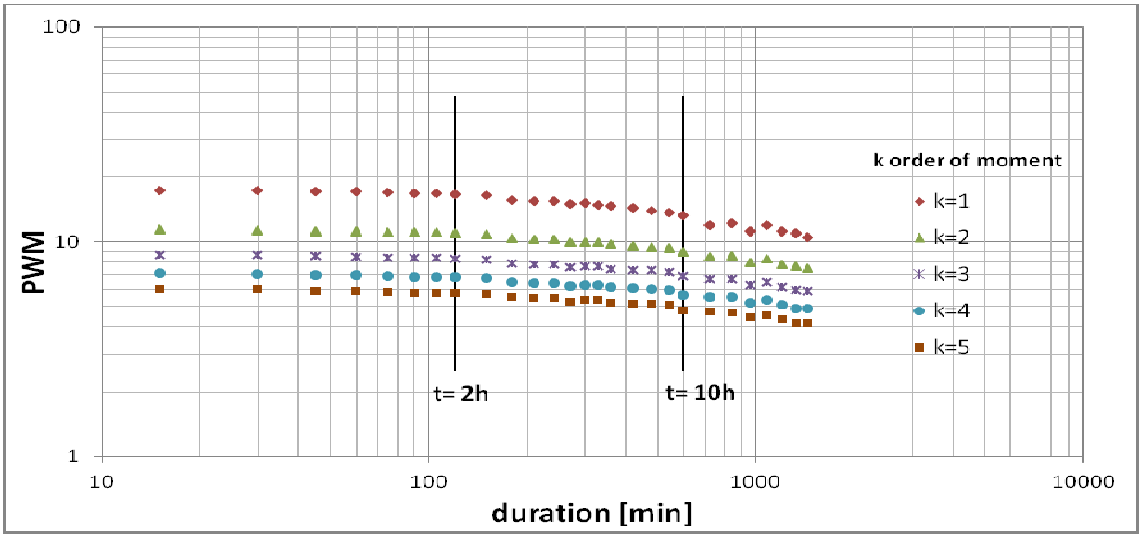

(b) Station2

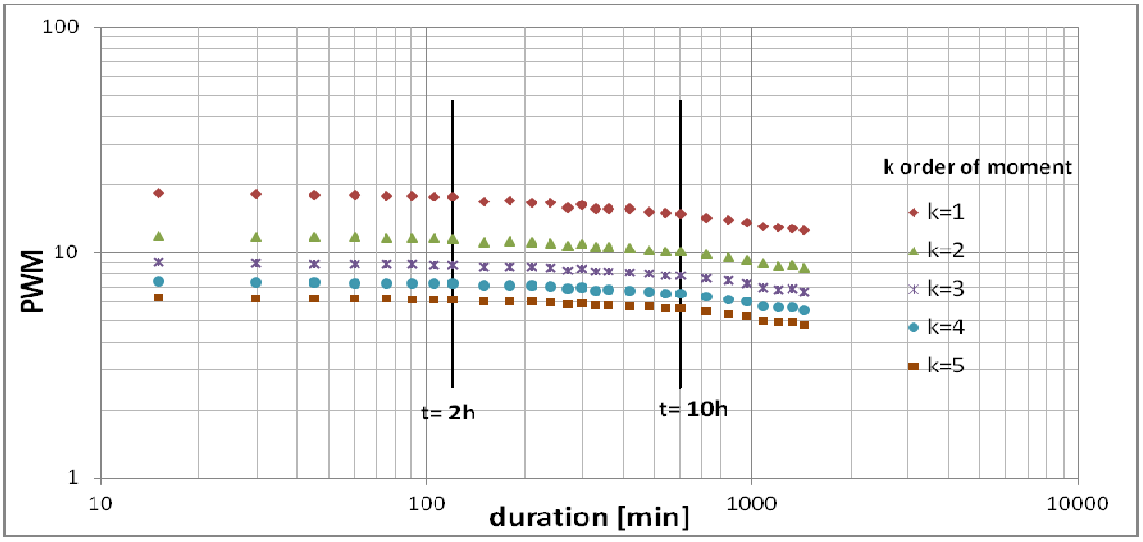

(c) Station3

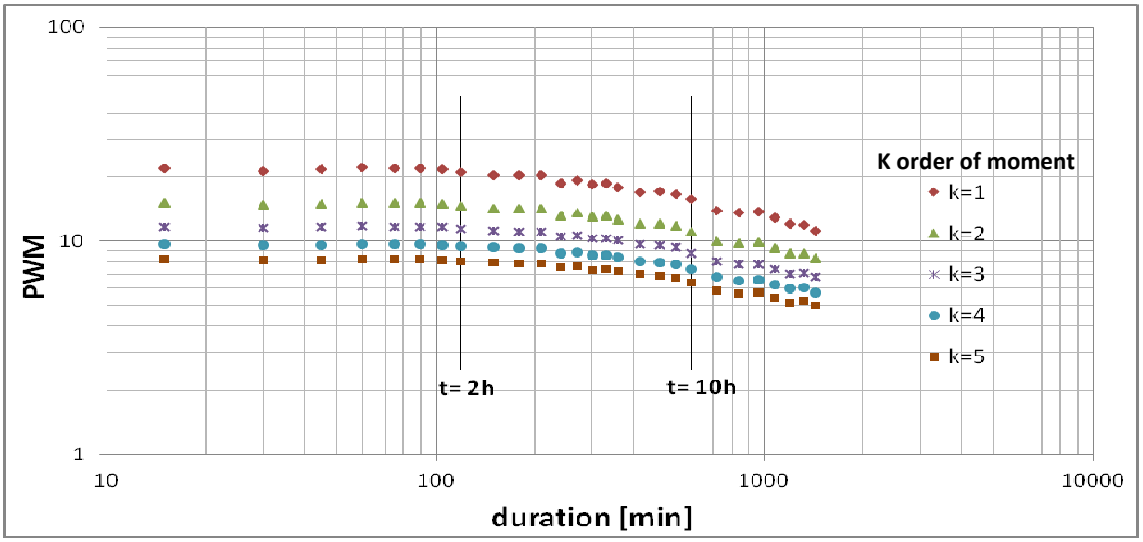

Figure 3.10: The relationship between log-transformed values of probability weighted moments (PWM) of various orders and various runoff durations at (a) station 1, (b) station 2, (c) station 3

Figure 3.11 shows the relationship between the scaling exponents and various orders of PWM for the three divided pieces at the three 15_minute flow stations. It is clear that a linear relationship exists between scaling exponents and various orders of PWM. The scaling exponents increase slightly with the order of PWM in the second and third piece (2h—10h and 10h—24h), but remain stable in the first piece (15 minute—2h). This indicates that the property of simple scaling of runoff rate exists in the three analyzed stations. Furthermore, the scaling properties at station 1 and 2 are more similar than when compared with station 3. The reason for it may be that the first two flow stations are located within close proximity (see Figure 3.1).

(a) Station 1

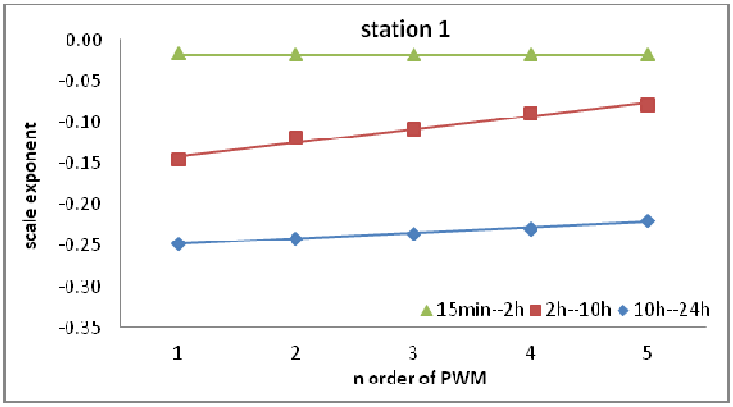

(b) Station 2

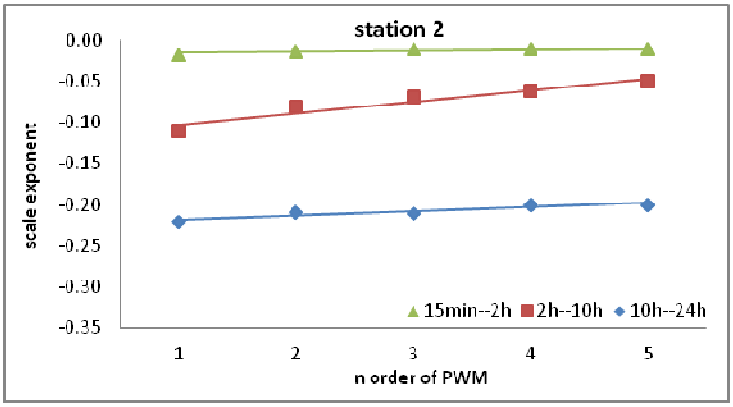

(c) Station 3

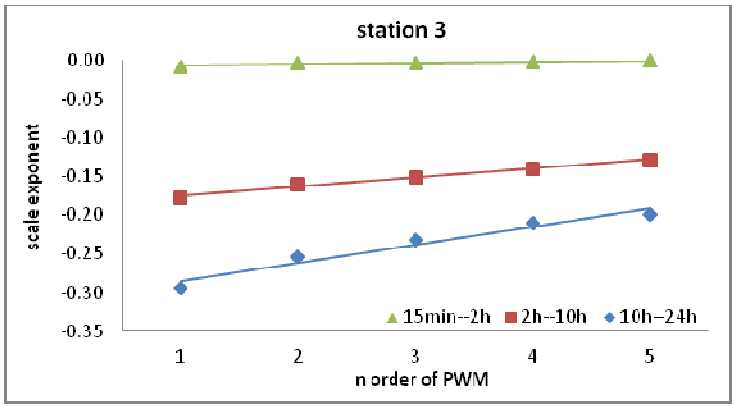

Figure 3.11: The relationship between scaling exponents and various orders of probability weighted moments (PWM) at (a) station 1, (b) station 2, (c) station 3

Based on the above analysis, the piecewise scaling formulas are developed as follows:

$$\begin{cases} \log M^k\left(Q_{24h}\right) = \log M^k\left(Q_{10h}\right) + \alpha_1^k \log 2.4 \\ \log M^k\left(Q_{10h}\right) = \log M^k\left(Q_{2h}\right) + \alpha_2^k \log 5 \\ \log M^k\left(Q_{2h}\right) = \log M^k\left(Q_{15\min}\right) + \alpha_3^k \log 8 \end{cases} \tag{3.17}$$

where α_1^k, α_2^k, α_3^k are the scaling exponents for various orders of PWM in the first (15_minute—2h), second (2h—10h) and third piece (10h—24h) respectively; Q_{15_minute} represents the observed annual 15_minute extreme values; Q_{2h} and Q_{10h} represent the annual 2-hour and 10-hour extreme values respectively using the aggregated 15_minute continuous flow series.

According to the obtained scaling exponents (α_1^k, α_2^k, α_3^k) of various orders of PWM and pieces for the three 15_minute flow stations , the three scaling equations are applied separately to all 45 daily flow stations in our study catchment to compute PWMs of annual instantaneous peak flows. The GEV distribution is then utilized for estimating the design values of peak flow for four different return periods (T=10, 20, 50, 100 years).

The cross validation results of simple scaling method are illustrated in Figure 3.12, where a comparison of RMSE and bias among the three 15_minute resolution flow stations is presented. Here, the reference error (Observed) is the same as for the former two regression models and the four return periods. It shows the difference between the average daily flow and instantaneous peak flow at the same event.

(a)

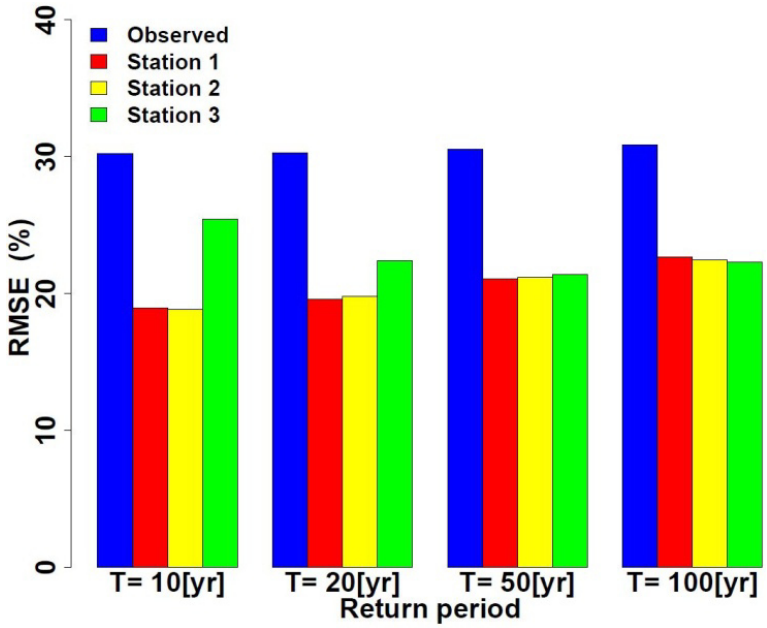

(b)

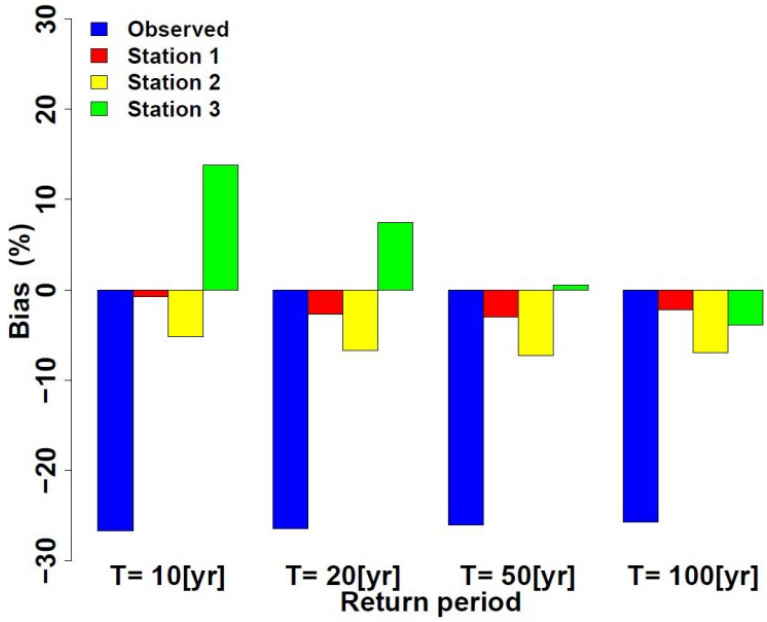

Figure 3.12: The RMSE (a) and bias (b) results from simple scaling method averaged for all 45 gauges

It can be seen from Figure 3.12(a) that the three simple scaling models also produce good results considering the flood frequencies. Generally, the difference of RMSE between station 1 and 2 is small, with an average RMSE of approximately 20% for the four return periods. It reduces the observed error by 10% and no obvious dependence of RMSE exists with increasing return period. The most significant difference between station 3 and the other two stations is that station 3 exhibits greater RMSE (by 6%) at the T=10 year recurrence interval, but for the more important larger return periods, it performs as well as the other two 15_minute flow stations. Compared with the RMSE, the differences in bias (see Figure 3.12 (b)) between the three stations are more apparent, ranging from -3% to 0, -8% to -5% and -4% to 14% respectively for each station. For the longer return periods (T=50, 100 years), the bias results indicate an underestimation of the design peak flows for all three scaling models. In summary, the scaling model generated from station 1 displays the best overall performance according to the above performance analysis and is recommended for application here. Due to the sparse station network and limited record length of the 15_minute runoff gauges, the relationship between the selected station locations and scaling attributes could not be investigated in more detail.

Comparative results for the three methods

Table 3.5 The comparative results for the three methods

		Simple regression approach		Multiple regression analysis		Scaling analysis		
RMSE (%)	Observed (daily)	Quantile regression	PWM regression	Fuller	Q~QLE	station1	station2	station3
T=10[yr]	30.23	20.66	20.72	18.12	16.22	18.95	18.84	25.46
T=20[yr]	30.30	20.93	21.07	19.21	15.96	19.60	19.78	22.42
T=50[yr]	30.55	21.77	21.90	21.31	16.75	21.08	21.19	21.42
T=100[yr]	30.85	22.79	22.78	23.25	18.41	22.69	22.46	22.29
Bias (%)								
T=10[yr]	-26.68	-11.84	-11.99	-10.01	2.55	-0.77	-5.20	13.83
T=20[yr]	-26.42	-11.18	-11.52	-11.90	2.28	-2.66	-6.72	7.46
T=50[yr]	-26.05	-10.60	-10.95	-14.66	2.24	-3.04	-7.28	0.55
T=100[yr]	-25.73	-10.51	-10.40	-16.70	2.58	-2.17	-6.92	-3.89

The three methods in terms of their performance in predicting the IPF from MDF are compared. The final comparative results for the four return periods are illustrated in Table 3.5. The observed error in the second column denotes the direct comparison between the observed maximum daily flow and its corresponding peak flow. The RMSE of it (around 30% for each return period) suggests for some catchments the average maximum daily flow will be much lower than the corresponding peak flows without post correction. It is clear that the multiple regression analysis performs best with the average value of RMSE 16.8% and Bias 2%. The

simple regression approach performs poorest since the magnitude of the estimation error is larger (around 20% for each return period) and it underestimates the peak flows significantly. Overall the scaling analysis based on the three hourly flow stations corresponds well and the first two stations perform better than the third one regarding their Bias results.

3.4 Conclusions and discussions

In this chapter, three different methods are proposed to provide a relatively simple way for this estimation of instantaneous peak flows from maximum daily flows in northern Germany.

The first method, a simple regression model, provides a coefficient to correct the underestimation of the design daily flow. The expression is based on the linear relationship between IPF and MDF regarding their quantile and PWM values. it presents a good comparison of the difference between IPF and MDF and is computationally very favorable. The final RMSE and bias results prove it to be a useful approach for estimating the peak flows for flood studies.

In the second method, a stepwise multiple regression model, special attention is given to the extraction of the proper predictors. The MDFs, the longest flow path and the minimum elevation in this case have been selected as predictors in the final regression equation using stepwise regression and considering partial correlations. According to the multiple regression analysis, the longest flow path is highly correlated with peak flow and also highly interrelated with basin area which is most significantly related with flow. This explains that the longest flow path is found to be one of the final explanatory variables. However, unlike in previous studies the minimum elevation showed a higher performance than the catchment area (eg. Taguas et al. 2008 and Fuller 1914). A physical explanation is given by the structure of the catchment. Using the area alone does not sufficiently differentiate between headwaters in the upper and the lower parts of the catchment. This study confirms that the scaling of the response is much related to hill slope and channel properties, where the elevation of the outlet is useful information. A side effect of the result is the fact that the lowest point of the catchment can be easily obtained because it is approximately the same value as the geodetic elevation of the gauging station, which is often published with the maximum flow data.

In comparison with the classical Fuller's equation, the proposed multiple regression model noticeably improves the accuracy of the estimation results. Despite a small overestimation, the multiple regression model performs best among the three models and for longer return periods its comparative performance becomes even more remarkable. Although this case study is carried out for Aller-Leine catchment in northern Germany, the knowledge and the methods can be applied to other areas.

The last method, a piecewise simple scaling model, provides promising insights into the temporal issues between peak flow and its corresponding maximum daily flow. The hypothesis of piecewise simple scaling combined with the GEV distribution, is used to explore the link between PWMs of IPF and MDF, given short-term 15_minute continuous flow data for three discharge gauges. The formulas obtained from the three 15_minute flow stations are then applied to the 45 daily gauges individually. The validation results reveal that the three piecewise simple scaling models are capable of deriving peak flow when only maximum daily flow is available. Compared with the regression models, the scaling model is more efficient because the parameters of the scaling model can be determined exclusively by one station with sufficient continuous high resolution flow data. Therefore, this method could be used for correcting a single station only. However, criteria for selecting a proper high resolution donor station are not clear and further investigation is required to establish regional scaling formulas.

It is difficult to perfectly represent IPFs with MDFs regarding the flood frequency analysis. For all three proposed methods, the stream flow data are considered to be the only decision variable. As discussed, all of them can provide a significantly better result compared with using MDFs directly and they can be easily applied. The first two methods are highly depend on the peak data availability for a sufficient set of stations, which may restrain its use in areas with poor peak flow data. The next step will be related to using hydrological models together with rescaling approaches in order to be able to consider land use or climate changes for the estimation of design flows.

Chapter 4

4 Estimation of IPF from MDF using hydrological Model

The primary aim in this chapter is to explore the possibility of deriving frequency distributions of IPFs using hydrological modelling with daily and hourly time steps in comparison.

4.1 Methods

The conceptual semi distributed model HBV has been chosen and is operated on an hourly and a daily time step respectively. Two calibration schemes are applied, which are based on hydrographs and multiple flow statistics, respectively. For the latter different aspects of the runoff statistics: the winter (November-April) extremes distribution, summer (May-October) extremes distribution, flow duration curve and annual extreme series are considered. An automatic optimization procedure based on dynamically dimensioned search algorithm (DDS) algorithm is introduced for solving a single overall objective calibration problem. The frequency analysis of the extreme values is based on the generalized extreme value distribution (GEV) with L moments (see Hosking and Wallis (1997)).

To make an appropriate choice for a specific design problem, The estimates of IPFs from daily simulations with post-correction of flows and hourly simulations with pre-processing of precipitation are compared. The simulated annual maximum daily and hourly extremes are subsequently analyzed for four return periods (T=10, 20, 50, 100yr). The results from hourly simulation lead to estimations of IPFs with the desired recurrence interval. It is referred as pre-processing approach. The obtained maximum daily flow (MDF) quantiles are subsequently transformed into IPFs with a multiple regression model. This is called post-correction approach.

4.1.1 Hydrological modelling

HBV model

The HBV model is a conceptual hydrological model for simulating runoff with reasonable requirements of hydrological data and computing power. Its application lies in flood forecasting, irrigation scheme planning, water balance studies and study of climate change impact on hydrological processes. The model was named after the abbreviation of Hydrologiska Byråns Vattenbalans-avdelning (Hydrological Bureau Waterbalance-section) and originally developed at the Swedish Meteorological and Hydrological Institute (SMHI) in early 1970s (SMHI 2008). The basic modeling philosophy behind this model is:

- The model should be based on a reasonable scientific foundation;
- Data demands should be met in the study areas;
- The model must be understandable by modelers and properly validated;
- The model performance can be utilized to justify the model complexity.

Nowadays, the HBV model has been developed into different versions and forms although only minor changes in the basic model structure are made. The applied hydrological model in this study is a version of the HBV model modified by Wallner et al. (2013). Here, the introduction of land use and potential evaporation time series as input is the main difference from the original HBV model (see Wallner et al. (2013)).

Model structure

HBV consists of a snow module, a soil moisture routine, a runoff generation and concentration routine within each sub basin and flood routing of the runoff in the river network. It is therefore possible to run the model for several sub-basins separately and then add the contributions from all the sub-basins. A schematic sketch of the HBV model version is presented in Figure 4.1. In this case, the input data are observations of precipitation, air temperature, crop coefficient and potential evaporation.

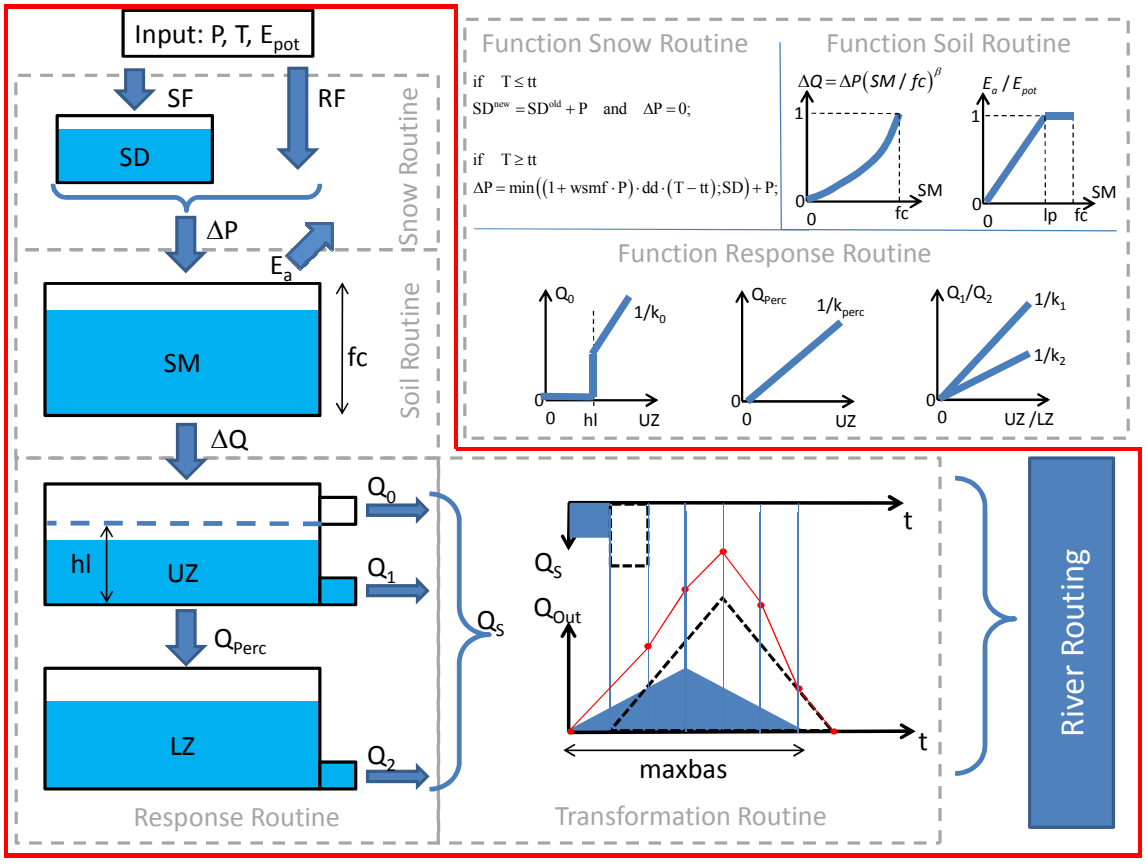

Figure 4.1: Conceptual structure of the modified version of the HBV from Wallner et al. (2013)

The snow routine represents snow melt and accumulation process by a simple degree day concept, based on the air temperature with a water holding capacity of snow. The snowmelt contributes to the runoff if the actual temperature (T) is higher than the threshold temperature (tt). Otherwise, the precipitation is in the form of snow. The amount of snow depth at t and t+1 time step can be calculated as:

$$SD_{t+1} = \begin{cases} SD_t + P_{t+1} \cdot \Delta t & if\ T_{t+1} \le tt \\ \max\left(SD_t - \Delta P_{t+1} \cdot \Delta t; 0\right) & if\ T_{t+1} > tt \end{cases} \tag{4.1}$$

where: SD = the snow depth storage

T = the actual temperature

tt = the threshold temperature, influenced by landuse

and the amount of runoff contributing rainfall at t and t+1 time step can be calculated as:

$$\Delta P_{t+1} = \begin{cases} 0 & if\ T_{t+1} \le tt \\ \min\left(\left(1 + wsmf \cdot P_{t+1}\right) \cdot dd \cdot \Delta t \cdot \left(T_{t+1} - tt\right); SD_t / \Delta t\right) + P_{t+1} & if\ T_{t+1} > tt \end{cases} \quad (4.2)$$

where: ΔP = the sum of rainfall and snowmelt while P = the precipitation

wsmf = the wet snow melt factor which accounts for a faster snow melt if precipitation occurs

dd = a degree day factor when there is no rainfall

The soil moisture is the main routine that determines the runoff generation and actual evapotranspiration. After the snow routine, the adjusted soil moisture at t+1 time step is calculated as:

$$SM'_{t+1} = SM_t + \Delta P_{t+1} \cdot \Delta t \quad (4.3)$$

where: *SM'*= adjusted soil moisture at t+1 time step

SM= old soil moisture

It consists of two parts. The actual evapotranspiration is calculated in the first part as the following equation. This method solves the problem of the requirement of the water supply and the landuse data to compute the real evapotranspiration. The water supply is represented by the soil parameters the actual water content. The crop coefficient is used to consider specific landuse.

$$E_{a,t+1} = \begin{cases} \min\left(k_{c,t+1} \cdot E_{pot,t+1} \cdot \dfrac{SM'_{t+1}}{lp \cdot fc}; \dfrac{SM'_{t+1}}{\Delta t}\right) & if\ SM'_{t+1} \le lp \cdot fc \\ \min\left(k_{c,t+1} \cdot E_{pot,t+1}; \dfrac{SM'_{t+1}}{\Delta t}\right) & if\ SM'_{t+1} > lp \cdot fc \end{cases} \quad (4.4)$$

where: Ea = actual evapotranspiration

Kc= crop coefficient

Epot= potential evaporation

lp= limit for potential evaporation

fc= maximum soil moisture storage

The second part of soil routine is to calculate the contribution of precipitation or snow melt to the runoff which is directly linked to the response routine. The adjusted soil moisture taking place from the soil zone is:

$$SM''_{t+1} = SM'_{t+1} - E_{a,t+1} \cdot \Delta t \tag{4.5}$$

where: SM''= adjusted soil moisture at t+1 time step

The runoff depended on the state of soil water content and the soil paramters is described by a power funtion as:

$$\Delta Q_{t+1} = \min\left(\Delta P_{t+1} \cdot \left(SM''_{t+1} / fc\right)^{\beta}; SM''_{t+1} / \Delta t\right) \tag{4.6}$$

where: ΔQ= generated runoff

β=shape factor if it smaller than 1 the effect that greater water supply contribute to greater runoff can be reduced and the contribution to the next routine is great, even for small actual soil water content.

The final moisture state at t+1 time step is then calculated as:

$$SM_{t+1} = SM''_{t+1} - \Delta Q_{t+1} \cdot \Delta t \tag{4.7}$$

The response routine estimates runoff generated from rainfall after the soil moisture routine which consists of one upper nonlinear reservoir and one lower linear reservoir. The flow generated from these hypothetical reservoirs assumes to obey Darcy's law. The contributing runoff ΔQ is directly linked to the upper reservoir. The surface runoff will occur if the water content in the upper reservoir exceeds the threshold value hl and the storage change and surface flow is calculated by:

$$UZ'_{t+1} = UZ_t + \Delta Q_{t+1} \cdot \Delta t$$

(4.8)

where: UZ′= adjusted water content of the upper reservoir

UZ= actual water content of the upper reservoir

$$Q_{0,t+1} = \max\left(\frac{1}{k_0} \cdot \left(UZ'_{t+1} - hl\right); 0\right) \tag{4.9}$$

where: Q_0 = surface runoff

k_0 = storage coefficient for upper reservoir, upper outlet

hl = threshold value in upper reservoir

with the updated soil water content in upper reservoir (see Eq. (4.10)) the interflow and the percolation to the lower reservoir are calculated by:

$$UZ''_{t+1} = UZ'_t - Q_{0,t+1} \cdot \Delta t \tag{4.10}$$

$$Q_{1,t+1} = \frac{1}{k_1} \cdot UZ''_t \tag{4.11}$$

$$UZ'''_t = UZ''_t - Q_{1,t+1} \cdot \Delta t \tag{4.12}$$

$$Q_{perc,t+1} = \frac{1}{k_{perk}} \cdot UZ'''_t \tag{4.13}$$

where: UZ″ and UZ‴= updated water content of upper reservoir
Q_1=interflow
k1 =storage coefficient for upper reservoir, lower outlet
Q_{perk} =percolation
K_{perk} = storage coefficient for percolation from upper to lower reservoir

Therefore, the final actual water content of the upper reservoir at t+1 time step is:

$$UZ_{t+1} = UZ'''_t - Q_{perc,t+1} \cdot \Delta t \tag{4.14}$$

The outflow from the lower reservoir is consider to be the base flow with the linear relationship between storage and flow:

$$LZ'_t = LZ_t + Q_{perc,t+1} \cdot \Delta t \tag{4.15}$$

$$Q_{2,t+1} = \frac{1}{k_2} \cdot LZ'_t \tag{4.16}$$

$$LZ_{t+1} = LZ'_t - Q_{2,t+1} \cdot \Delta t \tag{4.17}$$

where: LZ′ and LZ =actual water content of the lower reservoir
Q_2= baseflow
k_2 = the storage coefficient for lower reservoir

The total runoff at the outlet of a certain basin is then smoothed by the use of a simple triangular transformation function. The routing parameter maxbas describes the approximate delayed time steps of this transfer function. This is the runoff at the outlet of a sub-basin (or catchment). If more sub-basins are connected to each other the river routing is realized by the Muskingum method. Two parameters, mk and mx, have to be derived for this method. Details can be found in the literature, e.g. Chow et al. 1988.

The model parameters are explained in Table 4.1 and only 6 parameters indicated with grey color are selected for the calibration. These are all conceptual parameters which are often not easy to estimate from physical catchment properties. Besides, they have been tested to be sensitive with respect to their impact on model output. Further details about the model parameters can be found in Hundecha and Bárdossy (2004) and Wallner et al. (2013).

Table 4.1 Hydrological model parameters with units and meaningful range for this study

Module	Optimized HBV model parameters	Description and unit	Prior range
Snow	wsmf	wet snow melt factor accounting for faster snow melt when precipitation occurs [mm^{-1}]	1 — 4
	tt	threshold temperature for snowmelt [°C]	-2 — 2
	dd	degree day factor accounting for daily amount of snowmelt [$mm°C^{-1}d^{-1}$]	0.5 — 5
Soil	fc	the maximum soil moisture storage [mm]	30 — 600
	β	a shape coefficient [-]	0.5 — 8.0
Response	hl	a threshold value of water content in the upper reservoir [mm]	1 — 30
	k0	top recession coefficient of the upper reservoir [d]	0.25 — 5.00
	k1	second recession coefficient of the upper reservoir [d]	5— 50
	k2	recession coefficient of the lower reservoir [d]	10— 500
	K_{Perc}	storage coefficient of the percolation [d]	3 — 50
Tansform Routing	maxbas	base length of the triangular unit hydrograph [h]	3 — 10
	mx	weighting factor [-]	0.1 — 0.4
	mk	retention constant [h]	0.25— 10

Optimization algorithms: Dynamically Dimensioned Search algorithm (DDS)

Almost all runoff simulation models contain effective conceptual or physical model parameters that are either difficult or impossible to measure directly. Therefore, applications of these models are required that model parameters should be adjusted to obtain the predictions closely enough replicating the observed system response data. The tradition approach to solve this problem is manually by trial and error which may be difficult to implement for some complex model calibration situations and extremely labor intensive. Automatic calibration is described as an optimization algorithm based search for a set of model parameters that can minimize the model prediction errors compared with available measured data for the system being modeled. As compared with manual calibration, automatic calibration is fast and the confidence of the model simulations can be explicitly stated (Madsen 2000; Sorooshian and Dracup 1980; Sorooshian and Gupta 1983).

Research into optimization methods has led to several optimization algorithms, such as, the shuffled complex evolution developed at the University of Arizona (SCE-UA) (Duan et al. 1993), PEST (Kim et al. 2007) and Dynamically Dimensioned Search algorithm (DDS). In this thesis, the focus is on long term continuous hydrological modeling with the conceptual model HBV at both a daily and an hourly time step for subsequent flood frequency analysis using DDS algorithm. The scheme of DDS algorithm implemented to calibrate the HBV model is shown in Figure 4.2.

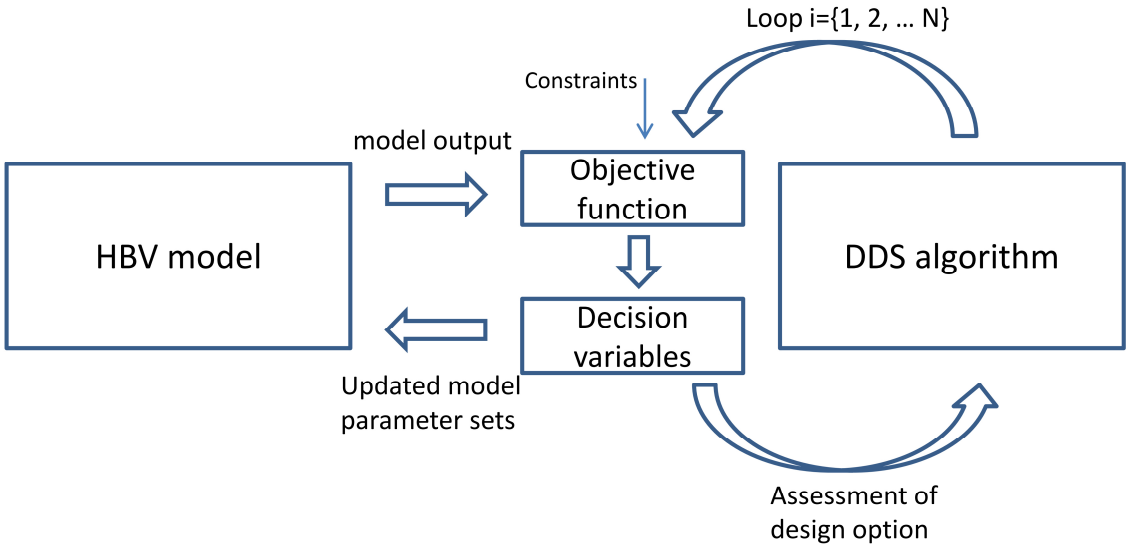

Figure 4.2: The scheme of DDS algorithm interacted with HBV model

The dynamically dimensioned search (DDS) is a stochastic, single objective search algorithm which has been proved to be efficient in finding 'good quality' global solutions (see Tolson and Shoemaker (2007)). Based on the way the neighborhood can be dynamically adjusted

when the dimension of the search changes, it is unique in relation to current optimization algorithms. To be more specific, the DDS perturbation variances remain constant if the objective function keeps the same. The number of decision variables perturbed from their current best value decreases as the number of function evaluations becoming close to the maximum function evaluation limit.

Tolson and Shoemaker (2007) suggested the value of 0.2 for the scalar neighborhood size perturbation parameter (r) which associates the standard deviation of a random perturbation size with a fraction of the model parameter's range. The DDS algorithm searches globally at the start then becomes a more local search as the number of iterations reaches the maximum allowable number of function evaluations. The model parameters being calibrated in automatic calibration are the decision variables and the number of model parameter values being changed is the dimension being varied to generate a new search neighborhood. Initially, a subset of dimensions for perturbation is selected completely at random without reference to sensitivity information and perturbed by values randomly sampled from a normal distribution. Then the number of perturbed parameters decreases with an increasing number of iterations to let the solver search more globally at the beginning and more locally at the end of the optimization process. In this study, the DDS algorithm is implemented to calibrate the HBV model in a lumped mode on both daily and hourly time steps with a total evaluation number of 2000 iterations.

Six steps are involved in the DDS algorithm as:

Step 1: define DDS inputs including neighborhood perturbation size parameter, r =0.2; lower and upper bounds (x^{min}, x^{max}) and initial solution for all the model parameters being optimized, $X^{t=0}=[x_1,\ldots x_D]$, and the maximum number of evaluation times M.

Step 2: set the iteration counter to 1, k=1 and evaluate the objective function F with the given initial solution, assuming $X^{best}=X^{t=0}$ and $F_{best}=F(X^{t=0})$.

Step 3: for d =1,…D decision variables, modify all the decision variables x_d according to the following rule:

$$x_d^{new}=\begin{cases} x_d^{best}+\left(x_d^{\max}-x_d^{\min}\right)\cdot r\cdot N(0,1) & if \quad U(0,1)<1-\dfrac{\ln(k)}{\ln(M)} \\ x_d^{best} & otherwise \end{cases} \tag{4.18}$$

where x_d is the best achieved for the entry decision variable d, N(0,1) is a standard normal distribution with a mean of 0 and standard deviation 1; U(0,1) is a uniform distribution and a random number can then be generated in the interval [0,1]; k is the current iteration count.

Step 4: The one dimensional decision variable perturbations in this step can generate new decision variable values outside of the box constraints. In order to make the new decision variable respect the bounds in the DDS algorithm, the minimum and maximum decision variable limits represent as reflecting boundaries. The values of the decision variables will be adjusted if necessary:

$$x_d^{new} = \begin{cases} x_d^{\min} + \left(x_d^{\min} - x_d\right) & if \quad x_d < x_d^{\min} \\ x_d^{\max} - \left(x_d - x_d^{\max}\right) & if \quad x_d > x_d^{\max} \end{cases} \tag{4.19}$$

or

$$x_d^{new} = \begin{cases} x_d^{\max} & if \quad x_d < x_d^{\min} \\ x_d^{\min} & if \quad x_d > x_d^{\max} \end{cases} \tag{4.20}$$

Step5: evaluate $F(X^{new})$ and update current best solution if necessary:

$$F_{best} = F\left(X^{new}\right); X^{best} = X^{new} \quad if \quad F\left(X^{new}\right) \le F_{best} \tag{4.21}$$

Step6: set iteration count k=k+1 and check stopping criterion:
if k=M, stop or else go to step 3.

Noted that regardless of whether the maximum function evaluation number is 10 or 10,000, the DDS algorithm scales the search strategy from global in the initial iteration to more local in the final iteration.

Calibration strategies

For the purpose of operational predictions, the usefulness of a hydrological model mainly depends on how well the model can be calibrated. If the parameters are poorly estimated, the model behavior of the catchment of interest can be quite different from those actually observed. Therefore, appropriate calibration is a key issue in hydrological modeling since all the models have parameters that need to be specified or identified, and much attention has been required to it.

Two different calibration strategies, representative of different ways of interpreting the calibration process to evaluate model performances with respect to estimation of IPFs are compared. The first one is referred to hydrograph calibration (hydr_d) which associates the model parameters with flow time series process. The second strategy (CDF_d) results in the determination of a set of parameters associated with four different flow statistics.
The objective functions used for both strategies are a combination of Nash-Sutcliffe coefficient (NSC) after Nash and Sutcliffe (1970) for different flow criteria.

For the calibration against the observed hydrograph where the model is forced with observed daily climate data, the objective function is:

$$OF_1 = 0.5 \cdot NSC + 0.5 \cdot NSC_{\log} \tag{4.22}$$

where NSC_{log} stands for the NSC calibrated with log transformed flows. The log-transformed discharges to emphasize low flows to provid equal attention to both high and low flows.

In the light of the second CDF_d strategy a weighted total Nash-Sutcliffe coefficient (NSC) is computed from the following objective function.

$$OF_2 = 0.275 \cdot NSC_{CDF-SUM} + 0.275 \cdot NSC_{CDF-WIN} + 0.20 \cdot NSC_{FDC} + 0.25 \cdot NSC_{MDF} \tag{4.23}$$

where the index CDF stands for the Cumulative distribution function of daily extremes for summer (SUM) and winter (WIN) respectively; FDC is flow duration curve and MDF is annual maximum daily flow series; As the main focus of this paper is the simulation of extremes the sum of weights for summer and winter is set to 55%. The remaining 45% are then portioned between annual maximum daily series and flow duration curve.

Traditional approach to determine the success of hydrological models often depend on the minimization of the differences between observed and simulated runoff time series, namely using hydrograph calibration (hydr_d). It can fully describe the water balance variability and provides an effective way of simulating the observations through the process of calibration. But, calibration on the exact hydrograph gives rise to limited feedback on areas of model deficiency and sensitivity to model parameters. Since it cannot give variable importance of the performance with flow magnitudes, this method may results with unsatisfactory extreme values.

CDF_d calibration strategy requires sufficient information content to make reliable estimation of parameters. This presents considerable insight into catchment runoff response and also enables us to assess how well the hydrological model is able to predict the flow response of the catchment without dependency on hydrograph fitting. Since it focuses on reproducing the observed discharge frequency distribution, better IPF simulation results are expected. Besides, this method is able to evaluate the model performance when observation time periods for model input data and discharge do not overlap.

4.1.2 Disaggregation rainfall model

A large variety of rainfall disaggregation methods have appeared in hydrological literature and used in hydrological applications such as urban hydrology, flood risk assessment and erosion investigations (Jebari et al. 2012; Licznar et al. 2011). For the calibration of the models long, high-resolution time series of rainfall are necessary. Observed time series of this kind are often too short. On the contrary, time series from non-recording rainfall stations (daily values) exist for much longer periods and with a higher network density. The disaggregation of these values using information of the time-series from nearby recording stations can be a possible solution for the data scarcity (Koutsoyiannis et al. 2003). For this study a multiplicative random cascade model (Güntner et al. 2001; Olsson 1998) is used, that has been modified and adapted to the study region in Northern Germany (Müller and Haberlandt 2015).

The scheme of the basic version of cascade model is shown in Figure 4.3. The cascade model is micro-canonical, so the rainfall amount is conserved exactly during the disaggregation procedure for each time step. The rainfall amount of one coarse time step (here daily) is divided into *b* finer time steps with equal length, where *b* is called the branching number. With *b =2* in the first disaggregation step a temporal resolution of 12 h is achieved. For further disaggregation steps, temporal resolutions of 6 h, 3 h and finally 1.5 hour are achieved. There are three possibilities (P) as to how the rainfall amount splits in each time interval: dry/wet with P(0/1), wet/dry with P(1/0), wet/wet with P(x/1-x) illustrated in Eq. (4.24).

$$W_1, W_2 = \begin{cases} 0 \; and \; 1 & with \; P(0/1) \\ 1 \; and \; 0 & with \; P(1/0) \\ x \; and \; 1-x & with \; P\left(x/(1-x)\right); 0 < x < 1 \end{cases} \tag{4.24}$$

where W_1 and W_2 are multiplicative weights and their sum is equal to 1.

The basic version of the cascade model requires four parameters which depend on the position and the rainfall volume of each time step. There are four classes of position of a time step: starting boxes (dry-wet-wet) preceded by a dry time step, succeeded by a wet time step; ending boxes (wet-wet-dry); enclosed boxes (wet-wet-wet) and isolated boxes (dry-wet-dry) (Olsson 1998). These parameters for the model can be estimated from the nearest recorded high resolution stations and running the model backwards.

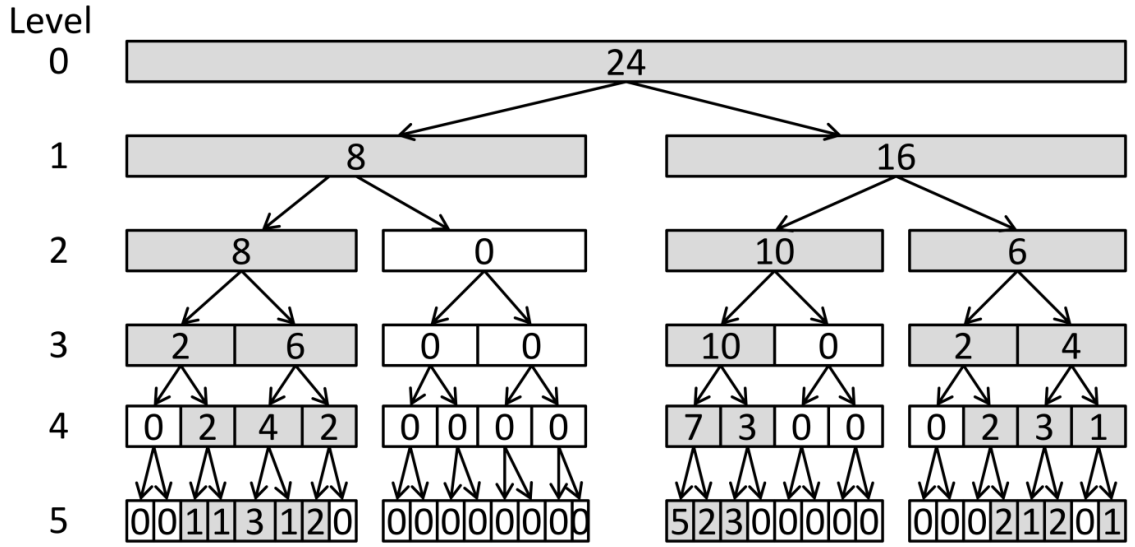

Figure 4.3: Scheme of the basic cascade model for rainfall disaggregation (modified from Müller and Haberlandt 2015)

Since the above disaggregation procedure starting with daily values can only result in a temporal resolution of 1.5h or 0.75h rainfall data while hourly rainfall data are needed in most cases. To overcome this problem, here, the model divides the observed daily precipitation into three equal sized non-overlapping boxes in the first step. Then the branch number b=2 is selected for the following disaggregation steps. Therefore, rainfall time series with resolutions of 1h can be obtained. The scheme of the updated version of the cascade model is shown in Figure 4.4. Depending on the wet or dry state of the adjacent time intervals and rainfall amount, the parameters for the model are estimated from the nearest hourly recording stations. For more details about the disaggregation procedure, see Müller and Haberlandt (2015).

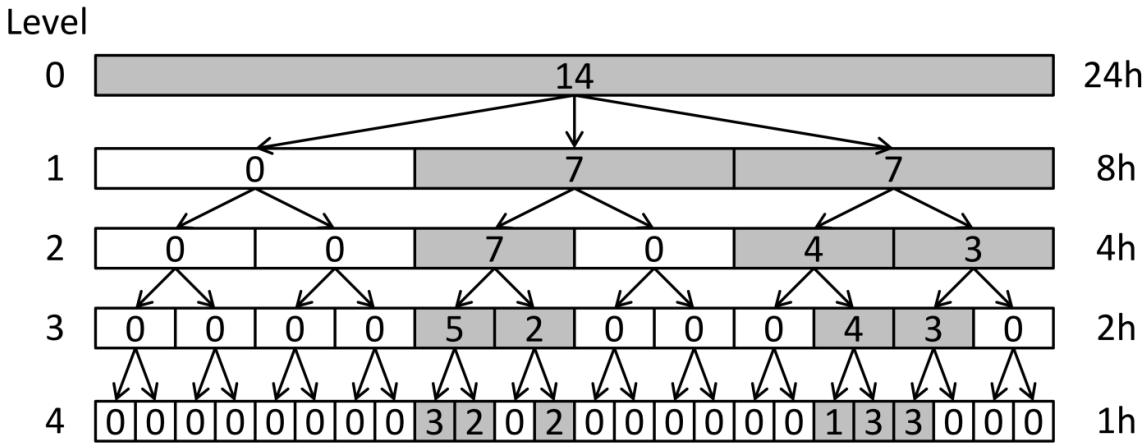

Figure 4.4: Scheme of the updated cascade model for rainfall disaggregation (modified from Müller and Haberlandt 2015)

The possibilities of splitting during the first disaggregation steps are as follows:

$$W_1, W_2, W_3 = \begin{cases} 1,0 \; and \; 0 & with \; P(0/0/1) \\ 0,1 \; and \; 0 & with \; P(0/0/1) \\ 0,0 \; and \; 1 & with \; P(0/0/1) \\ \frac{1}{2}, \frac{1}{2} \; and \; 0 & with \; P\left(0/\frac{1}{2}/\frac{1}{2}\right) \\ \frac{1}{2}, 0 \; and \; \frac{1}{2} & with \; P\left(0/\frac{1}{2}/\frac{1}{2}\right) \\ 0, \frac{1}{2} \; and \; \frac{1}{2} & with \; P\left(0/\frac{1}{2}/\frac{1}{2}\right) \\ \frac{1}{3}, \frac{1}{3} \; and \; \frac{1}{3} & with \; P\left(\frac{1}{3}/\frac{1}{3}/\frac{1}{3}\right) \end{cases} \tag{4.25}$$

As the impact of diurnal variation of the evaporation and temperature is of low importance for this study, the daily temperature values are regarded as constant over the whole day, while the daily evaporation values are uniformly divided over 24 hours.

4.1.3 Post correction and pre-processing approaches

Post-correction approach

For the post-correction approach the hydrological model is operated at a daily time step followed by a subsequent correction of the daily extremes into instantaneous peak flows (IPFs). An advantage of it is the availability of longer (more than 30 years in our case) and higher quality observation records based on the denser runoff and climate networks.
The approach consists of three steps:

Step 1: Calibrate the hydrological model on daily flow statistics (CDF_d) and hydrograph (hydr_d) respectively.

Step 2: Select the sample of the annual maximum daily winter/summer flows from the simulations and fit Generalized Extreme Value (GEV) distributions to both samples. Estimate the daily flow quantiles for four different return periods (T=10, 20, 50, 100 yr).

Step 3: Post correct the MDF quantiles using multiple regression equation which has already been derived in our former research to obtain the IPF from MDF (See Chapter 3):

$$HQ_{IPF} = \alpha_1 \cdot HQ_{MDF} + \alpha_2 \cdot lst\_fp + \alpha_3 \cdot Elv\_ds + \alpha_0 \quad (4.26)$$

where α_0 … α_3 are regression coefficients; HQ_{MDF} denotes the daily flow quantiles obtained from hydrological simulations and HQ_{IPF} denotes the estimated instantaneous peak flow quantiles; lst_fp and Elv_ds respesent longest flow path and minimum elevation of study basins respectively.

Pre-processing approach

In order to provide a basis for the direct simulation of instantaneous peak flows, synthetic hourly precipitation has been used given the restricted availability of long continuous rainfall series data with high temporal and sufficient spatial resolution. This method consists of the following points:

- Disaggregate the observed daily precipitation into hourly precipitation. In order to consider the uncertainty in the disaggregation process, 10 realizations of hourly rainfall are generated from historical daily data (see section 4.1.2).

- The calibration of the model with CDF_h strategy is carried out using disaggregated precipitation from the first step and observed flow statistics on an hourly base of the same time period. The objective function to assess the hourly model performance is OF_3.

  $$OF_3 = 0.275 \cdot NSC_{CDF-SUM} + 0.275 \cdot NSC_{CDF-WIN} + 0.20 \cdot NSC_{FDC} + 0.25 \cdot NSC_{IPF} \quad (4.27)$$

  where the index CDF stands for the Cumulative distribution function of hourly extremes for summer (SUM) and winter (WIN) respectively; FDC is flow duration curve and IPF is annual instantaneous peak flow series.

- Derive the mean flow quantiles obtained from the 10 GEV distributions which are obtained from the 10 disaggregation realizations. The parameters for hydr_h are derived by calibration of the model on shorter hourly hydrographs where the objective function is the same as Eq. (4.22), except for the time step of the flows.

Evaluation of the performance of estimating IPFs

The Root mean square error (RMSE), bias and Nash-Sutcliffe coefficient (NSC) (Nash and Sutcliffe 1970) are the criteria applied for the evaluation of model performance. The root mean square error is given by:

$$RMSE = \sqrt{\frac{1}{N}\sum_{i=1}^{N}\left(\frac{HQ_i^* - HQ_i}{HQ_i}\right)^2} \tag{4.28}$$

the bias criterion is:

$$Bias = \frac{1}{N}\cdot\sum_{i=1}^{N}\left(\frac{HQ_i^* - HQ_i}{HQ_i}\right) \tag{4.29}$$

where N is the number of stream flow stations; HQ_i^* and HQ_i denote estimated and observed peak flow values respectively.

NSC is computed as:

$$NSC = 1 - \left[\frac{\sum_{i=1}^{n}\left(HQ_i^{obs} - HQ_i^{sim}\right)^2}{\sum_{i=1}^{n}\left(HQ_i^{obs} - HQ^{mean}\right)^2}\right] \tag{4.30}$$

where n is the total number of observations; HQ_i^{obs} and HQ_i^{sim} are the ith observed and modeled peak flows; HQ^{mean} is the mean of the observed peak discharge.

4.2 Study area and Data

The investigations are carried out for 18 catchments within the Aller-Leine River basin in northern Germany (see Figure 4.5). Its detailed catchment descriptions are given in Chapter 3. The 18 study catchments are located in different geomorphologic and climatologic areas. Three sample catchments highlighted in Figure 4.5 are selected to demonstrate selected results in detail for the following results section. Table 4.2 summarizes some of the hydrological characteristics of those catchments. The size of the catchments is from 45 km^2 to 633 km^2 and the annual precipitation varies between 730 mm/year to around 1500mm/year.

The third column in the table shows the time window of observed discharge as daily flows and monthly peak flow series.

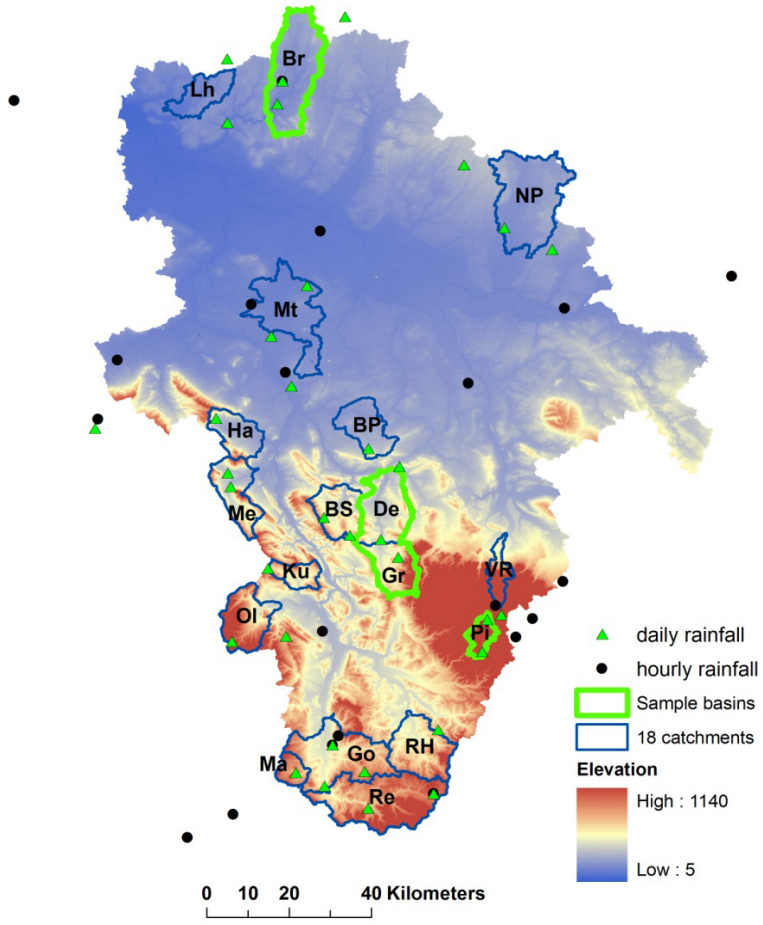

Figure 4.5: The locations of 18 subbasins of Aller-Leine catchment in northern Germany

Appropriate processing is performed to establish the distribution of important catchment characteristics based on the obtained different GIS digital data pertaining to the sub basins. These include a digital elevation model (DEM) with a resolution of 10 meters, a land use map and a river net work. The three characteristics (Area, longest flow path and minimum elevation) in Table 4.2 are derived from the digital elevation model (DEM). The portion of the forest land use type is derived from the land cover map CORINE2000 (see EUR 1994). Daily precipitation data from 244 stations covering the whole study area are obtained from the German Weather Service. Besides, there are 100 recording stations providing the hourly data.

Table 4.2 List of catchments and their basic descriptors

Nr (-)	basin name (-)	observed flow record (year)	annual precipitation (mm/year)	Area (Km2)	Longest flow path (m)	Min elevation (m)	urban (%)	agricultural (%)	forest (%)
1	BS	1968--2007	840.16	127	19689	96.8	4.81	67.99	27.37
2	BP	1967--2007	733.9	116	25747	67.5	6.33	87.58	6.26
3	Br	1962--2007	872.32	285	41802	41.0	4.7	42.75	51.91
4	Go	1959--2006	791.61	633	62868	141.5	7.03	66.95	26.04
5	Gr	1962--2006	1004.74	125	23915	129.4	7.91	48.85	43.22
6	Ha	1974--2007	838.62	104	25244	74.8	6.71	55.5	37.98
7	Ku	1962--2006	910.93	61.8	13524	130.2	1.97	70.39	27.73
8	Lh	1955--2007	854.3	100	25987	24.8	0.94	57.51	41.8
9	Ma	1964--2006	835.91	45	12035	196.2	0.98	67.63	31.49
10	Mt	1967--2007	748.98	242	36744	36.6	28.1	54.34	16.7
11	NP	1967--2006	737.17	334	40583	55.5	3.46	62.01	34.44
12	Ol	1962--2006	1004.16	149	25339	128.6	1.7	31.8	66.43
13	Pi	1952--2006	1537.94	44.5	17112	339.6	0.51	0.24	99.1
14	Re	1964--2006	793.69	321	43413	182.9	5.29	66.09	28.64
15	RH	1962--2006	781.71	184	24915	154.7	6.9	72.46	20.8
16	VR	1964--2006	1136.36	57.5	22158	133.1	15.88	19.19	65.18
17	De	1978--2007	899.57	309	49067	90.9	5.63	56.25	38.08
18	Me	1962--2007	889.15	136	27856	81.9	6.38	58.37	35.28

Records of precipitation with hourly temporal resolution are available around 6 years at a daily time step for the period between 1951 and 2008. The other climate data applied to force the hydrological model, such as temperature and evaporation are available for both temporal resolutions and time periods. Table 4.3 gives an overview of the time periods of these measurements.

Table 4.3 Time windows of hydrological data

variable	Daily	Hourly
runoff	29-44 yr	2004-2008
monthly peak flow	(-)	31-44 yr
precipitation	1951-2008	2003-2008
temperature	1951-2008	2003-2008
evaporation	1951-2008	2003-2008

4.3 Results

In this section, first the calibration results of the hydrological model using the observed daily data as input and using the two different calibration strategies (CDF_d and hydr_d) are presented. The multiple regression model is applied to post correct the simulated maximum daily flows (MDFs) into instantaneous peak flows (IPFs). Then the corresponding hourly simulation results by applying disaggregated daily rainfall data (CDF_h and hydr_h) are discussed. The performance and uncertainty of the four alternatives are finally compared for the purpose of estimating IPFs for the 18 catchments.

Note, that the conclusions are made based on a relative comparison involving only calibration results. A real validation of the hydrological model using a different data period is not feasible because of the short hourly observation period on one hand and the required full peak flow sample for calibration on extreme value statistics on the other hand.

4.3.1 Daily simulations with post-correction

Performance of the hydrological model calibrated on flow statistics (CDF_d)

Figure 4.6 shows comparisons between the fitted probability distributions of daily extremes in winter and summer for the sub-basins Br, De and Pi. These flood frequency results are calculated using observed and simulated daily flow data for over 30 years. The red solid line denotes the fitted GEV distribution on the observed annual daily extremes (black dots). The red dashed lines enclose the 90% confidence interval obtained by using bootstrap method after Efron and Tibshirani (1986). The black line corresponds to the simulated distributions,

generated using the parameter sets that achieve the best performance for the selected flow statistics. Since the small sample size may give rise to poor fitting of CDFs for observations, the comparison is then based on the more smooth and robust theoretical CDFs.

It is apparent from Figure 4.6 that the distribution functions corresponding to the simulated extremes seem to fit the functions derived from observations quite well in winter although there are some deviations in summer for both observed and simulated cases at the higher return periods. In those cases, given the observations only, there could be doubts about the accuracy of the observed peaks and ability of the hydrological model to simulate the flow peaks of similar magnitude corresponding to the same storm events that give rise to the observed peaks. Therefore, more care should be taken for the extrapolation of the fitted distributions in summer since extraordinary extremes appear more often than in winter season.

The uncertainty bands of the observed annual extreme values differ significantly in summer and winter. The wider extent of confidence interval in summer indicates greater uncertainty than in winter. Br catchment shows the best fits between the probability distributions derived from the observed and simulated flow peaks in both summer and winter season.

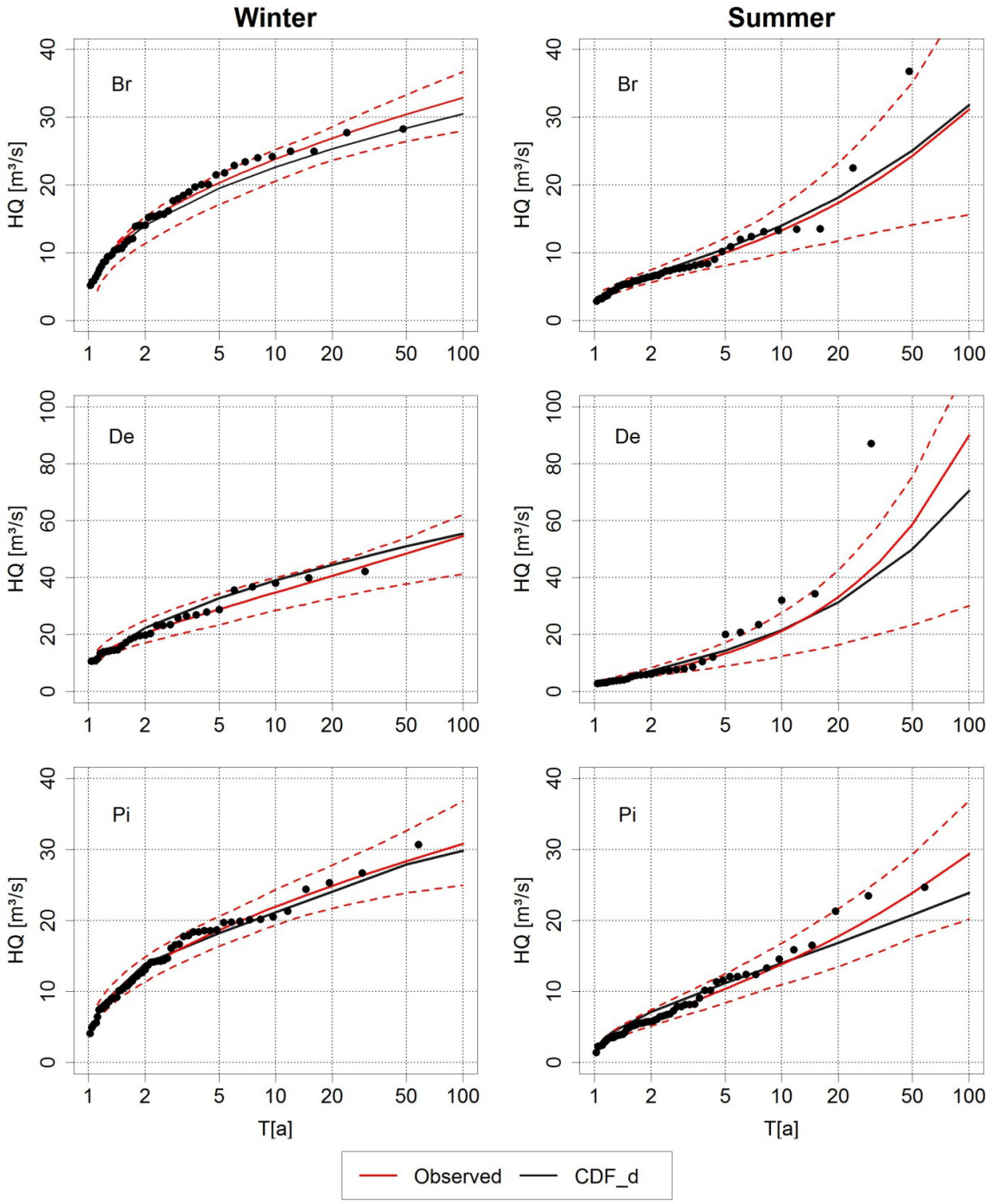

Figure 4.6: Observed and simulated fitted CDFs to daily extremes in winter and summer for the three sample catchments (Br/De/Pi); red dashed lines enclose the 90% confidence interval against observed peak flows

In order to investigate the performance of the hydrological model regarding winter and summer extremes for all 18 catchments, the fitted GEV distributions using observed and

simulated extremes are compared. For that a goodness of fit Chi-square test is performed and Figure 4.7 shows the results in the form of p-values. The red dashed line indicates a 5% significant level. A better the fit to the model is indicated by a larger p value. As can be seen, the estimation of winter peaks is far more robust than those in summer with median values (middle black line) in summer and winter of 0.05 and 0.41 respectively. This is consistent with the results obtained above regarding the three sample catchments.

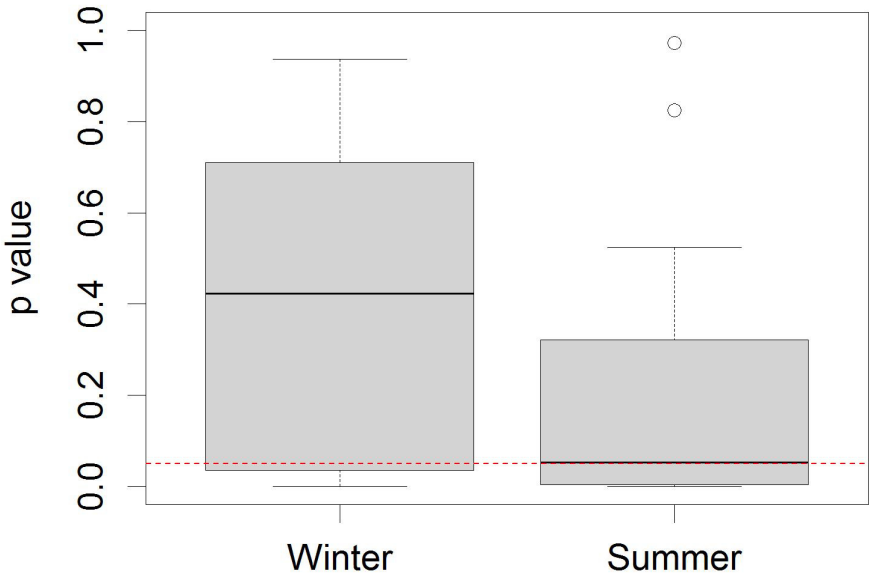

Figure 4.7: Boxplots of the p value over 18 catchments for the fitted GEV distribution between observed and simulated daily extremes in winter and summer respectively; red dashed line indicate the confidence line (a=0.05)

Figure 4.8 shows the visual assessments of simulated and observed flow duration curves (FDCs) (0.05, 0.25, 0.5, 0.75, 0.95, 0.975 Quantile). One can see that the general fit between simulated (red dashed line) and observed (blue line) FDCs is satisfactory although there are some overestimations in the low flow part of FDCs for the first two catchments. It is likely a result of higher weighting of high flows during the calibration process. In addition, quantative assessments of FDCs for all 18 sub catchments to check the overall quality of a given simulation are shown in Table 4. The average NSC value is 0.87 with a tendency to overestimation suggested by a positive bias value 20%.

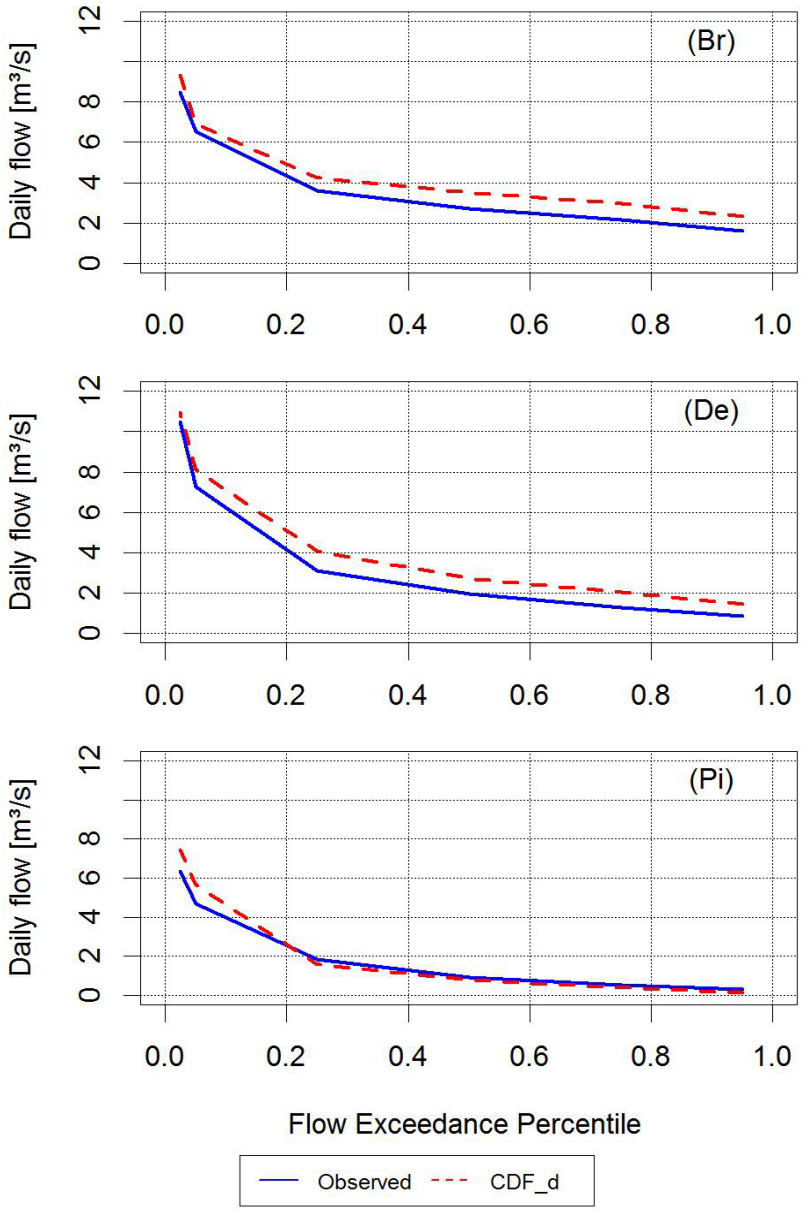

Figure 4.8: Comparison of observed and simulated daily flow duration curve (FDC) for the three sample catchments

Table 4.4 Calibration results of flow duration curve (FDC) using daily observed precipitation

FDC	Ku	Go	Re	VR	Br	De	RH	Lh	Pi	Me	Ha	BS	NP	Gr	BP	Ol	Ma	Mt
NSC [-]	0.95	0.96	0.94	0.94	0.91	0.92	0.74	0.60	0.93	0.98	0.91	0.89	0.96	0.91	0.93	0.98	0.94	0.95
Bias [%]	23.25	15.12	33.11	32.29	14.53	35.93	15.72	11.16	-12.07	10.81	17.99	19.75	17.74	32.33	32.44	18.57	42.07	9.23

Figure 4.9 illustrates the post correction results using multiple regression model (Ding et al. 2014) for a return period of 50 and 100 years among the whole study area in winter and summer. IPF (Obs) and IPF (Sim) indicate the quantiles of observed and simulated instantaneous peak flows respectively. R^2 is the coefficient of determination and RMSE is the root mean square error. As might be expected, the estimation of the higher return period peaks (T=100yr) are subject to greater amounts of estimation error in both summer and winter season while the estimations in winter (RMSE=0.202) is better than in summer (RMSE=0.237)

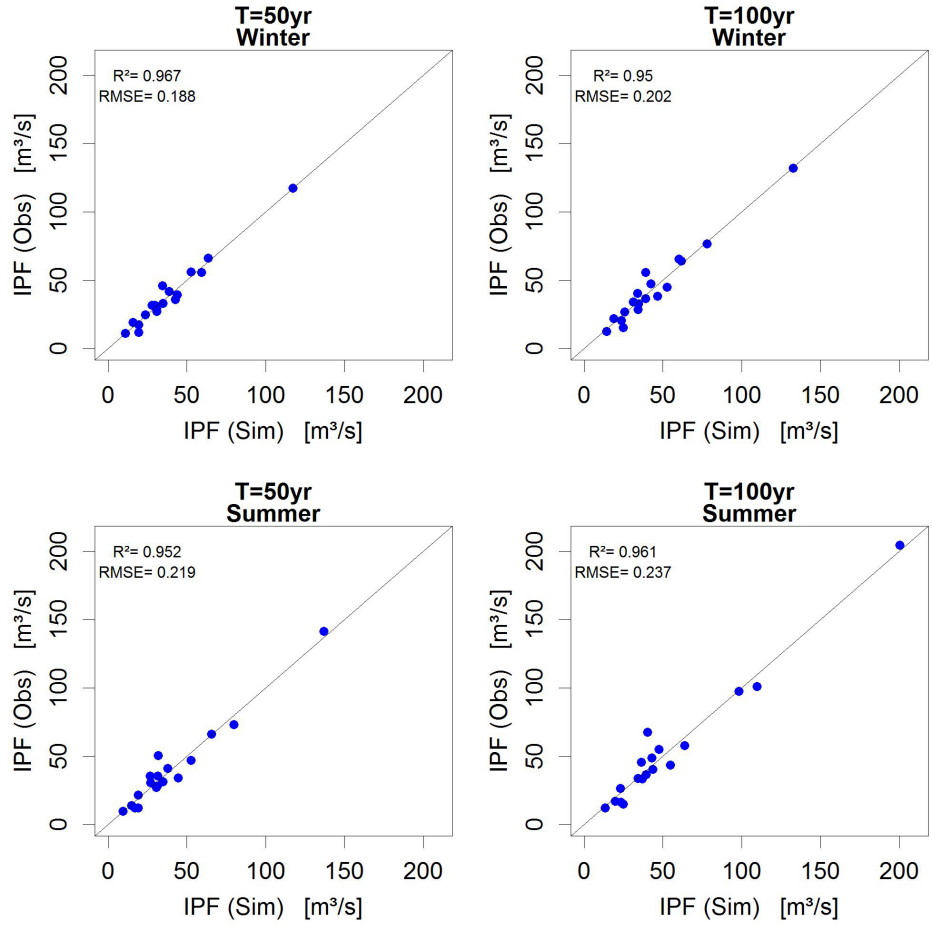

Figure 4.9: Comparison between the observed and simulated instantaneous peak flow in winter and summer using the CDF_d strategy at recurrence intervals of 50 and 100 years

Table 4.5 gives the results of multiple regression coefficients for all 18 sites where the simulated annual maximum daily flows obtained by using the CDF_d strategy are regressed with the observed annual instantaneous peak flows.

Table 4.5 Final results of multiple regression coefficients for all 18 sub catchments using CDF_d strategy

Regression Coefficients	α_0	α_1	α_2	α_3
T=10 yr	1.817	1.927	-0.00021	0.023
T=20 yr	2.846	1.916	-0.00030	0.032
T=50 yr	2.156	1.748	-0.00032	0.058
T=100 yr	-0.762	1.598	-0.00025	0.091

Performance of the hydrological model calibrated on daily hydrograph (hydr_d)

Turning to daily hydrograph simulation, it is important to notice that, all the observed climate and flow data are used here for calibration. Figure 4.10 shows only a portion of the calibration result (2005 and 2006 yr) at the three sample catchments. It can be seen that, in general, the low flows and the medium peak flows are estimated well although occasional underestimation of the higher peak flows are noticed in De and Pi catchments. Table 4.6 details the calibration results for all the 18 catchments in the form of their NSC and Bias value. One can see that good model fits to the observed flow time series data are achieved by hydrograph simulation, with NSC value between 0.70 and 0.89 and Bias between -1.31% and 5%.

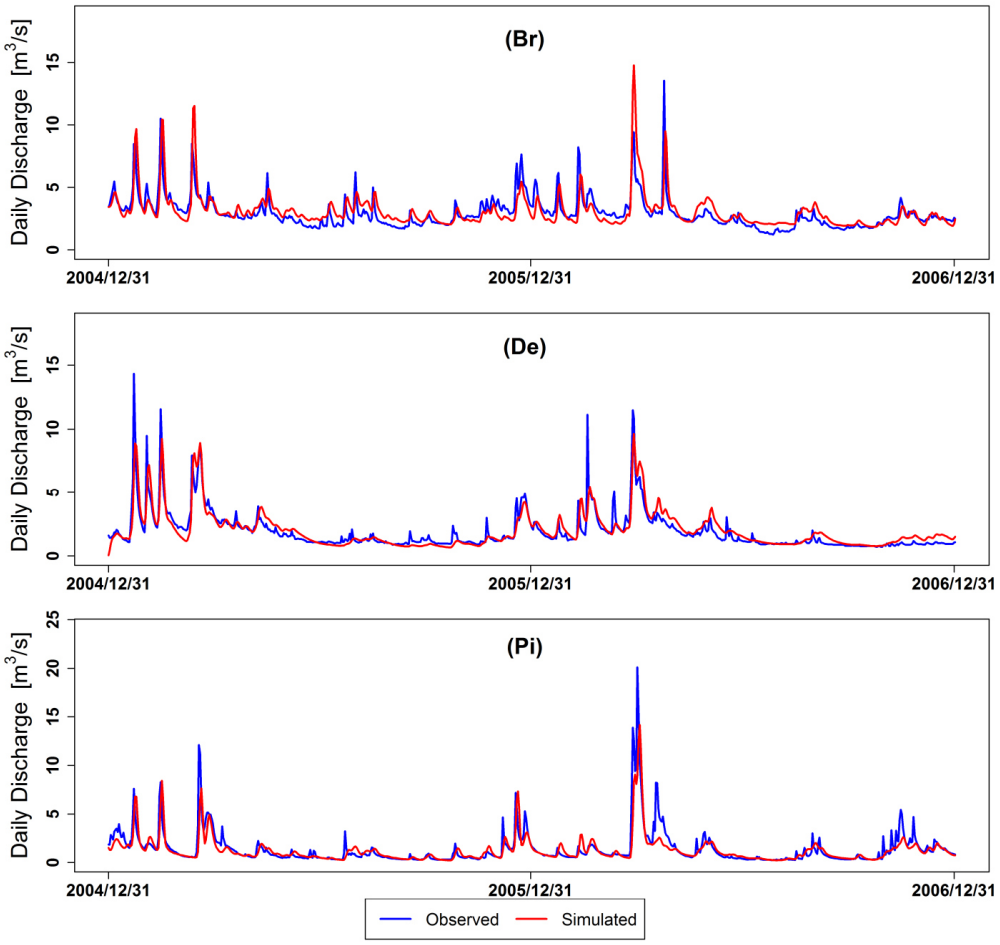

Figure 4.10: Example of observed and simulated daily hydrographs for the three sample catchments

Table 4.6 Calibration results for daily hydrographs over the whole record periods

hydr_d	BS	BP	Br	Go	Gr	Ha	Ku	Lh	Ma	Mt	NP	Ol	Pi	Re	RH	VR	De	Me
NSC [-]	0.76	0.75	0.80	0.89	0.79	0.8	0.75	0.71	0.73	0.81	0.74	0.83	0.82	0.82	0.74	0.70	0.85	0.81
Bias [%]	5	5	-0.56	-0.84	-0.25	1.18	3.15	-0.55	5.07	-1.11	-1.9	0.34	-1.31	0.44	-0.27	4.52	1.77	-0.8

Figure 4.11 shows the post correction results with respect to the selected maximum daily flow series from the hydrograph simulation. The discrepancies between the observed and simulated IPFs demonstrated here confirm the findings in Figure 4.9 with slightly worse estimation results for all the cases. Especially, the values of RMSE in winter are much higher than the ones obtained from CDF_d strategy.

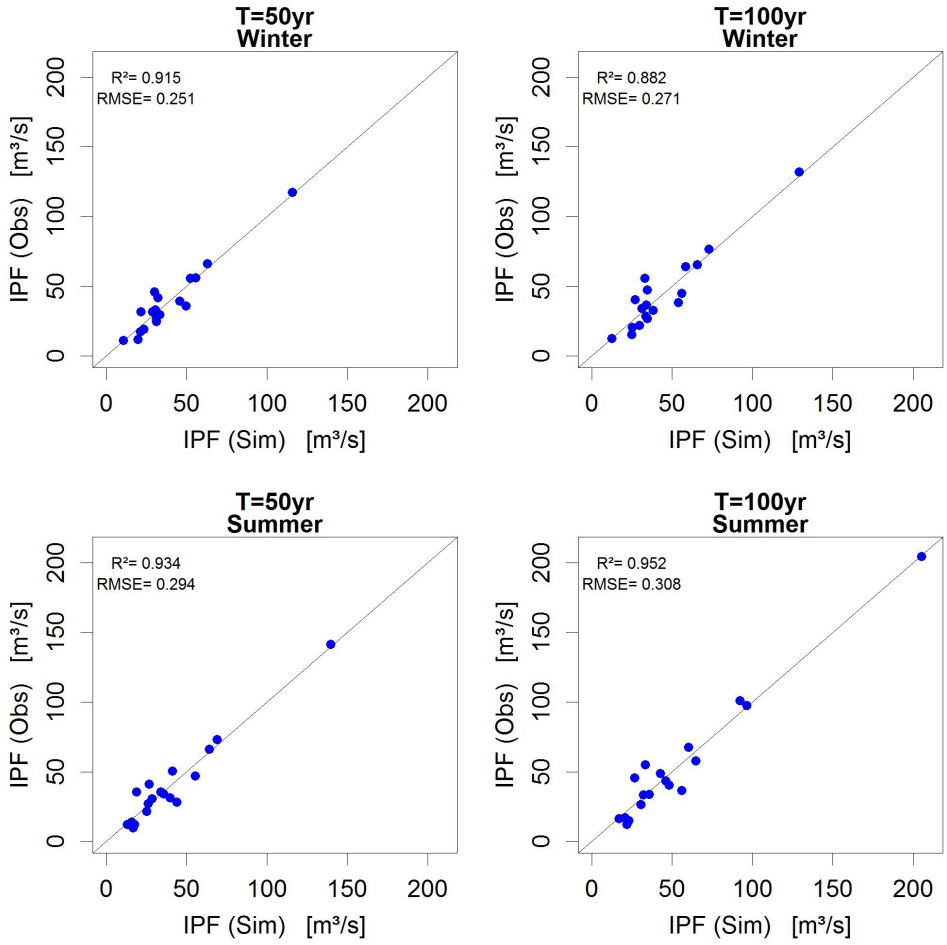

Figure 4.11: Comparison between the observed and simulated instantaneous peak flow in winter and summer using the hydr_d strategy at recurrence intervals of 50 and 100 years

Table 4.7 Final results of multiple regression coefficients for all 18 sub catchments using the hydr_d strategy

Regression Coefficients	α_0	α_1	α_2	α_3
T=10 yr	3.219	2.373	-0.00015	0.022
T=20 yr	8.842	2.900	-0.00040	0.003
T=50 yr	14.761	3.005	-0.00058	-0.012
T=100 yr	14.737	2.816	-0.00048	-0.005

Table 4.7 gives the final results of multiple regression coefficients for all 18 sites where the simulated annual maximum daily flows obtained using the hydr_d strategy are regressed with

the observed annual instantaneous peak flows. The comparison of regression coefficient α_0 in Table 4.5 and Table 4.7 indicates the hydrograph simulation leads to underestimation of peak flows. This case is especially true for the long return periods (T=50, 100yr) where α_0 =2.156,-0.762 for CDF calibration while α_0 around 14.7 for hydrograph calibration.

4.3.2 Hourly simulations with pre-processing

The results presented in this section are based on continuous hydrological simulations at an hourly time step for the whole observed period. The hydrological model is forced by disaggregated daily climate data and the obtained results from the two calibration strategies CDF_h and hydr_h are compared with the results from the corresponding daily simulations.

Performance of hydrological model calibrated on flow statistics (CDF_h)

Figure 4.12 shows comparisons between the fitted GEV distributions for the three sample catchments in summer and winter season. The red and black solid lines are the results based on observed and simulated annual maxima respectively. The red dashed lines enclose 90% confidence interval of the observed IPFs, represented by black dots. Compared with the corresponding results shown in Figure 4.6, it is apparent in Figure 4.12 that the fitted probability distributions from the simulated and observed peaks seem to match fairly well although with a slight overestimation. Unlike the significant underestimation of flows at higher return periods in summer for daily simulations (see Figure 4.6), a better agreement between the observed and simulated data fitted to GEV distributions can be seen here at T=100yr. However, it can also be noted that the agreement between the observed and simulated CDFs for lower return periods is a bit poorer than the corresponding daily simulations. Both the CDF_h and CDF_d strategies are more likely to identify a proper parameter set that reproduce the annual extremes of the observed flow data in winter than in summer.

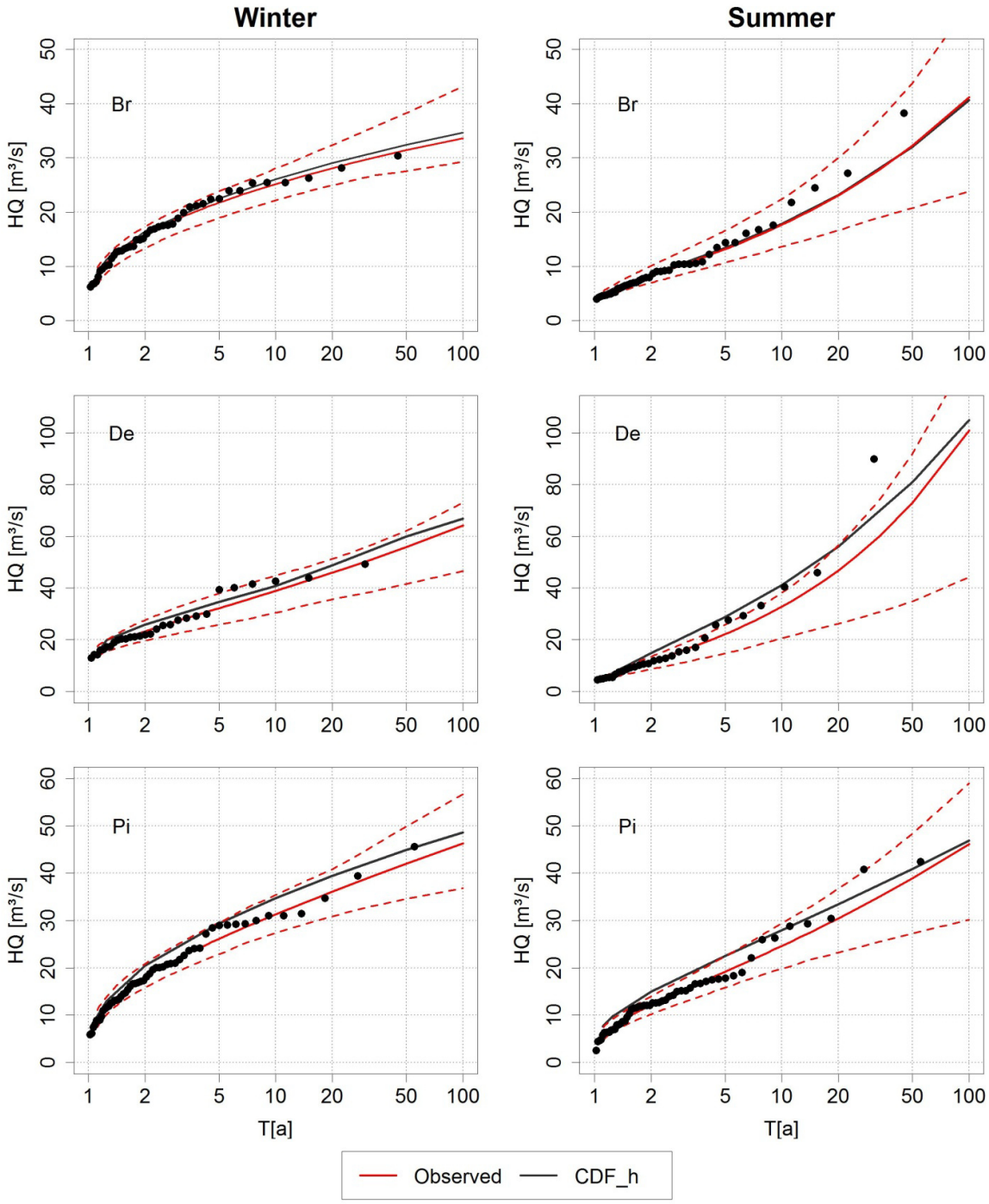

Figure 4.12: Observed and simulated fitted CDFs to hourly extremes in winter and summer for the three sample catchments (Br/De/Pi); red dashed lines enclose the 90% confidence interval against observed peak flows

Figure 4.13 shows the p-value results in winter and summer by Chi-square test where the better "goodness of fit" between the simulated and observed IPF frequency curves for all 18

catchments is indicated by a bigger p value. Those results support the findings in Figure 4.7, that the agreement of fitted frequency distributions using observed and simulated peaks is more robust in winter. Additionally, the parameter sets estimated by CDF calibration with the disaggregated daily precipitation give rise to a better fit between the observed and simulated GEV distribution curves in summer.

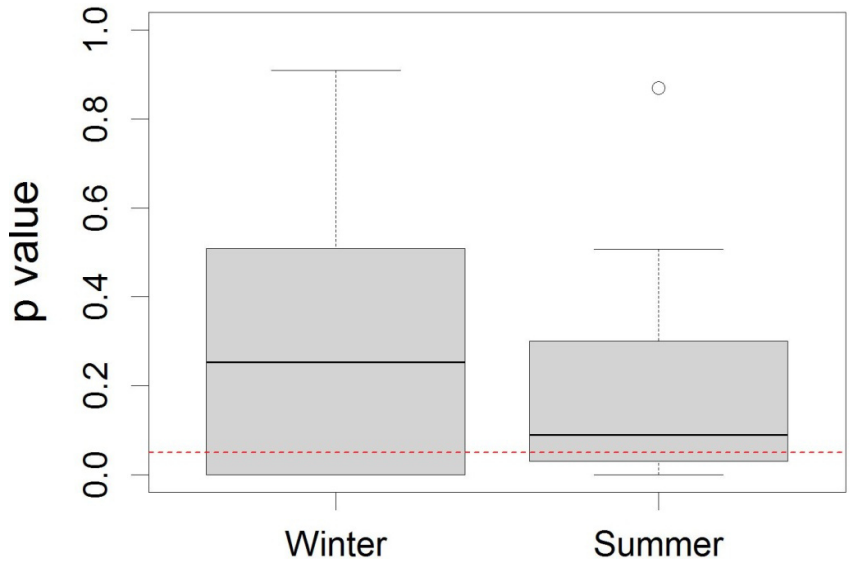

Figure 4.13: Boxplots of the p value over all sub catchments for the fitted GEV distribution on observed and simulated hourly extremes in winter and summer respectively; red dashed line indicate the confidence level of 95% (a=0.05)

A direct comparison of simulated and observed daily FDCs is done by aggregating the hourly simulated flow time series into daily values (Figure 4.12). Compared with Figure 4.6, it is apparent that, given the choice of the same target quantiles (0.05, 0.25, 0.5, 0.75, 0.95, 0.975), the aggregated hourly simulations are closer to the observed daily data series in these three sample catchments. The remaining results from the other 14 catchments except Lh shown in Table 4.8 also agree with it. The poorer estimation performance in Lh can be explained by the pre-processing procedure since the available daily and hourly rainfall stations involved in the disaggregation are not within the basin (see Figure 4.5). Given the relatively small sample size for FDC estimation, it is likely to have perfect NSC value (NSC=1) results, such as BP and Ol catchments.

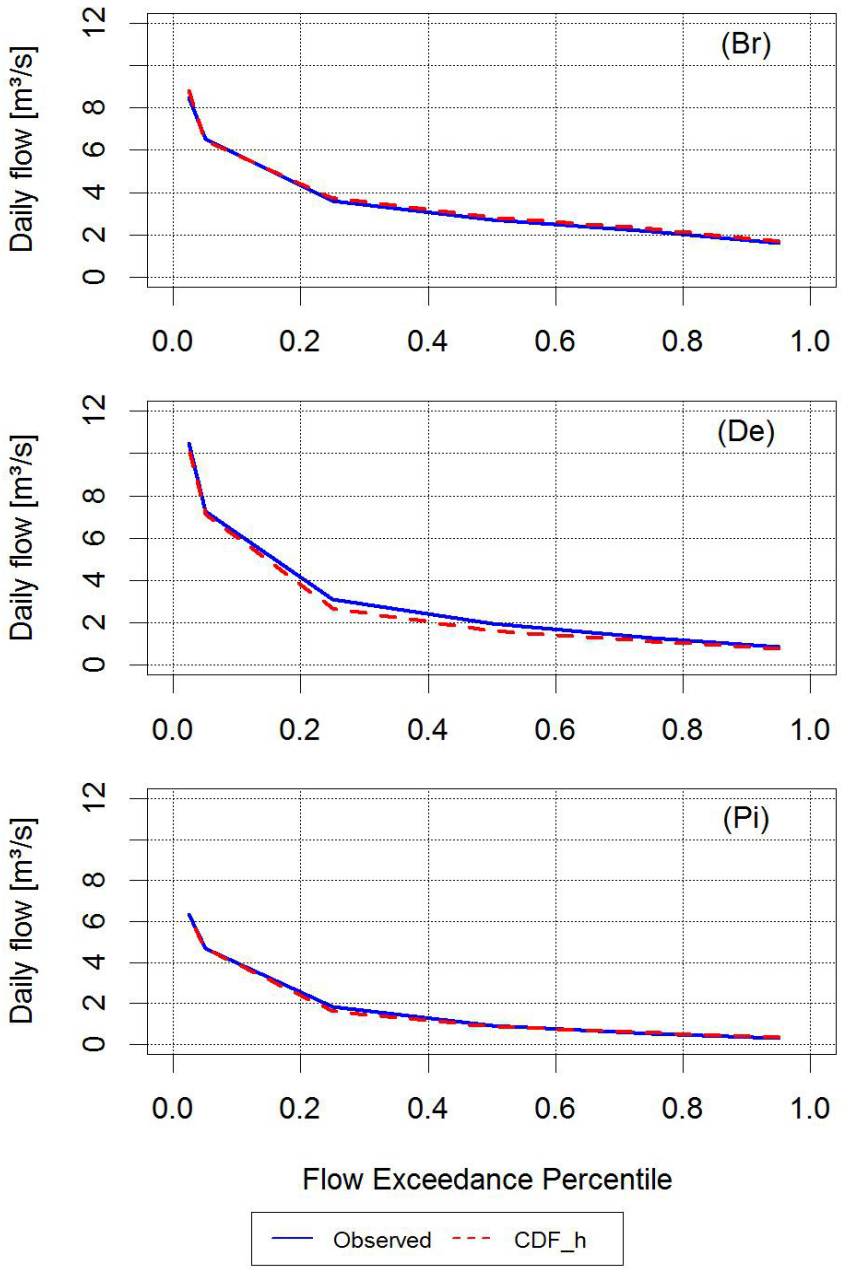

Figure 4.14: Comparison of observed and simulated daily flow duration curve (FDC) for the three sample basins at an hourly time step

Table 4.8 Calibration results of flow duration curve (FDC) using the Nash-Sutcliffe criterion (NSC) and the bias criteria

FDCs	Ku	Go	Re	VR	Br	De	RH	Lh	Pi	Me	Ha	BS	NP	Gr	BP	Ol	Ma	Mt
NSC [-]	0.94	0.99	0.97	0.92	0.97	0.96	0.94	0.51	0.97	0.89	0.96	0.95	0.98	0.99	1.00	1.00	0.81	0.98
Bias [%]	21.76	-4.88	5.19	33.31	12.78	-12.21	20.95	32.82	-11.43	30.61	23.21	26.50	0.79	6.87	0.31	2.57	-5.83	-13.23

Performance of hydrological model calibrated on hydrograph (hydr_h)

Turning to hourly hydrograph simulation, the visual assessment of the simulation of the three sample catchments is shown in Figure 4.15 and Table 4.9 details the quantitative assessment for all the 18 catchments. It can be seen, that the hydrological model describes the runoff dynamics well with the Nash values varied between 0.7 and 0.91 and Bias values varied between -15.5% and 13.62%.

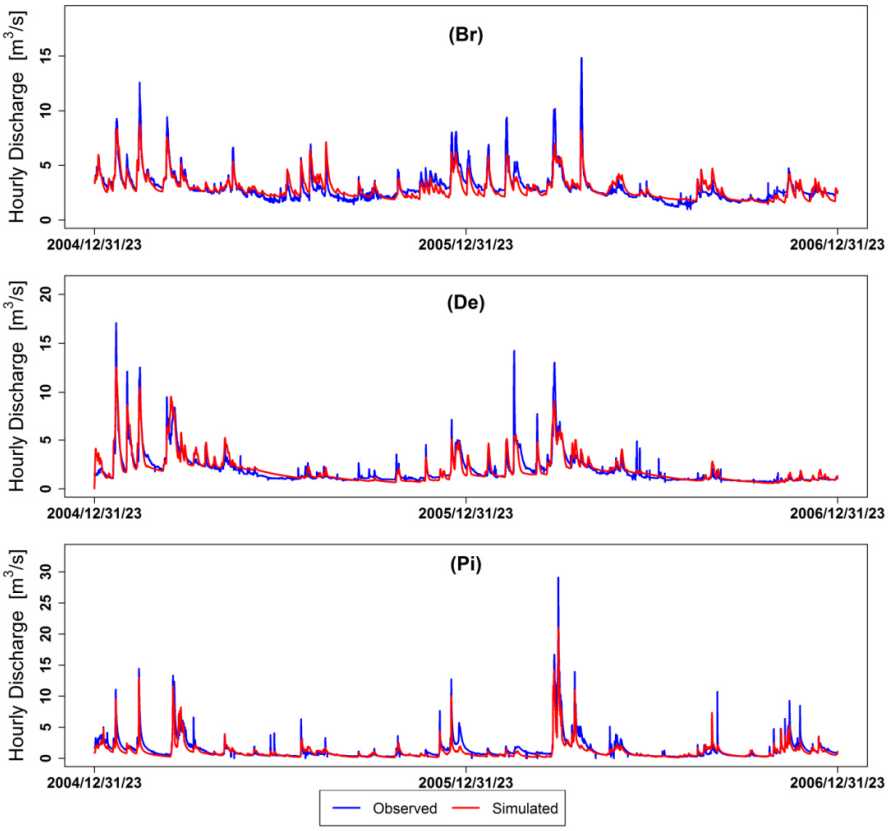

Figure 4.15: Comparison of observed and simulated hydrographs based on hourly observed precipitation for the three sample catchments

Table 4.9 Calibration results of continuous hourly hydrograph over the whole record periods

hydr_h	BS	BP	Br	Go	Gr	Ha	Ku	Lh	Ma	Mt	NP	Ol	Pi	Re	RH	VR	De	Me
NSC [-]	0.82	0.75	0.82	0.84	0.8	0.84	0.75	0.7	0.72	0.81	0.85	0.91	0.85	0.78	0.73	0.72	0.82	0.74
Bias [%]	7.83	13.62	-0.41	-0.61	12.3	3.71	-7.75	0.6	-2.66	0.09	2.98	3.29	-15.5	-2.9	2.14	-1.22	4.2	-5.67

4.3.3 Comparison between post-correction and pre-processing approaches

Uncertainty is inherent in any flood frequency estimation which results from various sources, such as the analytical techniques applied, the hydrological model regarding its structure and parameters and the limitations of the observed data series.

Figure 4.16 shows a comparison for the estimation of the 100 yr IPFs including uncertainty bands for the three sample catchments using all different methods (CDF_d, CDF_h, hydr_d, hydr_h). In order to consider the error from the hydrological model, 50 parameter sets are optimized for each method to obtain 50 sets of simulated flow peaks. Subsequently, bootstrap is applied to estimate the confidence intervals for the estimated 100 yr IPF with the observed and all sets of simulated flow peaks. For each parameter set, 500 samples of the same length as calibration period are generated using bootstrapping. This provides 25000 samples for estimation of the uncertainty range in this figure. The result based on the observed data series is referred to as OBS.

The uncertainty bands of OBS in summer are generally wider than in winter for the three sample catchments. Good estimation of IPFs is obtained by calibrating the model on flood frequency curves at both daily and hourly time steps (CDF_d and CDF_h) where CDF_h gives rise to a larger uncertainty range. The traditional calibration on hydrograph with observed long term daily (hydr_d) and short term hourly rainfall (hydr_h) performs generally poor. However, the daily hydrograph simulation (hydr_d) generates smaller uncertainty and better estimation results than the corresponding hourly simulation results (hydr_h). These findings are only proved in the three example catchments.

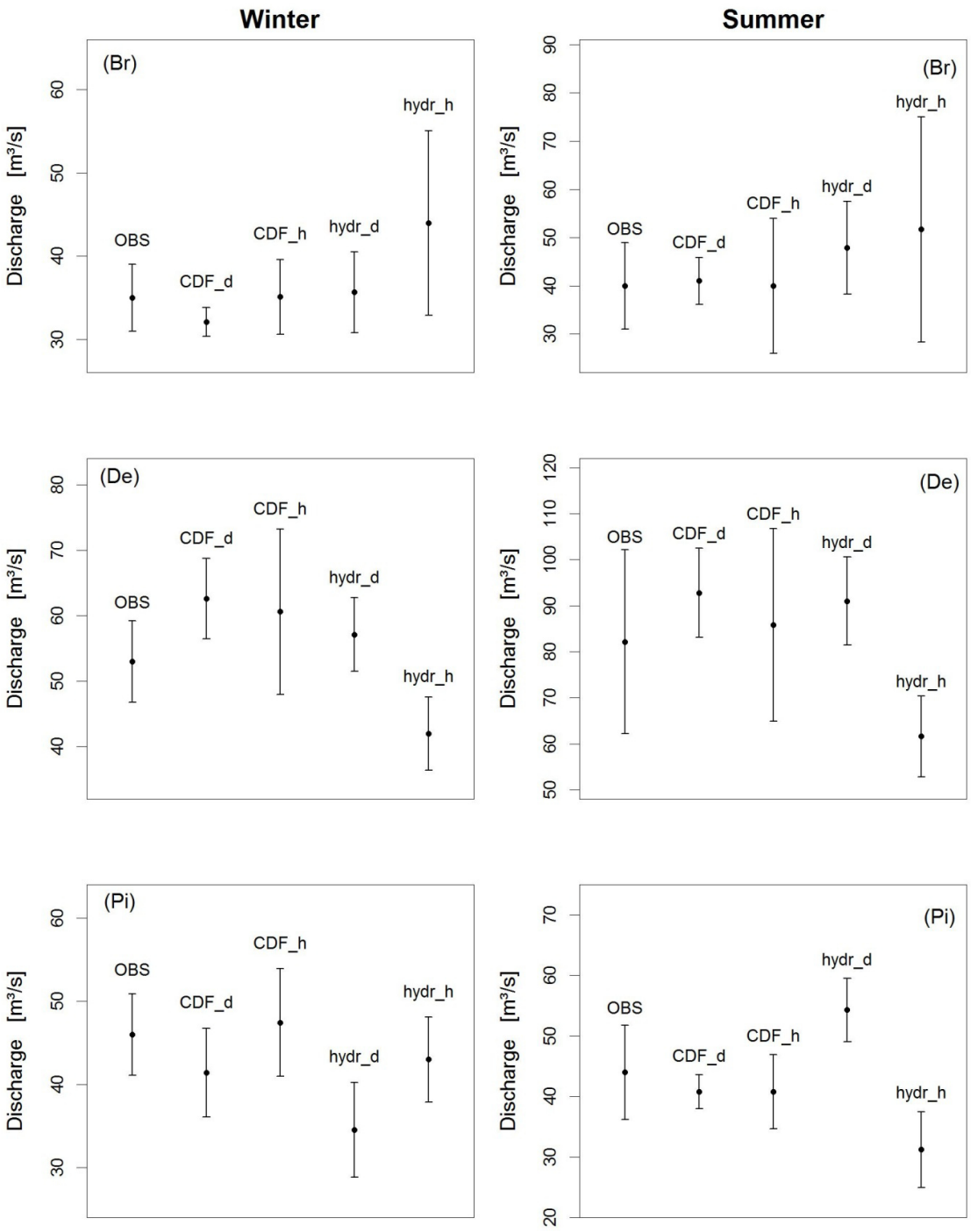

Figure 4.16: Estimated 100yr IPFs with 90% confidence bands for the three sample catchments by calibrating the model on flow statistics and hydrograph at daily and hourly step

Finally, to sum up the contrast between daily simulation with post correction and hourly simulation with pre-processing over the whole study area for four different return periods (T=10, 20, 50, 100yr) in summer and winter, the RMSE and bias criteria, are estimated to check the overall quality of a given simulation strategy. Figure 4.17 illustrates the averaged results for 18 gauges using daily observed climate data with post correction and disaggregated daily data with pre-processing to estimate the design IPFs by calibration on flood distributions. Accordingly, the results of Figure 4.18 are based on calibration using hydrographs.

The first column (MDF-IPF) represents the differences between the estimated quantiles of instantaneous peak flows (IPFs) and the corresponding maximum daily flows (MDFs) without any correction. As can be seen the immediate replacement of IPF with MDF can lead to significant underestimation with an average RMSE 30% and Bias -30% in winter and 35% and -35% in summer for the four return periods. The estimation from daily calibration with post correction is shown in the second column (CDF_d). The third column shows the estimation error from calibration at an hourly time step using disaggregated climate data as input (CDF_h).

Figure 4.17 shows in general that the model calibration at both temporal steps (daily and hourly) is able to effectively predict the IPF. However, using disaggregated daily rainfall as input provides the better overall estimation results with RMSE of 15 % in winter and 19% in summer although there is a slight underestimation in summer. The accuracy by calibrating the model on daily flow statistics with post correction is stable in summer and winter where the average RMSE is 22% with Bias 4%.

Turning to the hydrograph calibration strategy, Figure 4.18 shows the advantage of the hydr_d approach to estimate the IPFs where observed long-term daily rainfall data as input are combined with subsequent post-correction of daily peaks. This is more notable in the summer season. The RMSE from hydr_d is 25% and 27% for the return period of 50 yr and 100 yr, respectively while the hydr_h using disaggregated daily precipitation gives 30% for both periods.

Besides, the bias shows that there is a significant underestimation of IPFs in summer (-18%) and overestimation in winter (10%) when using the disaggregated daily precipitation (hydr_h). The daily simulation with post-correction (hydr_d) produces only small overestimation for both seasons (6% and 4% respectively).

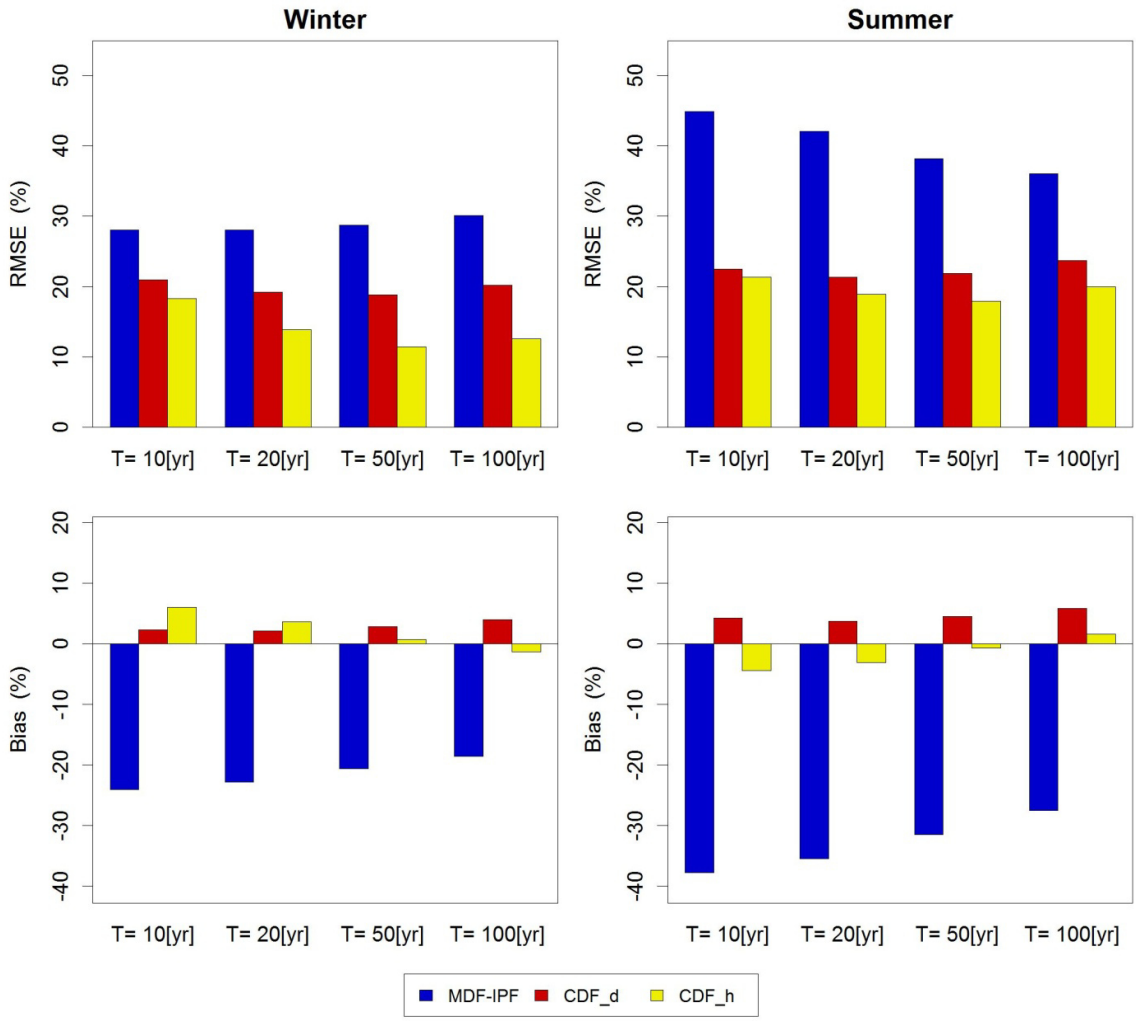

Figure 4.17: Comparison of the root mean square error (RMSE) and Bias using the CDF_d and CDF_h for summer and winter season averaged over 18 gauges

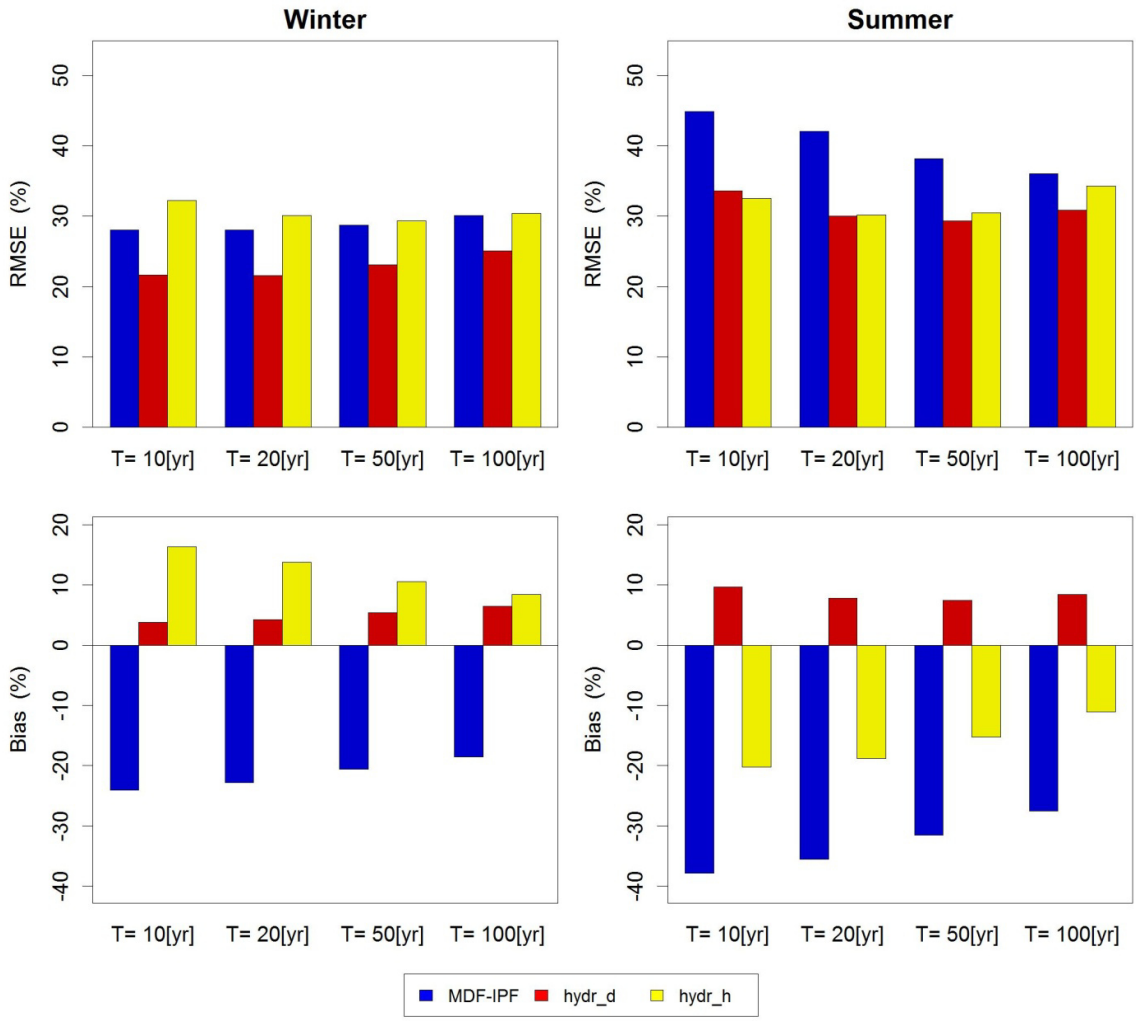

Figure 4.18: Comparison of the root mean square error (RMSE) and Bias using the hydr_d and hydr_h for summer and winter season averaged over 18 gauges

4.4 Conclusions and discussions

This research compares two different approaches for the estimation of instantaneous peak flows (IPFs), namely, post-correction and pre-processing. Observed daily rainfall and 10 realizations of hourly disaggregated rainfall data are used as input of the rainfall-runoff model HBV. The calibration strategies for model parameter estimation incorporate standard hydrograph calibration and calibration on flow statistics based on winter/summer extremes distributions, flow duration curve for 18 sub catchments in the Aller-Leine river basin, Germany.

The results for the three sample catchments shows that, the parameters sets obtained from both flood frequency estimation and hydrograph simulation are found to be acceptable within the current hydrological modeling limits. This is in consist with the findings in (Haberlandt and Radtke 2014 and Cameron et al. 1999).

In general the final comparison of the different methods for design IPF estimation suggests:

(1) The multiple regression model developed from observed MDFs and IPFs data series is capable to estimate the IPFs with the modeled MDFs regarding flood frequency analysis.
(2) Generally, the model performances using flow statistics calibration strategy (CDF) are better than using the traditional hydrograph calibration strategy (hydr) according to the obtained RMSE and bias results.
(3) The best overall performance for design IPF estimation for all catchments is obtained when disaggregated rainfall data are used for calibration on the observed probability distribution of peak flows (CDF_h). However, the requirement to have available observed long recorded peak flow data fitted to the probability distributions may limit its application in catchments with poor data records.
(4) The daily simulation with post-correction using the same calibration method, namely (CDF_d) is the second best approach. Compared with CDF_h, it has fewer limitations regarding the length of the observation period of peak flows since the data on a daily basis are more available in most cases. This can help the decision makers and modelers to clarify ideas about how to choose the proper estimation strategy conditioned on available data.
(5) The daily simulation with post-correction (hydr_d) provides better estimation results of IPFs than the corresponding hourly simulation (hydr_h) when the calibration strategy is based on hydrographs. It can be used for estimation of design IPFs when there are not long enough peak flow data available to carry out CDF calibration.

Although the results are obtained for a specific study region, it is assumed, that they hold in general also for other regions with similar characteristics. It would be beneficial to have more case studies also involving other hydrological models. Further work is under way considering not only this scaling of the flows but regionalization for unobserved catchments simultaneously.

Chapter 5

5 Estimation of IPF from MDF in ungauged areas

As watershed models become increasingly useful and sophisticated, there is a need to extend their applicability to basins where they cannot be calibrated or validated to estimate IPF. Little is known so far how the regional relationships between model parameters and catchment characteristics impact the ability to model stream flows in ungauged areas. Therefore, it would be beneficial to take further work considering not only the scaling strategies of daily flows but also regionalization techniques for unobserved catchments.

The tradition regionalization approach includes two steps: (1) estimation of hydrological model parameters at each site, then (2) attempts to obtain the relationship between model parameters with catchment characteristics. In this chapter, a methodology for the regionalization of HBV model is introduced which involves calibration of a hydrological model to many sub catchments simultaneously, instead of the previous two-step approach. Besides, the dual objective of reproducing the flow statistics of observed daily flows and additionally, to avoid 'equifinality' (see Beven and Freer 2001) by using a proper transformation function has been taken into account.

The following sections outline the regional calibration methodology and provide an evaluation of the overall strategy by comparing the estimation results of IPF with the corresponding results from Chapter 4.

5.1 Methods

The modified version of the conceptual hydrological model HBV is also used here and the detailed description can be found in Chapter 4. Inspired by the linear transfer function applied successfully in many regionalization studies (Hundecha and Bárdossy 2004; Seibert 1999; Wallner et al. 2013; Yadav et al. 2007), this method is designed to give a different insight of estimation of instantaneous peak flow from simulated daily flow in ungauged areas.

The model parameters are linked with the catchment characteristics and can be estimated uniformly for all sub catchments based on the selected catchment characteristics. The traditional way to obtain the transfer function is to first calibrate the model for each sub catchment independently and then attempt to build a regional relationship betweeen the optimized model parameters with the hydrological indicators (such as land use/cover

parameters, climate characteristics) (Abdulla and Lettenmaier 1997). It can generate several different parameter sets which would reach the same model performance and the derived relationship therefore is likely to be weak or even 'false'. Here, to avoid this problem a predefined functional form of the relationship between the model parameters and catchment characteristics is used and then the model is calibrated for all sub catchments simultaneously. The transfer function implemented in this work is based on the previous work carried out by Wallner et al. 2013 and Hundecha and Bárdossy 2004. It is in a linear form as:

$$\Psi_{p,b} = \sum_{i=1}^{I} \alpha_{p,i} \cdot S_{b,i} + \sum_{j=1}^{J} \beta_{p,j} \cdot L_{b,j} + \gamma_p \cdot slope \cdots + e \qquad (5.1)$$

where $\psi_{p,b}$ is the hydrological model parameter value for the specific parameter p and the specific basin b. the variables $S_{b,i}$ and $L_{b,j}$ represent different soil and land use characteristics for basin b. e is the random error in regression analysis.

By establishing such a relationship, the model is calibrated by simultaneous estimations of the regression coefficients of the transfer function (α, β, γ, …) and of the model parameters p. Therefore, the regression coefficients of the transfer function keep unique for all the study basins whereas different basins have different parameter sets. Table 5.1 shows the selected calibrated 6 HBV model parameters and their corresponding linked catchment characteristics. The meaning for each symbol can be found in the first row of Table 5.2.

Table 5.1 Predefined relationship between model parameters and their corresponding catchment descriptors for the linear transfer function (see also Table 5.2)

Model parameter	Combination of catchment descriptors		
tt	Melv	aspR	
fc	FC	PV	
β	Bslop	fc	LUF
hl	Bslop	FC	LUF
K0	Bslop	Lst_fp	Kf
Perc	Bslop	Kf	BFR

In order to get the instantaneous peak flow, the multiple regression method derived in chapter 3 is applied here to post correct the simulated MDFs into IPFs. The optimization technique

DDS is utilized to achieve an effective and optimum estimation of the regression coefficients and parameters. Since the model is operated for several basins simultaneously, there is a need to aggregate all the different objective function into one objective function. Then, the sum of the individual objective functions of all the sub catchments is considered in DDS program. The objective function for this regionalization method is as follows:

$$OF = 0.25 \cdot NSC_{FFC-SUM} + 0.25 \cdot NSC_{FFC-WIN} + 0.25 \cdot NSC_{FDC} + 0.25 NSC_{MDF} \quad (5.2)$$

where the index CDF stands for the cumulative distribution function of daily extremes for summer (SUM) and winter (WIN) respectively; FDC is flow duration curve and MDF is annual maximum daily flow series; As the main focus is the simulation of extremes the sum of weights for summer and winter is set to 50%. The remaining half is then portioned between annual maximum daily series and flow duration curve.

5.2 Study area and data

The investigations are carried out for 18 catchments within the Aller-Leine River basin in northern Germany (see Figure 4.6). The 18 study basins are located in different geomorphologic and climatologic areas. For each sub catchment there are 11 catchment descriptors applied in this research and one can find the details in Table 5.2 from column 2 to 12. The second row of the table shows the reference symbol of each descriptor. The first six characteristics (Area – aspR) are derived from a Digital Elevation Model (DEM) with a resolution of 10 meters. The main orientation (aspR) ranges between 0 and 1, the bigger the value, the greater the portion of the basin orient to the north. The soil properties of effective field capacity (Fc), saturated hydraulic conductivity (Kf) and total pore volume (TPV) are estimated from the German digital soil data base BÜK1000 (see Hartwich et al. 1995). The portion of the forest land use type is derived from the land cover map CORINE2000 (see EUR 1994). Based on the observed runoff with an automatic base flow filter the recession constants are calculated in different hydrogeological units (HGUs) (Arnold et al. 1995). The mean recession constants for each basin are weighted according to the contributing area of the HGUs.

Table 5.3 gives an overview of the time periods of these measurements. Observed discharge is available as daily flows and monthly peak flow series within the period from 1951 to 2008 with lengths between 29 to 44 years for all the 18 catchments. The other climate data applied to force the hydrological model, such as temperature and evaporation are available for the same time periods.

Table 5.2 List of catchments and their basic descriptors

name	Area	minimum elevation	Mean elevation	Longest flow path	Basin slope	Main aspect	Raito of forest	Field Capacity	Conductivity	total pore volume	Mean recession constant
	Area	Elv_ds	Melv	lst_fp	Bslop	aspR	LUF	FC	Kf	TPV	BFR
(-)	(Km^2)	(m)	(m)	(km)	(%)	(-)	(%)	(vol.%)	(mm $h^{-1)}$	vol.%	(d)
BS	127	96.8	156.94	19.689	199.05	0.65	27.37	18.26	82.51	24.3	63
BP	116	67.5	90.58	25.747	95.35	0.85	6.26	20.82	62.78	33.9	37
Br	285	41.0	58.87	41.802	76.49	0.43	51.91	12.31	282.11	35.7	102
Go	633	141.5	315.84	62.868	299.31	0.49	26.04	16.57	117.39	27.3	100
Gr	125	129.4	208.43	23.915	269.32	0.56	43.22	15.92	92.6	29.5	56.4
Ha	104	74.8	93.42	25.244	152.64	0.42	37.98	19.17	66.52	37.7	42.1
Ku	61.8	130.2	219.9	13.524	237.97	0.38	27.73	14.26	109.96	37.8	37.5
Lh	100	24.8	54.87	25.987	53.60	0.52	41.8	13.89	238.99	32.6	102
Ma	45	196.2	275.58	12.035	312.56	0.56	31.49	12.25	125.98	19.9	34
Mt	242	36.6	61.76	36.744	53.83	0.63	16.7	14.42	206.25	36.7	64.6
NP	334	55.5	65.02	40.583	77.06	0.67	34.44	13.96	248.68	43.4	56
Ol	149	128.6	284.6	25.339	328.04	0.63	66.43	17.41	130.93	30.5	56
Pi	44.5	339.6	586.09	17.112	634.67	0.32	99.1	7.8	166.87	20.4	35
Re	321	182.9	273.74	43.413	341.49	0.49	28.64	15.96	127.09	27.3	100
RH	184	154.7	206.07	24.915	254.36	0.56	20.8	16.99	150.82	26.5	100
VR	57.5	133.1	467.03	22.158	435.86	0.79	65.18	13.98	145.27	20.1	35
De	309	90.9	258.02	49.067	208.87	0.56	38.08	17.33	84.44	29.5	56.4
Me	136	81.9	395.54	27.856	199.88	0.75	35.28	17.39	84.28	36.3	38

Table 5.3 Time windows of hydrological data

variable	Daily
runoff	29-44 yr
monthly peak flow	(-)
precipitation	1951-2008
temperature	1951-2008
evaporation	1951-2008

5.3 Results

In this section the performance of the hydrological model with and without regionalization strategies for estimation of design IPF has been compared. Four different flow statistics are used to represent the goodness of fit of the calibrated daily flows to the observed flows, namely, winter/summer extremes distributions, flow duration curve, annual daily extremes. The results of calibration of the hydrological model without regionalization are obtained from Chapter 4. For the regionalized results, the hydrological model is applied by estimation of regression coefficients of the transfer function and model parameters simultaneously for all 18 sub catchments.

5.3.1 Comparison of model performances with and without regionalization

Figure 5.1 shows comparisons between the fitted probability distributions of daily extremes in winter and summer for the sub-basins Br, De and Pi with and without regionalized model parameters. It is based on the observed and simulated daily flow data for over 30 years. The light grey (CDF_Reg) line corresponds to the simulated distributions, generated using the regionalized parameter sets while the dark grey line (CDF_d) is the simulated distributions without regionalization. The red solid line denotes the fitted GEV distribution on the observed annual daily extremes (black dots). The red dashed lines enclose the 90% confidence interval for the observations obtained by using a bootstrap method after Efron and Tibshirani (1986).

It is apparent from Figure 5.1 that the distribution functions corresponding to the simulated extremes by CDF_d strategy seem to fit the functions derived from observations much better than by CDF_Reg strategy in both winter and summer seasons. This fact indicates that the hydrological model is better able to simulate the extreme flows when it is calibrated independently at each site, especially in summer season. However, for both regionalization

and without regionalization cases, some underestimations of the design peak flows at the higher return periods can be noticed. There could be doubts about ability of the hydrological model to simulate the peaks of similar magnitude corresponding to the same storm events that give rise to the observed peaks. Therefore, more care should be taken for the selection and use of specific efficiency criterions since they place different emphasis on different types of observed and simulated behaviors.

The uncertainty bands of the observed annual extreme values differ significantly in summer and winter. The wider extent of the confidence interval in summer indicates greater uncertainty than in winter. The discrepancies between the probability distributions derived from the observed and two types of simulated flow peaks in both summer and winter season are smallest in De catchment.

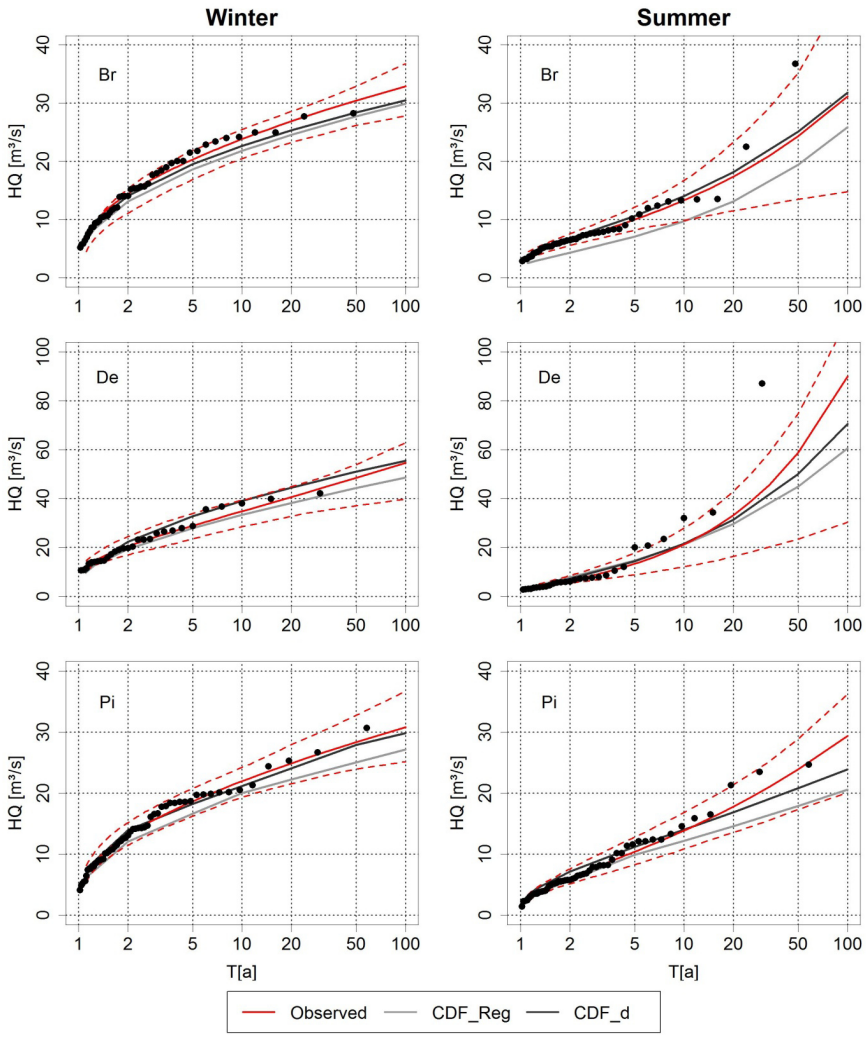

Figure 5.1: Observed and simulated fitted CDFs to daily extremes in winter and summer for the three sample catchments (Br/De/Pi) with and without regionalization; red dashed lines enclose the 90% confidence interval against observed peak flows

In order to investigate hydrological model performance in terms of fitting both winter and summer extremes to the GEV distributions for all 18 catchments, the results based on regionalization are compared the ones without regionalization. For that a goodness of fit Chi-square test is performed and Figure 5.2 gives a visual comparison of the results in the form of p-values. The left green violin is without regionalization and the right red one is with regionalization. A larger the p value shows a better model fit. As can be seen, the estimation of winter peaks for both cases is far more robust than those in summer. However, the use of regionalization shows fewer advantages in representation of the observed extremes distributions.

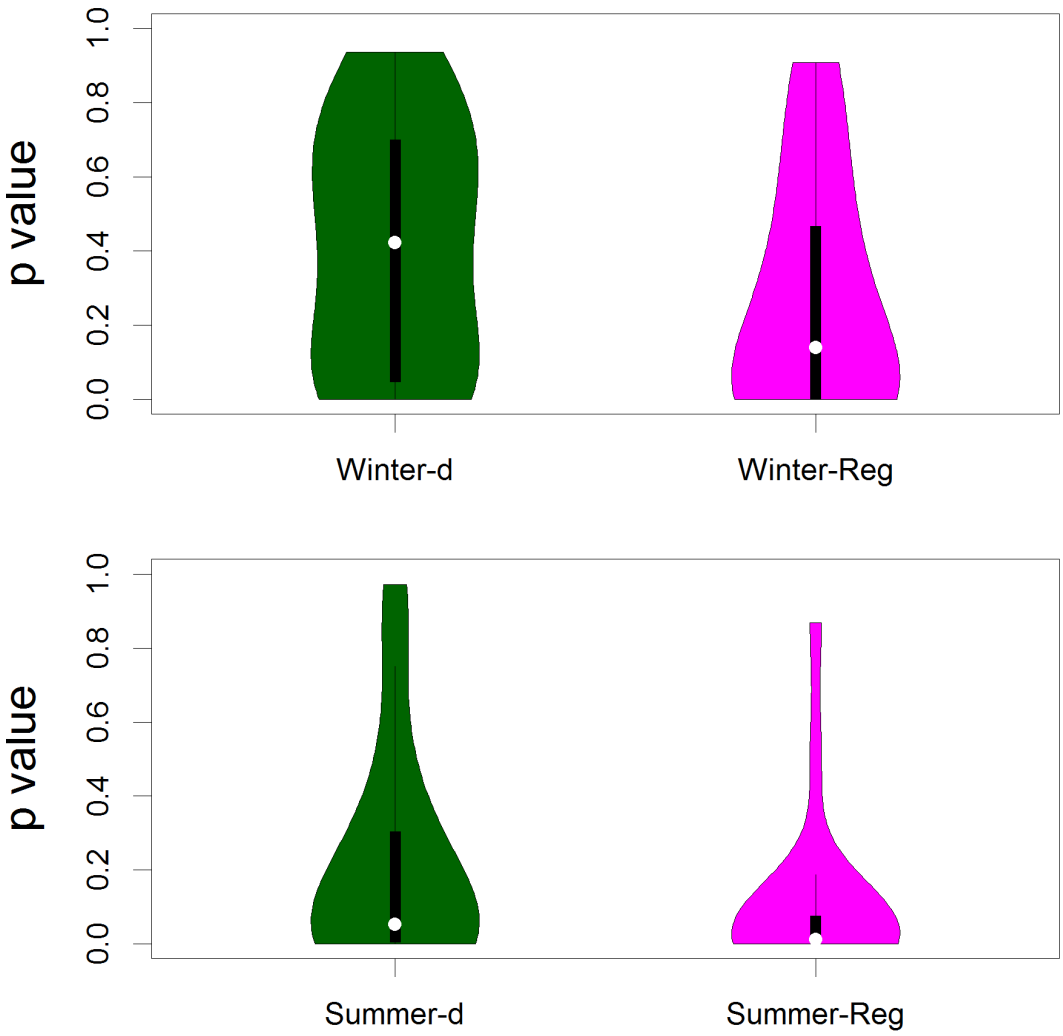

Figure 5.2: Violin plots of the p value over all sub catchments for the fitted GEV distribution between observed and simulated daily extremes in winter and summer respectively; suffix '-d' and '–Reg' indicate with and without regionalization

Figure 5.3 shows the comparison for simulated and observed flow duration curves (FDCs) in terms of 6 quantile values (0.05, 0.25, 0.5, 0.75, 0.95, 0.975 Quantile). The blue solid point indicates the observations; the red (FDC_d) and green (FDC_Reg) points are simulated results by calibrating the hydrological model without and with regionalized parameter sets respectively.

It is noticeable that the general goodness of fit between simulated and the observed 6 quantiles of FDC is satisfactory for both of the two approaches although there is a slightly overestimation generated by FDC_d method for Br catchment. The assessments for all the 18 sub catchments shown in Table 5.4 confirm the above findings. For hydrological modeling

with regionalized parameters, the average NSCs is 0.88 with a trend of overestimation suggested by a positive bias value 34.8% while without regionalization, the average NSC value is 0.87 with a positive bias value of 20%.

Table 5.4 Calibration results of flow duration curve (FDC) using the Nash-Sutcliffe criterion (NSC) and the bias with and without regionalization

		Ku	Go	Re	VR	Br	De	RH	Lh	Pi	Me	Ha	BS	NP	Gr	BP	Ol	Ma	Mt
NSC[-]	FDC_d	0.94	0.96	0.95	0.51	0.98	0.93	0.84	1	1	0.97	0.95	0.67	0.87	0.88	0.79	0.99	0.56	0.95
	FDC_Reg	0.95	0.96	0.94	0.44	0.91	0.92	0.74	0.8	0.93	0.98	0.91	0.89	0.96	0.91	0.93	0.98	0.74	0.95
Bias[%]	FDC_d	28.6	12.34	32.69	42.14	-8.51	38.36	56.67	-0.61	-15.47	22.36	27.77	53.46	32.35	37.76	31.91	-2.94	29.06	37.58
	FDC_Reg	23.25	15.12	33.11	32.29	14.53	35.93	15.72	11.16	-12.07	10.81	17.99	19.75	17.74	32.33	32.44	18.57	42.07	9.23

Table 5.5 gives the results of multiple regression coefficients for all 18 sites where the simulated annual maximum daily flows obtained from the regionalization approach are regressed with the observed annual instantaneous peak flows.

Table 5.5 Final results of multiple regression coefficients for all 18 sub catchments using regionalization

Regression Coefficients	α_0	α_1	α_2	α_3
T=10 yr	1.748	1.792	-0.00010	0.016
T=20 yr	1.677	1.966	-0.00016	0.019
T=50 yr	0.844	2.184	-0.00028	0.028
T=100 yr	-1.123	2.324	-0.00040	0.041

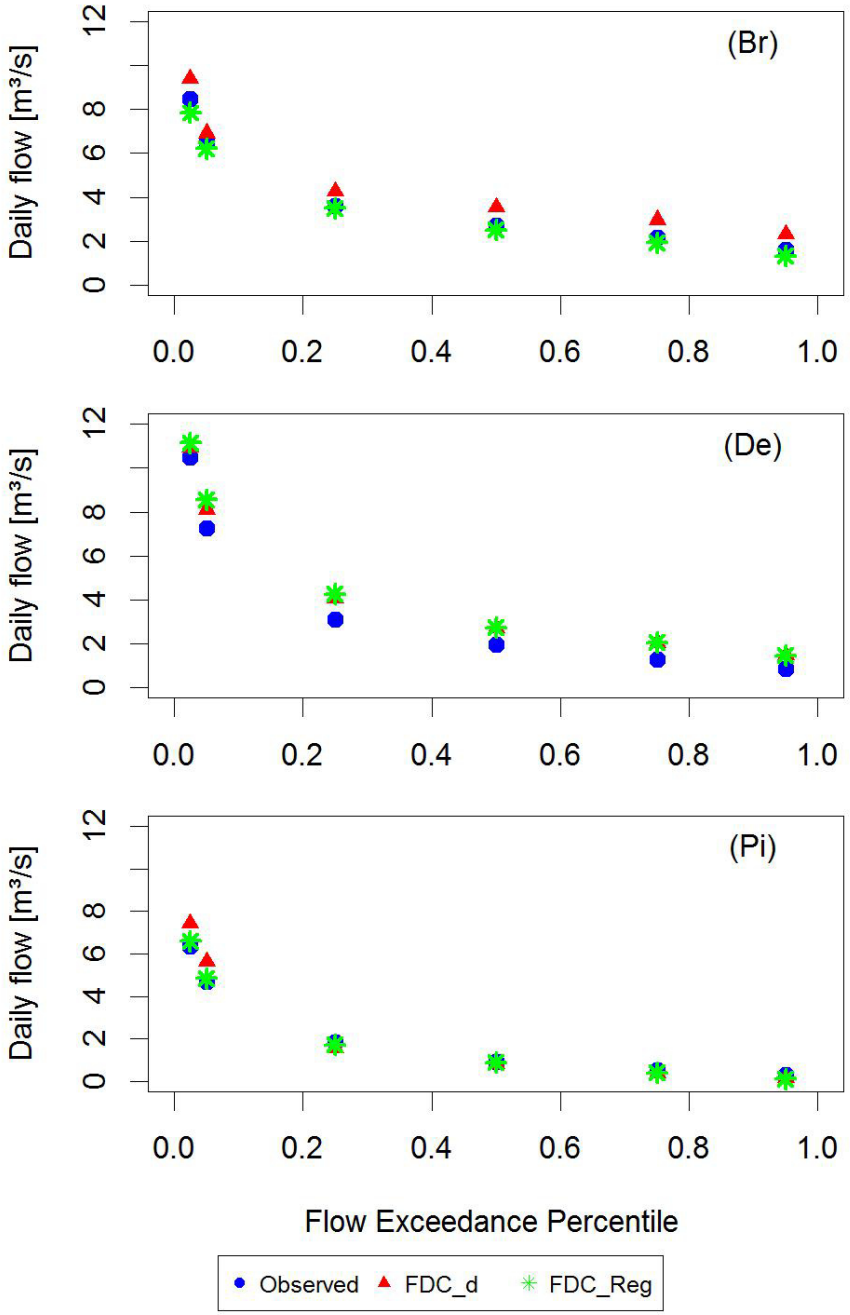

Figure 5.3: Comparison of observed and simulated daily flow duration curve (FDC) for the three sample catchments by calibrating the hydrological model without and with regionalized parameter sets respectively

Table 5.6 illustrates the post correction results for the above two approaches using the multiple regression model for a return period of 50 and 100 years among the whole study area

in winter and summer. As mentioned before, CDF_d and CDF_Reg indicate the flow statistic calibration strategy combined with and without regionalization respectively. R^2 is the coefficient of determination and RMSE is the root mean square error. The high values of R^2 indicate a good overall agreement between observed and simulated peaks for both cases. However, the comparison of RMSE shows CDF_d gives a significantly better representation of the observed peak flows at T=50yr and T=100yr than CDF_Reg and this is especially true in winter season.

Table 5.6 Comparison between the observed and simulated instantaneous peak flow using the CDF strategy combined with and without regionalization in winter and summer at recurrence intervals of 50 and 100 years

	Winter		**Summer**	
R^2 [-]	CDF_d	CDF_Reg	CDF_d	CDF_Reg
T=50 yr	0.967	0.967	0.952	0.954
T=100 yr	0.95	0.95	0.961	0.966
RMSE [%]	CDF_d	CDF_Reg	CDF_d	CDF_Reg
T=50 yr	18.801	27.319	21.906	30.921
T=100 yr	20.178	32.528	23.677	32.991

To further understand the difference of performance between regionalization and without regionalization, the distribution of RMSE for the 100yr flood from observed instantaneous peak flow series (IPFs) and the corresponding simulated ones for the whole area is shown in Figure 5.4 and Figure 5.5 respectively. It can be seen from Figure 5.4 the RMSE generated with regionalization in summer is from 1% to 80% whereas the corresponding range in Figure 5.5 is only between 0.2% and 42%. This trend also continues in winter season with smaller errors using regionalized parameters sets. For both cases, the overall distribution of error among the whole study area is similar. Major discrepancies are observed for Mt where the largest error for CDF_Reg case is following in summer and winter seasons. An opposite behavior is noticed in BP sub catchment with RMSE generated from CDF_Reg 1.4% in summer and 27.8% in winter while the corresponding results from CDF_d are 41.8% in summer and 2.1% in winter. The loss in model performance using CDF_Reg method suggests that the ability of the hydrological model to match high flows could be decreased by the regionalized parameters. Meanwhile, the model and parameter uncertainty could also be accredited to these unsatisfactory results.

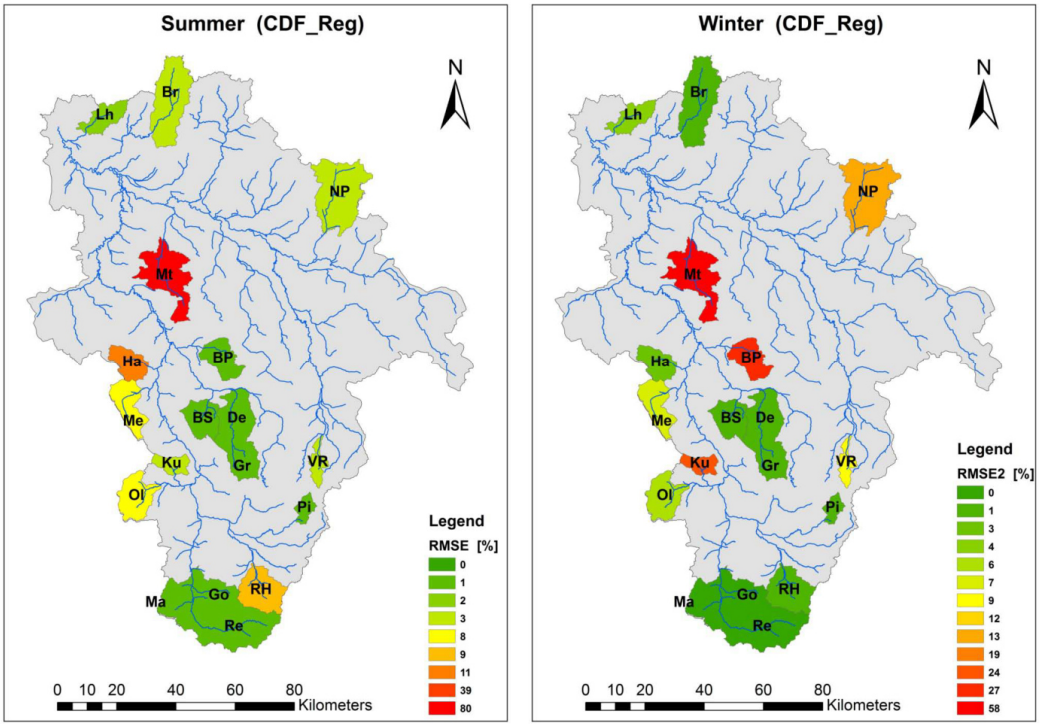

Figure 5.4: RMSE for estimating the 100yr flood in all 18 catchments using regionalized HBV model parameters

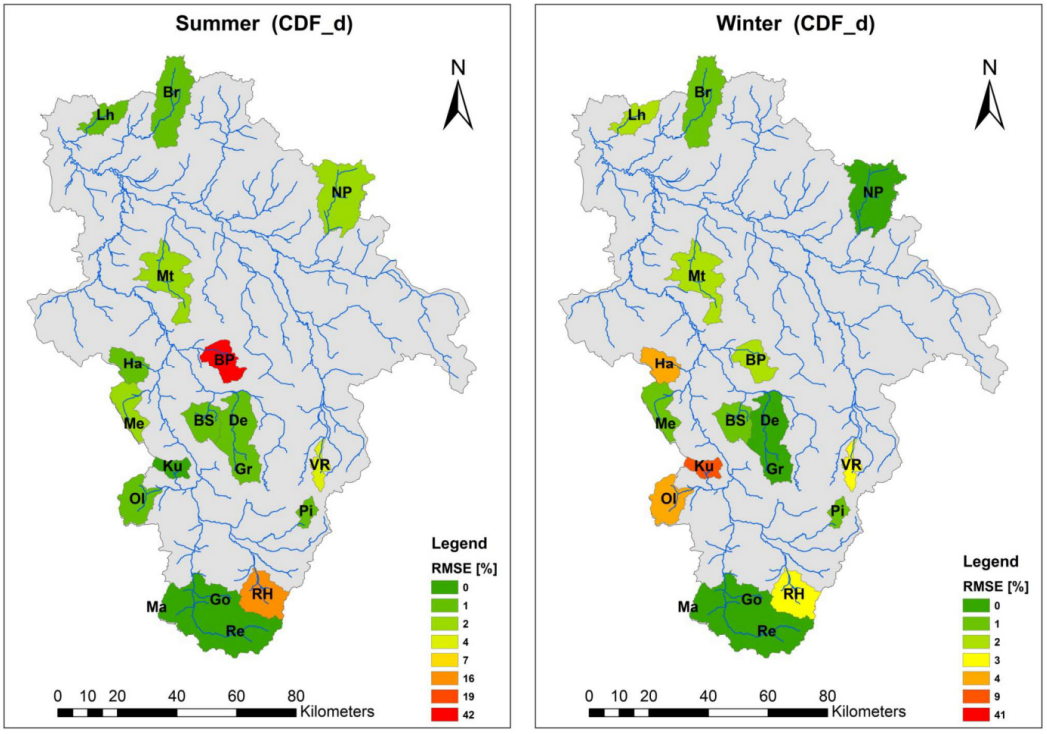

Figure 5.5: RMSE for estimating the 100yr flood in all 18 catchments using individually calibrated HBV model parameters

5.3.2 Final comparison between CDF calibration with regionalization and without regionalization

Finally, to sum up the contrast between CDF simulation with and without regionalization over the whole study area for four different return periods (T=10, 20, 50, 100yr) in summer and winter, the RMSE and bias criteria, are used. Figure 5.6 illustrates the results using daily observed climate data with post correction and without post correction to estimate the design IPFs by calibration on flood distributions.

The first column (MDF-IPF) represents the differences between the estimated quantiles from observed instantaneous peak flows (IPFs) and the corresponding observed maximum daily flows (MDFs) without any correction. The estimation from daily calibration with regionalization also without post correction is shown in the second column (MDF(Reg)-IPF). The comparison between the first column and the second column shows that the simulated maximum daily flows generated by the hydrological model with regionalized parameters are not acceptable for the purpose of estimation of IPFs. The third (CDF_Reg) and fourth (CDF_d) columns show the estimation error from daily calibration post-correction and with and without regionalization respectively.

As can be seen from the Figure 5.6 that immediate replacement of IPFs with observed or simulated MDFs can lead to significant underestimation in both seasons for four return periods and this tends to be even worse with using the simulated MDFs (average RMSE=46% in summer and 36% in winter). Additionally, the regionalization combined with post correction strategy (CDF_Reg) shows advantage of estimation of IPFs. The average RMSE for these four different return periods is reduced to 26.5% in winter and 31.5% in summer although there is a slight underestimation in both seasons (4.7% and 5.3%). The comparison of CDF_Reg approach with CDF_d approach reveals about 9% of the remaining accuracy is induced by calibrating the hydrological model without regionalization.

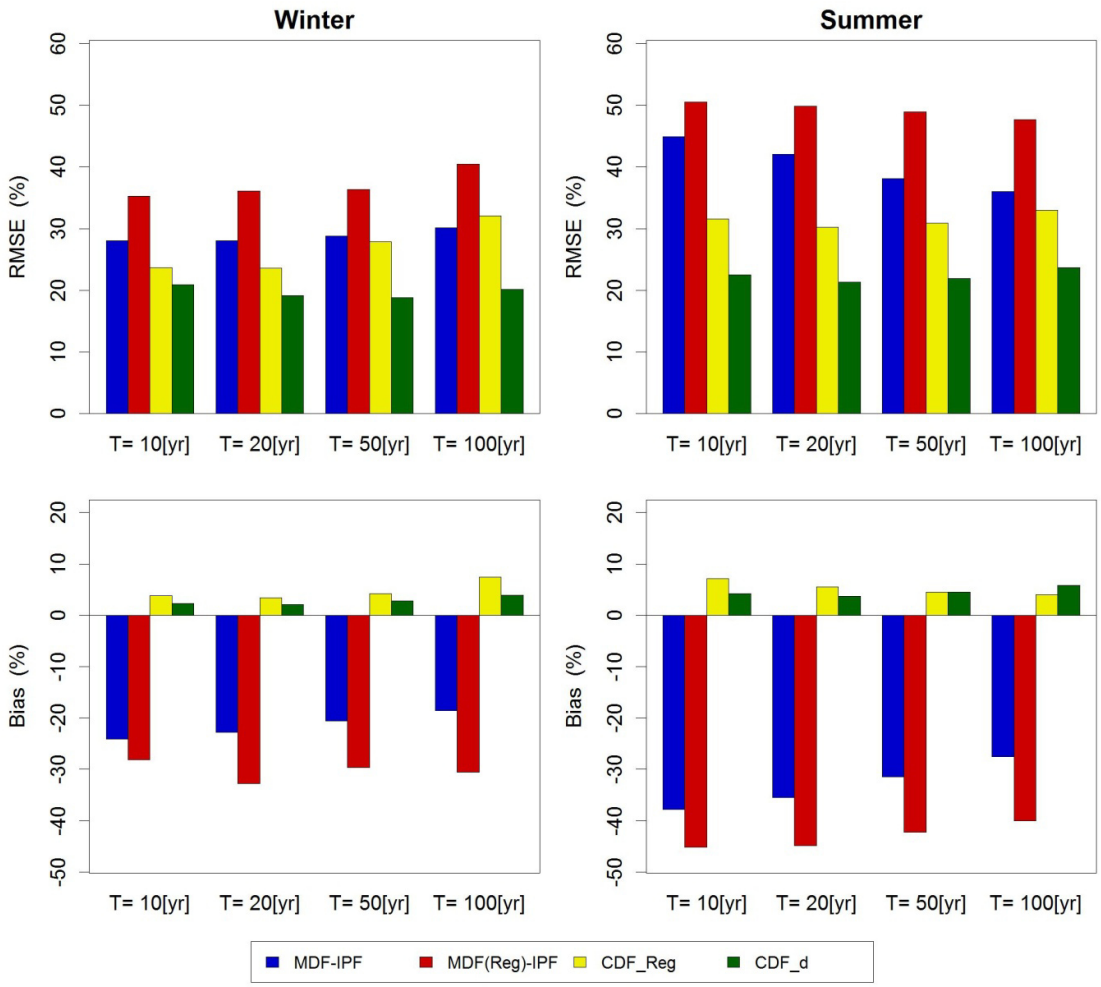

Figure 5.6: Comparison of root mean square error (RMSE) and Bias for estimating flood quantiles by with and without using regionalized parameter sets for the whole study area in both winter and summer season

5.4 Conclusions and discussions

In this chapter, the model performance regarding estimation of IPFs for 18 sites in Aller-Leine catchment is investigated with and without using regionalized parameter sets. The hydrological model is calibrated not only on flow statistics with the daily observed precipitation as input. The main findings can be summarized as follows:

It is found that the post correction step based on the multiple regression model is necessary and important to yield reasonable IPF results from simulated MDFs.

Based on the established function between model parameters and readily available information about catchment characteristics, regionalization of the HBV model parameters combined with post correction technique has been proved to be capable of estimating the IPFs from simulated MDFs in ungauged areas. However, the comparison of the results with and without regionalization indicates that the relative simplicity of parameter estimation may lead to worse model performance by calibrating the model simultaneously with regionalized parameter sets. It would be therefore recommended to classify the sub catchments according to their specific catchment characteristics in the future work.

In conclusion, this study provides important information to support the design peak flow estimation in ungauged areas which is essential for hydraulic infrastructures, flood management and planning for future development.

Chapter 6

Summary, conclusions and recommendations

The work reported in this thesis is carried out to determine suitable and feasible methods of estimating the instantaneous peak flow from the maximum daily flow in Aller-Leine catchment, Germany. Data include the daily flow time series and monthly peak flow from 50 flow gauges with the average recording length more than 30 years. In addition, daily precipitation data of 18 gauges have been disaggregated into hourly time step precipitation.

Chapter 3 deals with estimation of IPF from MDF conditioned on at-site observations using three different statistical methods, namely, simple regression method, multiple regression method and piecewise simple scaling method. The results have shown they can efficiently reduce the estimation error compared to using immediate replacement of quantiles of maximum daily flows (MDFs) with the corresponding quantiles of instantaneous peak flows (IPFs). The simple regression method provides an adjusted coefficient to correct the underestimation of the design daily flow. The expression is based on the linear relationship between IPF and MDF regarding their quantile and PWM values. The goodness fit test has proven the GEV distribution as being the best fit compared with all the other candidate distributions. The regression coefficients are then considered as the adjusted coefficients and this method is computationally very favorable. The final analysis of all three methods gives us a more comprehensive understanding of the difference between IPF and MDF.

For the stepwise multiple regression method, special attention is given to the extraction of the proper predictors. A number of catchment characteristics are selected and considered as the initial explanatory variables. The longest flow path and minimum elevation in this case have been selected as the final predictors in the regression equation by using the partial correlation method and stepwise regression. According to the previous multiple regression analysis, the longest flow path is highly correlated with peak flow and also highly interrelated with basin area which is most significantly related with flow. It is not surprising that the longest flow path is found to be the explanatory variable. However, unlike previous study results (eg. Taguas et al. 2008 and Fuller 1914) the minimum elevation is also taken into account here due to the above statistical analysis. In comparison with the classical Fuller's equation, the proposed multiple regression model noticeably improves the accuracy of the estimation results. Despite a small overestimation, the stepwise multiple regression method performs the best among the three models and for longer return periods its comparative performance becomes even more remarkable.

The last method, a piecewise simple scaling model, provides promising insights into the temporal issues between peak flow and its corresponding maximum daily flow. The hypothesis of piecewise simple scaling combined GEV distribution, is used to explore the link between PWMs of IPF and MDF, given the short-term 15_minute continuous flow data for three discharge gauges. Overall, the validation results reveal the three piecewise simple scaling models are capable of deriving peak flow when only maximum daily flow is available. Compared with the regression models, the scaling model is more efficient because the parameters of the scaling model are determined exclusively by the station with sufficient continuous highly resolution flow data. Therefore, this method could be used if only data available for a single station. However, the reason for the performance variance between different flow stations is at this stage not clear and a thorough investigation is required before it can be used in other basins. This indicates that the estimation of design IPF cannot be formulated to a single strict function based procedure. For a specific study case, the choices must be made according to the data availability and the particular circumstances of the problem.

Chapter 4 shows the comparison results to derive design IPFs using the HBV hydrological model which is operated on both daily and hourly time steps for 18 sub catchments in Aller-Leine catchment. There are two calibration strategies are involved: calibration on flow statistics and hydrographs. The model parameters sets obtained from both calibration strategies illustrated on the three sample basins are found to be acceptable within the current hydrological modeling limits. This is in consist with the findings in (Haberlandt and Radtke 2014 and Cameron et al. 1999). Overall the results also reveal the multiple regression model developed from Chapter 3 is capable to estimate the IPFs with the modeled MDFs regarding flood frequency analysis. The general model performances using flow statistics calibration strategy (CDF) are better than using the traditional hydrograph calibration strategy (hydr) according to the obtained RMSE and bias results. The best overall performance for design IPF estimation is CDF_h using disaggregated rainfall data and calibration on the observed probability distribution of peak flows. Discussion is provided on the issues of the applicability and limitations when those methods are applied in other areas. CDF_h requires long observed peak flow data fitted to the probability distributions which may limit its application in catchments with poor data records. The daily simulation CDF_d with post-correction using the same calibration method is the second best approach and it has fewer limitations regarding the length of the observation period of peak flows since the data on a daily basis are more available in most cases. For the traditional hydrograph calibration, the daily simulation with post-correction (hydr_d) provides better estimation results of IPFs than the corresponding hourly simulation (hydr_h). In some cases calibration on hydrographs is more preferable for estimation of design IPFs when there are not long enough peak flow data available to carry out CDF calibration.

Chapter 5 investigates estimation of IPFs in ungauged areas by regionalization of the HBV model parameters. The hydrological model in this chapter is calibrated only on flow statistics with the daily observed precipitation as input. The analysis is also carried out for the same study area as in Chapter 4. Since the calibration is carried out simultaneously for all sub catchments with different hydrological properties, the restriction of parameter estimation may lead to unacceptable model performance in some basins. It would be beneficial to classify the sub catchments according to their different catchment characteristics. In addition, the results reveal that the post correction on the simulated MDFs is an important step to yield more reasonable IPFs.

Although all those results are obtained for a specific study region, it is assumed, that they hold in general also for other regions with similar characteristics. It would be beneficial to have more case studies also involving other hydrological models.

The following steps are recommended for further development of estimation of IPFs in ungauged areas:

- Grouping of all the sub catchments according to their catchment characteristics by cluster analysis
- Regionalize the model parameters in each group and validate the regionalized parameter sets using Leave One Out Cross Validation (LOOCV)
- Comparing the performance of regionalization method with and without clustering

Literature

Abdulla, F.A., and Lettenmaier, D.P., 1997, Development of regional parameter estimation equations for a macroscale hydrologic model: Journal of Hydrology, v. 197, p. 230-257.

Acharya, A., and Ryu, J., 2014, Simple Method for Streamflow Disaggregation: Journal of Hydrologic Engineering, v. 19, p. 509-519.

Adamson, P.T., 1981, Southern African storm rainfall. Technical Report No. TR 102: Pretoria, RSA., Department of Water Affairs.

Ahilan, S., O'Sullivan, J.J., and Bruen, M., 2012, Influences on flood frequency distributions in Irish river catchments: Hydrology and Earth System Sciences, v. 16, p. 1137-1150.

Alexander, W.J.R., 2001, Flood Risk Reduction Measures: Incorporating Flood Hydrology for Southern Africa, Department of Civil and Biosystems Engineering, University of Pretoria, Pretoria.

Arnold, J.G., Allen, P.M., Muttiah, R., and Bernhardt, G., 1995, Automated Base Flow Separation and Recession Analysis Techniques: Ground Water, v. 33, p. 1010-1018.

Bárdossy, A., and He, Y., 2006, APPLICATION OF A NEAREST NEIGHBOUR METHOD TO A CONCEPTUAL RAINFALL-RUNOFF MODEL: Proceedings of the 7th International Conference on HydroScience and Engineering Philadelphia, USA September 10-13, 2006 (ICHE 2006).

Benito, G., Rico, A., Thorndycraft, V.R., Sanchez-Moya, Y., Sopena, A., Herrero, A.D., and Jimenez, A., 2006, Palaeoflood records applied to assess dam safety in SE Spain: River Flow 2006, Vols 1 and 2, p. 2113-2120.

Beven, K., and Freer, J., 2001, Equifinality, data assimilation, and uncertainty estimation in mechanistic modelling of complex environmental systems using the GLUE methodology: Journal of Hydrology, v. 249, p. 11-29.

Beven, K.J., Wood, E.F., and Sivapalan, M., 1988, On hydrological heterogeneity — Catchment morphology and catchment response: Journal of Hydrology, v. 100, p. 353-375.

Blazkova, S., and Beven, K., 2002, Flood frequency estimation by continuous simulation for a catchment treated as ungauged (with uncertainty): Water Resources Research, v. 38, p. 14-1-14-14.

Blazkova, S., and Beven, K., 2004, Flood frequency estimation by continuous simulation of subcatchment rainfalls and discharges with the aim of improving dam safety assessment in a large basin in the Czech Republic: Journal of Hydrology, v. 292, p. 153-172.

Bobee, B., 1999, Extreme flood events valuation using frequency analysis: a critical review: Houille Blanche-Revue Internationale De L Eau, v. 54, p. 100-105.

Boughton, W., and Droop, O., 2003, Continuous simulation for design flood estimation—a review: Environmental Modelling & Software, v. 18, p. 309-318.

Bouwer, L.M., Poussin, J., Papyrakis, E., Daniel, V.E., Pfurtscheller, C., Thieken, A.H., and Aerts, J.C.J.H., 2011, Methodology report on costs of mitigation v. WP04_2

Bozdogan, H., 1987, Model selection and Akaike's Information Criterion (AIC): The general theory and its analytical extensions: Psychometrika, v. 52, p. 345-370.

Bradley, A.A., and Potter, K.W., 1992, Flood frequency analysis of simulated flows: Water Resources Research, v. 28, p. 2375-2385.

Cameron, D.S., Beven, K.J., Tawn, J., Blazkova, S., and Naden, P., 1999, Flood frequency estimation by continuous simulation for a gauged upland catchment (with uncertainty): Journal of Hydrology, v. 219, p. 169-187.

Canuti, P., and Moisello, U., 1982, Relationship between the yearly maxima of peak and daily discharge for some basins in Tuscany: J. Hydrol.Sci, v. 27, p. 111–128.

Cawley, G.C., and Talbot, N.L.C., 2003, Efficient leave-one-out cross-validation of kernel fisher discriminant classifiers: Pattern Recognition, v. 36, p. 2585-2592.

Chadwick, A.J., Morfett, J.C., and Borthwick, M., 2004, Hydraulics in Civil and Environmental Engineering (4th edn.): Chapman and Hall, London, E & FN Spon.
Chambers, J.M., Cleveland, W.S., Kleiner, B., and Tukey, P.A., 1983, Graphical Methods for Data Analysis: Boston, PWS-Kent Publishing Co.
Chiew, F.H.S., and Siriwardena, L., 2005, Estimation of SimHyd parameter values for application in ungauged catchments: International Congress on Modelling and Simulation, Modelling and Simulation Society of Australia and New Zealand, p. 2883–2889.
Chow, V.T., Maidment, D.R., and Mays, L.R., 1988, Applied Hydrology: New York, USA, McGraw-Hill.
Colin, G., Christophe, V., and Paul, T., 2011, Guidance for assessing flood losses CONHAZ Report: Flood Hazard Research Centre – Middlesex University, v. WP06
Cordery, I., and Pilgrim, D.H., 2000, The state of the art of flood prediction, *in* Parker, D.J., ed., Floods, Volume II: London, UK, Routledge,, p. 185-197.
Cunnane, C., 1988, Methods and merits of regional flood frequency analysis: Journal of Hydrology, v. 100, p. 269-290.
D4E, 2007, Évaluations socio-économiques des instruments de prévention des inondations Paris, p. 117.
Dalrymple, T., 1960, Flood-frequency analyses, Manual of Hydrology: Part 3: Water Supply Paper, v. 1543.
Damm, M., 2010, Mapping Social-Ecological Vulnerability to Flooding [PhD thesis thesis]: Bonn, United Nations University.
Dastorani, M.T., Koochi, J.S., Darani, H.S., Talebi, A., and Rahimian, M.H., 2013, River instantaneous peak flow estimation using daily flow data and machine-learning-based models: Journal of Hydroinformatics, v. 15, p. 1089–1098.
Dawdy, D., Griffis, V., and Gupta, V., 2012, Regional Flood-Frequency Analysis: How We Got Here and Where We Are Going: Journal of Hydrologic Engineering, v. 17, p. 953-959.
De Michele, C., and Rosso, R., 1995, Self-similarity as physical basis for regionalization of flood probabilities: U.S.- Italy Research Workshop on the Hydrometeorology, Impacts, and Management of Extreme Floods.
Ding, J., Haberlandt, U., and Dietrich, J., 2014, Estimation of the instantaneous peak flow from maximum daily flow: a comparison of three methods: Hydrology Research (in press) doi:10.2166/nh.2014.085.
Draper, N.R., and Smith, H., 1998, Applied Regression Analysis, John Wiley and Sons, USA, p. Pp: 736.
Duan, Q.Y., Gupta, V.K., and Sorooshian, S., 1993, Shuffled complex evolution approach for effective and efficient global minimization: Journal of Optimization Theory and Applications, v. 76, p. 501-521.
Eagleson, P.S., 1972, Dynamics of flood frequency: Water Resources Research, v. 8, p. 878-898.
Efron, B., and Tibshirani, R., 1986, Bootstrap Methods for Standard Errors, Confidence Intervals, and Other Measures of Statistical Accuracy: Statistical Science, v. 1, p. 54-75.
Eleutério, J., 2012, Flood risk analysis:impact of uncertainty in hazard modelling and vulnerability assessments on damage estimations, National School of Water and Environmental Engineering of Strasbourg, France.
EUR, 1994, EUR 12585 - CORINE land cover project - Technical guide. European Commission. Office for Official Publications of the European Communities. Luxembourg.
Faulkner, D., and Wass, P., 2005, FLOOD ESTIMATION BY CONTINUOUS SIMULATION IN THE DON CATCHMENT, SOUTH YORKSHIRE, UK: Water and Environment Journal, v. 19, p. 78-84.
Fernandez, W., Vogel, R.M., and Sankarasubramanian, A., 2000, Regional calibration of a watershed model: Hydrological Sciences Journal, v. 45, p. 689-707.
Fill, H., and Steiner, A., 2003, Estimating Instantaneous Peak Flow from Mean Daily Flow Data: Journal of Hydrologic Engineering, v. 8, p. 365-369.

Fisher, R.A., and Tippett, L.H.C., 1928, Limiting forms of the frequency distribution of the largest or smallest member of a sample: Mathematical Proceedings of the Cambridge Philosophical Society, v. 24, p. 180-190.

Fortin, V., Bobee, B., and Bernier, J., 1997, Rational Approach to Comparison of Flood Distributions by Simulation: Journal of Hydrologic Engineering, v. 2, p. 95-103.

Fuller, W.E., 1914, Flood Flows: American Society of Civil Engineers, v. 77, p. 564-617.

Gebregiorgis, A.S., and Hossain, F., 2012, Hydrological Risk Assessment of Old Dams: Case Study on Wilson Dam of Tennessee River Basin: Journal of Hydrologic Engineering, v. 17, p. 201-212.

Greenwood, J.A., Landwehr, J.M., Matalas, N.C., and Wallis, J.R., 1979, Probability weighted moments: definition and relation to parameters of several distributions expressable in inverse form: Water Resources Research, v. 15, p. 6.

GREHYS, 1996, Presentation and review of some methods for regional flood frequency analysis: Journal of Hydrology, v. 186, p. 63-84.

Güntner, A., Olsson, J., Calver, A., and Gannon, B., 2001, Cascade-based disaggregation of continuous rainfall time series: the influence of climate: Hydrol. Earth Syst. Sci., v. 5, p. 145-164.

Guo, S.L., and Cunnane, C., 1991, Evaluation of the Usefulness of Historical and Palaeological Floods in Quantile Estimation: Journal of Hydrology, v. 129, p. 245-262.

Gupta, V.K., Mesa, O.J., and Dawdy, D.R., 1994, Multiscaling theory of flood peaks: Regional quantile analysis: Water Resources Research, v. 30, p. 3405-3421.

Gupta, V.K., and Waymire, E., 1990, Multiscaling properties of spatial rainfall and river flow distributions: Journal of Geophysical Research: Atmospheres, v. 95, p. 1999-2009.

Haberlandt, U., Ebner von Eschenbach, A.D., and Buchwald, I., 2008, A space-time hybrid hourly rainfall model for derived flood frequency analysis: Hydrol. Earth Syst. Sci., v. 12, p. 1353-1367.

Haberlandt, U., Heijden, S.v.d., Verworn, A., Berndt, C., Dietrich, J., Wallner, M., and Krause, F., 2015, Regionalisierung von Klimabeobachtungsdaten und WETTREG-Szenarien für Niedersachsen: Hannover, INSTITUT FÜR WASSERWIRTSCHAFT, HYDROLOGIE & LANDWIRTSCHAFTLICHEN WASSERBAU.

Haberlandt, U., and Radtke, I., 2014, Hydrological model calibration for derived flood frequency analysis using stochastic rainfall and probability distributions of peak flows: Hydrol. Earth Syst. Sci., v. 18, p. 353-365.

Haddad, K., and Rahman, A., 2012, Regional flood frequency analysis in eastern Australia: Bayesian GLS regression-based methods within fixed region and ROI framework – Quantile Regression vs. Parameter Regression Technique: Journal of Hydrology, v. 430–431, p. 142-161.

Hartwich, R., Behrens, J., Eckelmann, W., Haase, G., Richter, A., Roeschmann, G., and Schmidt, R., 1995, Bodenübersichtskarte der Bundesrepublik Deutschland 1:1000000 (BÜK 1000). Karte mit Erläuterungen, Textlegende und Leitprofilen Bimdesamstaöt für Geowissenschaften und Rohstoffe, Hannover.

Hill, P., and Mein, R., 1996, Incompatibilities between storm temporal patters and losses for design flood estimation: Hydrology and Water Resources Symposium, Hobart, Tasmania, Australia, p. 445–451.

Hosking, J.R.M., 1985, Algorithm AS 215: Maximum-likelihood estimation of the parameter of the generalized extreme-value distribution: Appl. Stat.,, v. 34, p. 301–310.

Hosking, J.R.M., 1990, L-Moments: Analysis and Estimation of Distributions Using Linear Combinations of Order Statistics: Journal of the Royal Statistical Society. Series B (Methodological), v. 52, p. 105-124.

Hosking, J.R.M., and Wallis, J.R., 1993, Some statistics useful in regional frequency analysis: Water Resources Research, v. 29, p. 271-281.

Hosking, J.R.M., and Wallis, J.R., 1997, Regional frequency analysis:an approach based on L-moments: Cambridge University Press ,New York, USA.

Hosking, J.R.M., Wallis, J.R., and Wood, E.F., 1985, Estimation of the Generalized Extreme-Value Distribution by the Method of Probability-Weighted Moments: Technometrics, v. 27, p. 251-261.

Hundecha, Y., and Bárdossy, A., 2004, Modeling of the effect of land use changes on the runoff generation of a river basin through parameter regionalization of a watershed model: Journal of Hydrology, v. 292, p. 281-295.

Jebari, S., Berndtsson, R., Olsson, J., and Bahri, A., 2012, Soil erosion estimation based on rainfall disaggregation: Journal of Hydrology, v. 436–437, p. 102-110.

Jenkinson, A.F., 1955, The frequency distribution of the annual maximum (or minimum) values of meteorological elements: Quarterly Journal of the Royal Meteorological Society, v. 81, p. 158-171.

Kapangaziwiri, E., and Hughes, D.A., 2008, Towards revised physically based parameter estimation methods for the Pitman monthly rainfall-runoff model: Water SA, v. 34, p. 183-192.

Katz, R.W., Parlange, M.B., and Naveau, P., 2002, Statistics of extremes in hydrology: Advances in Water Resources, v. 25, p. 1287-1304.

Kim, S.M., Benham, B.L., Brannan, K.M., Zeckoski, R.W., and Doherty, J., 2007, Comparison of hydrologic calibration of HSPF using automatic and manual methods: Water Resources Research, v. 43, p. W01402.

Kite, G.W., 1988, Frequency and Risk Analysis in Hydrology: Littleton, Colorado, Water Resources Publications.

Koutsoyiannis, D., Kozonis, D., and Manetas, A., 1998, A mathematical framework for studying rainfall intensity-duration-frequency relationships: Journal of Hydrology, v. 206, p. 118-135.

Koutsoyiannis, D., Onof, C., and Wheater, H.S., 2003, Multivariate rainfall disaggregation at a fine timescale: Water Resources Research, v. 39, p. 1173.

Kumar, D.N., Lall, U., and Petersen, M.R., 2000, Multisite disaggregation of monthly to daily streamflow: Water Resources Research, v. 36, p. 1823-1833.

Lamb, R., 2006, Rainfall-Runoff Modeling for Flood Frequency Estimation, Encyclopedia of Hydrological Sciences, John Wiley & Sons, Ltd.

Langbein, W.b., 1944, Peak discharge from daily records: US Geological survay Bulletin August, v. p.145.

Langbein, W.B., 1960, Plotting Positions in Frequency Analyses, U.S. Geological Survey Water Supply Paper 1543-A: Washington, D.C, p. A48-A51.

Licznar, P., Łomotowski, J., and Rupp, D.E., 2011, Random cascade driven rainfall disaggregation for urban hydrology: An evaluation of six models and a new generator: Atmospheric Research, v. 99, p. 563-578.

Madsen, H., 2000, Automatic calibration of a conceptual rainfall–runoff model using multiple objectives: Journal of Hydrology, v. 235, p. 276-288.

Madsen, H., Pearson, C.P., and Rosbjerg, D., 1997, Comparison of annual maximum series and partial duration series methods for modeling extreme hydrologic events: 2. Regional modeling: Water Resources Research, v. 33, p. 759-769.

Martins, E.S., and Stedinger, J.R., 2001, Historical information in a generalized maximum likelihood framework with partial duration and annual maximum series: Water Resources Research, v. 37, p. 2559-2567.

McIntyre, N., Lee, H., Wheater, H., Young, A., and Wagener, T., 2005, Ensemble predictions of runoff in ungauged catchments: Water Resources Research, v. 41, p. W12434.

Merz, B., Hall, J., Disse, M., and Schumann, A., 2010, Fluvial flood risk management in a changing world: Natural Hazards and Earth System Sciences, v. 10, p. 509-527.

Merz, R., and Blöschl, G., 2004, Regionalisation of catchment model parameters: Journal of Hydrology, v. 287, p. 95-123.

Messner, F., Penning-Rowsell, E., Green, C., Meyer, V., Tunstall, S., and van der Veen, A., 2007, Evaluating flood damages: guidance and recommendations on principles and methods, v. T09-06-01.

Montz, B.E., and Tobin, G.A., 1997, The environmental impacts of flooding in St. Maries, Idaho.
Müller, H., and Haberlandt, U., 2015, Temporal rainfall disaggregation with a cascade model: from single-station disaggregation to spatial rainfall: J. Hydrol. Eng (in press).
Muñoz, E., Arumí, J.L., and Vargas, J., 2012, A Design Peak Flow Estimation Method for Medium-Large and Data-Scarce Watersheds With Frontal Rainfall1: JAWRA Journal of the American Water Resources Association, v. 48, p. 439-448.
Nascimento, N., Machado, M.L., Baptista, M., and De Paula E Silva, A., 2007, The assessment of damage caused by floods in the Brazilian context: Urban Water Journal, v. 4, p. 195-210.
Nash, J.E., and Sutcliffe, J.V., 1970, River flow forecasting through conceptual models part I — A discussion of principles: Journal of Hydrology, v. 10, p. 282-290.
Olsson, J., 1998, Evaluation of a scaling cascade model for temporal rain- fall disaggregation: Hydrol. Earth Syst. Sci., v. 2, p. 19-30.
Oudin, L., Kay, A., Andréassian, V., and Perrin, C., 2010, Are seemingly physically similar catchments truly hydrologically similar?: Water Resources Research, v. 46, p. W11558.
Parajka, J., Merz, R., and Blöschl, G., 2005, A comparison of regionalisation methods for catchment model parameters: Hydrol. Earth Syst. Sci., v. 9, p. 157-171.
Pegram, G., and Parak, M., 2004, A review of the regional maximum flood and rational formula using geomorphological information and observed floods: WaterSA, v. 30 (3)
Pilon, P., 2004, Guidelines for reducing flood losses: United Nations Office for Disaster Risk Reduction (UNISDR), p. 79 p.
Pilon, P.J., and Harvey, K.D., 1994, Consolidated frequency analysis, Reference manual: a, Ottawa, Canada, Environment Canada.
Potter, K.W., 1987, Research on flood frequency analysis: 1983–1986: Reviews of Geophysics, v. 25, p. 113-118.
Rahman, A., Haddad, K., Zaman, M., Kuczera, G., and Weinmann, P., 2011, Design flood estimation in ungauged catchments: A comparison between the probabilistic rational method and quantile regression technique for NSW, Volume 14 (2), p. 127 - 139.
Reis Jr, D.S., and Stedinger, J.R., 2005, Bayesian MCMC flood frequency analysis with historical information: Journal of Hydrology, v. 313, p. 97-116.
Saddagh, M.H., and Abedini, M.J., 2012, Enhancing MIKE11 Updating Kernel and Evaluating Its Performance Using Numerical Experiments: Journal of Hydrologic Engineering, v. 17, p. 252-261.
Sangal, B., 1983, Practical Method of Estimating Peak Flow: Journal of Hydraulic Engineering, v. 109, p. 549-563.
Sangal, B., 1984, Closure to "Practical Method of Estimating Peak Flow" by Beni P. Sangal (April, 1983): Journal of Hydraulic Engineering, v. 110, p. 1165-1166.
Schulze, R., 1995, Hydrology and Agrohydrology: A Text to Accompany the ACRU 3.00 Agrohydrological Modelling System, Volume WRC Report No. TT 69/95: Pretoria, Water Research Commission.
Sefton, C.E.M., and Howarth, S.M., 1998, Relationships between dynamic response characteristics and physical descriptors of catchments in England and Wales: Journal of Hydrology, v. 211, p. 1-16.
Seibert, J., 1999, Regionalisation of parameters for a conceptual rainfall-runoff model: Agricultural and Forest Meteorology, v. 98–99, p. 279-293.
Servat, E., and Dezetter, A., 1993, Rainfall-runoff modelling and water resources assessment in northwestern Ivory Coast. Tentative extension to ungauged catchments: Journal of Hydrology, v. 148, p. 231-248.
Sivapalan, M., 2003, Prediction in ungauged basins: a grand challenge for theoretical hydrology: Hydrological Processes, v. 17, p. 3163-3170.
Sivapalan, M., Blöschl, G., Merz, R., and Gutknecht, D., 2005, Linking flood frequency to long-term water balance: Incorporating effects of seasonality: Water Resources Research, v. 41, p. W06012.

Sivapalan, M., and Samuel, J.M., 2009, Transcending limitations of stationarity and the return period: process-based approach to flood estimation and risk assessment: Hydrological Processes, v. 23, p. 1671-1675.
SMHI, 2008, Integrated Hydrological Modelling System - Manual Version 6.0,
Swedish Meteorological and Hydrological Institute.
Smith, J.A., 1992, Representation of basin scale in flood peak distributions: Water Resour. Res., v. 28, p. 2993-2999.
Smithers, J.C., and Schulze, R.E., 2000a, Development and evaluation of techniques for estimating short duration design rainfall in South Africa, WRC Report No. 681/1/00: Pretoria, RSA, Water Research Commission.
Smithers, J.C., and Schulze, R.E., 2003, Design Rainfall and Flood Estimation in South Africa: Pretoria, RSA, p. 156 pp.
Sorooshian, S., and Dracup, J.A., 1980, Stochastic parameter estimation procedures for hydrologie rainfall-runoff models: Correlated and heteroscedastic error cases: Water Resources Research, v. 16, p. 430-442.
Sorooshian, S., and Gupta, V.K., 1983, Automatic calibration of conceptual rainfall-runoff models: The question of parameter observability and uniqueness: Water Resources Research, v. 19, p. 260-268.
Stedinger, J.R., and Vogel, R.M., 1984, Disaggregation Procedures for Generating Serially Correlated Flow Vectors: Water Resources Research, v. 20, p. 47-56.
Stedinger, J.R., Vogel, R.M., and Foufoula-Georgiou, 1993a, Frequency analysis of extreme events, in: Handbook of hydrology,edited by: Maidment, D. R., MacGRAW-HILL: New York, USA, p. 18.11–18.66.
Stedinger, J.R., Vogel, R.M., and Foufoula-Georgiou, E., 1993b, Frequency analysis of extreme events. Handbook of Hydrology: New York, USA, McGraw-Hill.
Taguas, E.V., Ayuso, J.L., Pena, A., Yuan, Y., Sanchez, M.C., Giraldez, J.V., and Pérez, R., 2008, Testing the relationship between instantaneous peak flow and mean daily flow in a Mediterranean Area Southeast Spain: CATENA, v. 75, p. 129-137.
Tarboton, D.G., Sharma, A., and Lall, U., 1998, Disaggregation procedures for stochastic hydrology based on nonparametric density estimation: Water Resources Research, v. 34, p. 107-119.
Tasker, G.D., and Stedinger, J.R., 1989, An operational GLS model for hydrologic regression: Journal of Hydrology, v. 111, p. 361-375.
Tolson, B.A., and Shoemaker, C.A., 2007, Dynamically dimensioned search algorithm for computationally efficient watershed model calibration: Water Resources Research, v. 43, p. W01413.
USACE, 1994, Flood-Runoff Analysis: Washington, DC U.S. Army Corps of Engineers, p. 214pp.
Veijalainen, N., Lotsari, E., Alho, P., Vehvilainen, B., and Kayhko, J., 2010, National scale assessment of climate change impacts on flooding in Finland: Journal of Hydrology, v. 391, p. 333-350.
Viglione, A., Castellarin, A., Rogger, M., Merz, R., and Blöschl, G., 2012, Extreme rainstorms: Comparing regional envelope curves to stochastically generated events: Water Resources Research, v. 48, p. W01509.
Viglione, A., Merz, R., and Blöschl, G., 2009, On the role of the runoff coefficient in the mapping of rainfall to flood return periods: Hydrol. Earth Syst. Sci., v. 13, p. 577-593.
Villarini, G., Serinaldi, F., Smith, J.A., and Krajewski, W.F., 2009a, On the stationarity of annual flood peaks in the continental United States during the 20th century: Water Resources Research, v. 45, p. W08417.
Villarini, G., Smith, J.A., Serinaldi, F., Bales, J., Bates, P.D., and Krajewski, W.F., 2009b, Flood frequency analysis for nonstationary annual peak records in an urban drainage basin: Advances in Water Resources, v. 32, p. 1255-1266.

Wallis, J.R., Schaefer, M.G., Barker, B.L., and Taylor, G.H., 2007, Regional precipitation-frequency analysis and spatial mapping for 24-hour and 2-hour durations for Washington State: Hydrology and Earth System Sciences, v. 11, p. 415-442.

Wallner, M., Haberlandt, U., and Dietrich, J., 2013, A one-step similarity approach for the regionalization of hydrological model parameters based on Self-Organizing Maps: Journal of Hydrology, v. 494, p. 59-71.

Westerberg, I.K., Guerrero, J.L., Younger, P.M., Beven, K.J., Seibert, J., Halldin, S., Freer, J.E., and Xu, C.Y., 2011, Calibration of hydrological models using flow-duration curves: Hydrol. Earth Syst. Sci., v. 15, p. 2205-2227.

Wu, X.L., Xiang, X.H., Wang, C.H., Chen, X., Xu, C.Y., and Yu, Z.B., 2013, Coupled Hydraulic and Kalman Filter Model for Real-Time Correction of Flood Forecast in the Three Gorges Interzone of Yangtze River, China: Journal of Hydrologic Engineering, v. 18, p. 1416-1425.

Xiong, L., and Guo, S., 2004, Trend test and change-point detection for the annual discharge series of the Yangtze River at the Yichang hydrological station / Test de tendance et détection de rupture appliqués aux séries de débit annuel du fleuve Yangtze à la station hydrologique de Yichang: Hydrological Sciences Journal, v. 49, p. 99-112.

Xu, Z., Schumann, A., and Li, J., 2003, Markov cross-correlation pulse model for daily streamflow generation at multiple sites: Advances in Water Resources, v. 26, p. 325-335.

Yadav, M., Wagener, T., and Gupta, H., 2007, Regionalization of constraints on expected watershed response behavior for improved predictions in ungauged basins: Advances in Water Resources, v. 30, p. 1756-1774.

Yevjevich, V., 1982, Probability and Statistics in Hydrology (1st edn.): Littleton, Colorado, Water Resources Publications.

Young, C.B., McEnroe, B.M., and Rome, A.C., 2009, Empirical Determination of Rational Method Runoff Coefficients: Journal of Hydrologic Engineering, v. 14, p. 1283-1289.

Yu, P.-S., Yang, T.-C., and Lin, C.-S., 2004, Regional rainfall intensity formulas based on scaling property of rainfall: Journal of Hydrology, v. 295, p. 108-123.

Yu, P.S., and Tseng, T.Y., 1996, A model to forecast flow with uncertainty analysis: Hydrological Sciences Journal-Journal Des Sciences Hydrologiques, v. 41, p. 327-344.

Yu, P.S., and Yang, T.C., 2000, Using synthetic flow duration curves for rainfall–runoff model calibration at ungauged sites: Hydrological Processes, v. 14, p. 117-133.